Leaders in Deep Exploration

Quantec Geoscience

TITAN-24 DC - IP - MT SURVEY
GEOPHYSICAL REPORT
NORTH TISDALE PROJECT
(ONTARIO, CANADA)
ON BEHALF OF
MONETA PORCUPINE MINES INC.
(TIMMINS, ONTARIO, CANADA)

QUANTEC GEOSCIENCE LTD
146 SPARKS AVE, TORONTO, ONTARIO, M2H 2S4, CANADA
PHONE: (416) 306-1941 / FAX: (416) 306-1949
WWW.QUANTECGEOSCIENCE.COM

KEVIN KILLIN, P. GEO
SAMAN PERERA, MEHRAN GHARIBI &
MOJTABA DANESHVAR
17/02/2012

EXECUTIVE SUMMARY

INTRODUCTION

A Titan-24 DC-IP-MT survey was completed over the North Tisdale Project, North Tisdale, Ontario, Canada on behalf of Moneta Porcupine Mines Inc. Data were acquired along two parallel (~900m apart) N-S oriented lines and a total of 4 km (5.6 km with current extensions) DC-IP survey line and 4 km of test MT survey line were surveyed using 80 m station spacing. A pole-dipole configuration was used for DC and IP measurements.

SURVEY OBJECTIVES

The exploration objective of the Titan 24 DCIP & MT survey at North Tisdale Project was to map and define contact/lithologies to depth (known in near surface setting from drilling, etc) and determine any change in their character.

RESULTS

The resistivity subsurface distribution along the survey lines displays two conductive zones in the southern and northern parts. These high conductive zones with resistivity of 1- 100 Ωm are resolved in a high resistivity background with a resistivity of ~5000 Ωm. The geometry of these conductive anomalies resembles lithological contacts; probably associated with the interbedded graphitic argillite, or faults. Note that several tests were completed to reduce the effects of power lines on the inversion results. Auxiliary information is required to validate these results.

The chargeability distribution over the survey area indicates two IP anomalies, 70 mrads and 30 mrads, at locations corresponding with the observed conductive zones. Between these two zones resistive and moderately chargeable area is observed. This zone could be associated with lithological contact or fault with no conductive materials.

RECOMMENDATIONS

An Illustration of potential target zones is presented in Figure 4-9 and Figure 4-10. A total of 6 anomalies identified in the resistivity and chargeability models and are listed in the following table. The potential targets are prioritized as High, Moderate, or Low, and their intermediate ranges based on the category of the chargeability and conductivity of the anomalies as well as the size. The High priority anomalies are associated with large anomalies with high-moderate chargeability and high-moderate conductivity (category I). Category II denotes anomalies with high-moderate chargeability and moderate-low conductivity. A moderate-low chargeable and resistive anomaly is categorized as III.

The resolved anomalies are interpreted based on the reliability and repeatability of the DC, IP and MT inversion results. Because of cultural interferences observed in the survey area this interpretation must be treated with caution and should be validated by ground truthing. Any drilling efforts based on these interpretations must incorporate other geophysical and geological models and information to validate these results.

Anomaly ID	Chargeability (High/Mod/Low)	DC Conductivity (High/Mod/Low)	MT Conductivity (High/Mod/Low)	Size (Large/Mid/Small)	Category	Priority	#
L1E_IP1	High	High	Mod	Large	I	High	1
L1E_IP2	High-Mod	High	Mod	Mid	I	High	2
L2E_IP1	High	High	High	Large	I	High	3
L2E_IP2	High-Mod	High	Mod	Mid	I	High	4
L2E_IP3	High-Mod	Low	Mod	Mid	II	Moderate	5
L2E_IP4	Mod-Low	Low	Low	Mid-Small	III	Low	6

TABLE OF CONTENTS

LIST OF FIGURES

LIST OF TABLES

1 INTRODUCTION

This report presents the logistics and the results of the analysis of the Titan-24 DC - IP - MT data acquired from 2011/12/06 to 2011/12/14 over the North Tisdale Project, on behalf of Moneta Porcupine Mines Inc.

The survey includes 2 DC-IP-MT spreads along 2 N-S oriented lines with 80 m station interval and ~900 m line spacing (Figure 1-1 and Figure 1-2). A total of 4.0 km DC/IP survey line (5.6 km with current extensions) and 4 km of MT survey line were surveyed. A pole-dipole configuration was used for DC and IP measurements.

The first part of this report presents the inversion results, their geophysical interpretation, and some recommendations for future follow-up on the property.

The second part of the report presents the logistics of the survey, including the survey parameters and methodology, and the survey results (data) in digital documents.

1.1 SURVEY OBJECTIVES

The exploration objective of the Titan 24 DCIP & MT survey at North Tisdale Project was to map and define contact/lithologies to depth (known in near surface setting from drilling, etc), determine any change in their character, and detail anomalies found depending on importance. And complete second profile up to 800-1000m away on strike, depending on earlier results. Titan 24 should provide the following benefits:

Locating potential mineralization zones and/or associated alteration.

Mapping the resistivity and chargeability features of the subsurface assisting geologic interpretations.

The Titan 24 **D**istributed **A**cquisition **S**ystem (**DAS**; Sheard, 1998) employs a combination of multiplicity of sensors, 24-bit digital sampling, and advanced signal processing. It provides three independent datasets capable of measuring subsurface resistivity's (structure, alteration & lithology) and chargeability (mineralization) to depth.

The DC/IP component of the survey should provide an excellent means of delineating target mineralization within the top 500m to 750m pending geologic and cultural environment. The MT resistivity provides additional resistivity information from surface to depths beyond 1km. The MT resistivity is useful for mapping geological contacts with resistivity contrasts and deep conductors that may potentially represent alteration or mineralization.

1.2 GENERAL SURVEY INFORMATION

Quantec Project No.:	CA00916T
Client:	Moneta Porcupine Mines Inc.
Client Address	65, Third Avenue Timmins, Ontario, P4N 1C2 Canada
Client representative:	Rainer Skeries Phone: (705) 264-2296 Email: RSkeries@monetaporcupine.com
Project Name:	North Tisdale Project
Survey Type:	Titan-24 DC - IP - MT
Project Survey Period:	2011/12/06 to 2011/12/14
General Location:	Approximately 7.6 km NNE of Timmins
Province	Ontario
District	North Tisdale and South of Murphy Township
Nearest Settlement:	Timmins
Datum & Projection:	WGS84 / UTM Zone 17N
Latitude & Longitude:	Approx. 081°16’07”W, 48°32'00”N
UTM position:	Approx. 480160m E, 5375629m N

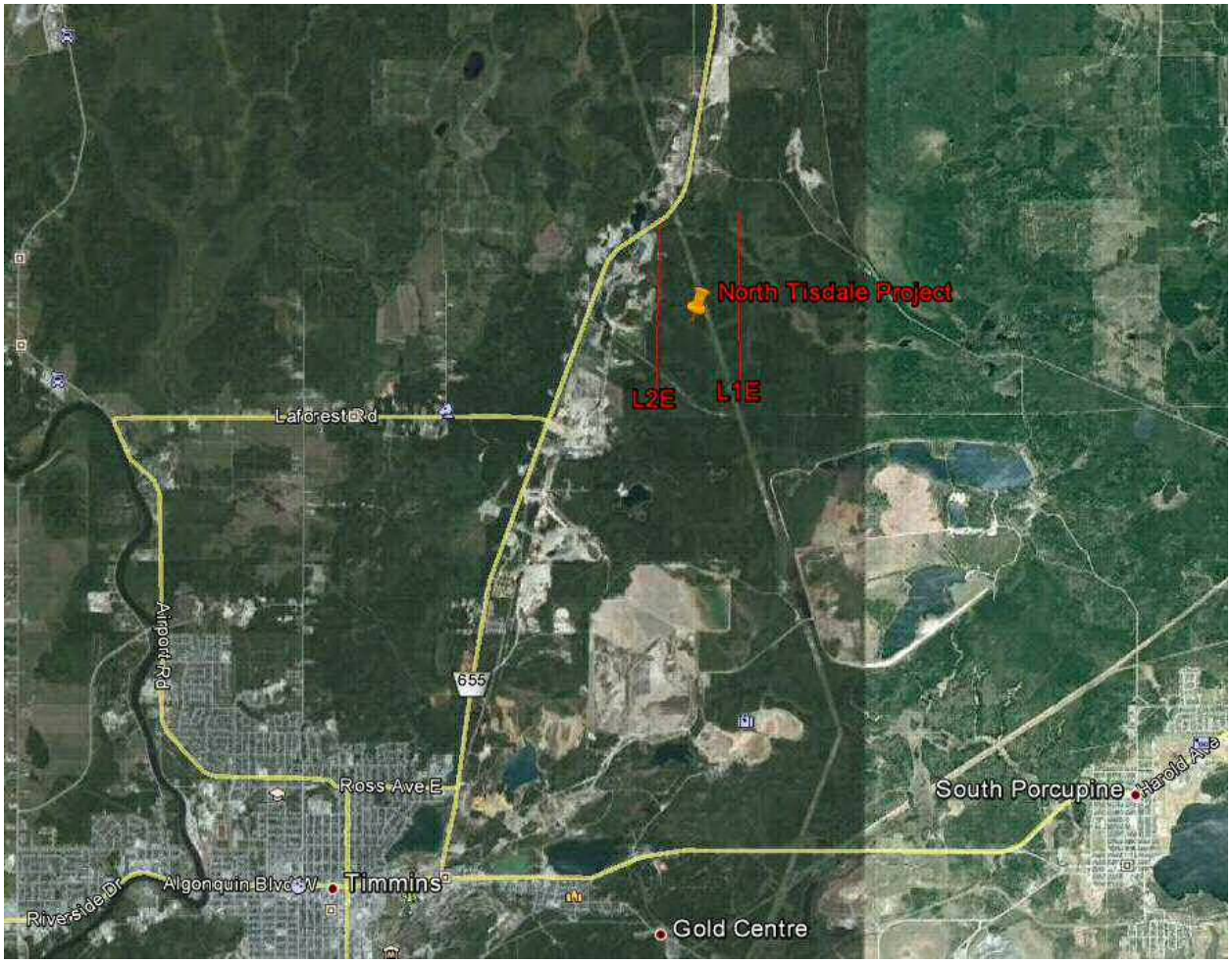

Figure 1-1: General Project Location[1].

[1] Image downloaded from Google Earth, Inset downloaded from Google Map, 2012/01/03.

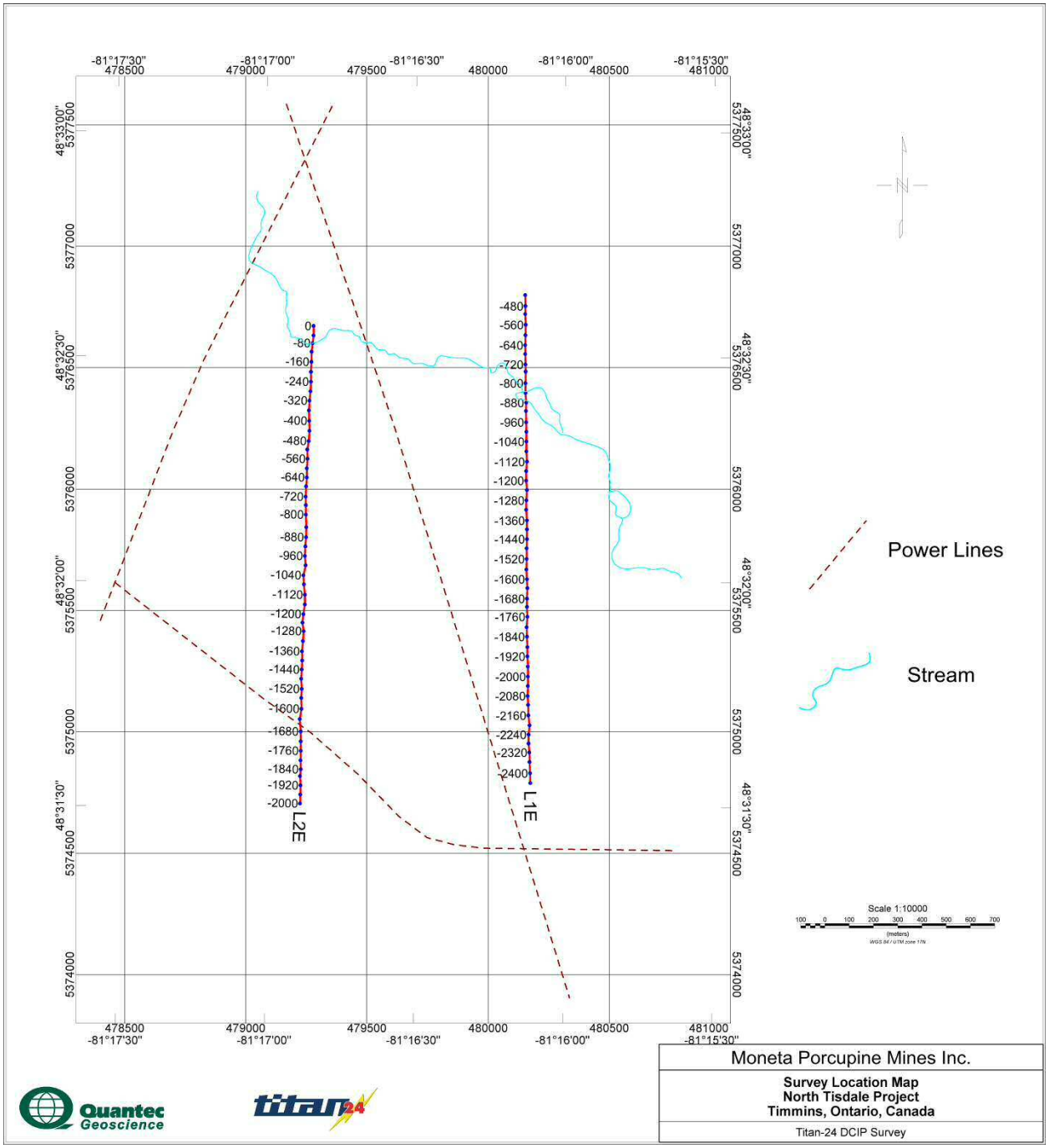

Figure 1-2: North Tisdale Project – Titan 24 Survey Lines and Approximate Power Line Location Map.

2 GEOLOGY[2]

The Property is underlain primarily by numerous east-westerly trending intercalated mafic and ultramafic volcanic flows and variably graphitic argillites and clastic sediments (Figure 2-1). Gold mineralization can be hosted in a variety of settings mainly within quartz-sulphide-carbonate stockwork zones occupying porphyry/mafic/ ultramafic/graphitic argillite contacts and/or structural zones. The primary target is considered to be the western extension of the Bell Creek-Owl Creek New Mine Trend setting believed to cross the central portion of the Property.

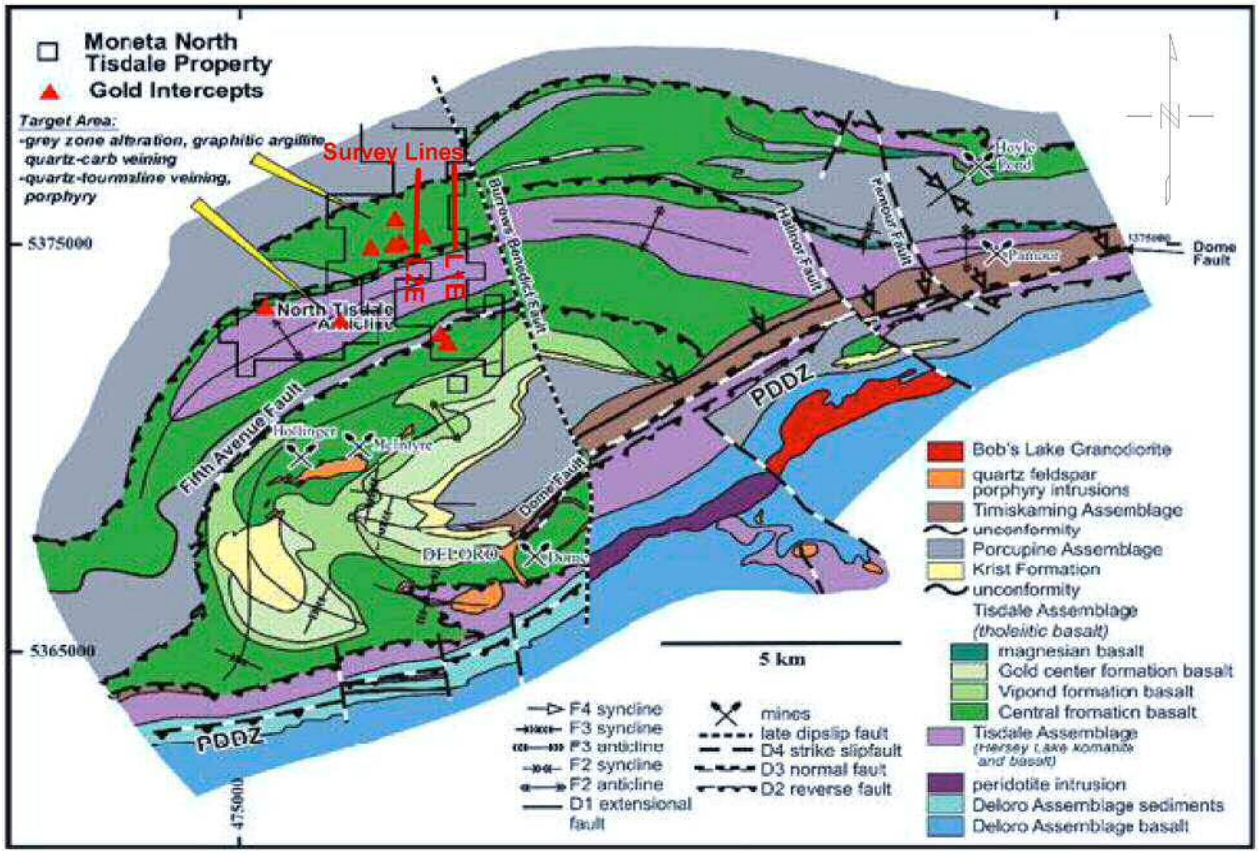

Figure 2-1: Approximate survey line locations superimposed on Regional Geology of the area

[2] After R. Bateman et al in Summary of Field Work and Other Activities 2004, Ontario Geological Survey, Open File Report 6145 and survey contract

3 RESULTS AND INTERPRETATION

This section presents the results of the 2D inversion of the Titan-24 data and interpretation in context with the survey objectives and significance to future exploration at North Tisdale Project.

The Titan-24 system acquires three types of geophysical data – magnetotelluric (MT), direct current resistivity (DC), and induced polarization (IP).

The MT and DC methods are used to resolve the resistivity distribution of the subsurface by measuring the electric potential (DC) and the variation of natural source electric and magnetic fields (MT). Resistivity can be an indicator of metallic mineralization, but is more often than not controlled by rock porosity and is therefore an indirect indicator of alteration and mineral grain fabric.

In the induced polarization method, electrical capacitance or chargeability of the subsurface is measured. Chargeability is a near-direct indicator of the presence of sulphide mineralization, in both massive and disseminated forms. Chargeable mineralization is most commonly various sulphides and graphite, but also includes clay-type minerals potentially making it a useful tool for base-metals exploration.

For each line surveyed, the DC-IP utilized a pole-dipole configuration with 80m dipoles with the current injection points located at every 80m between the potential dipoles along the lines. There was 440 m current extension at both the ends of each profile.

The MT utilized the same DC-IP dipoles, plus another set of 80m dipoles oriented perpendicular to the profile at every second site to acquire electric field data. One set of high-frequency and one set of low frequency magnetic sensors was used on the line. A remote site with the same magnetic sensor configuration was used to improve processing of the MT data.

Detailed information on the survey logistics, acquisition parameters and screen capture of the acquired data for the survey are provided in appendices at the end of this report.

The final inversion models are presented as cross-sections in Geosoft plot format along with an interpretation overlay and comments on the most significant results and recommended targets.

Detail results, i.e. observed DC-IP data and equivalent calculated responses for each model, are presented on a line per line basis in PowerPoint (or PDF) documents delivered in the digital archive (DVD) attached to this report.

3.1 OVERVIEW OF INVERSION PROCEDURE

3.1.1 DC RESISTIVITY & INDUCED POLARIZATION INVERSIONS

DC-IP is an electrical method that uses the injection of current and the measurement of voltage difference along with its rate of decay to determine the subsurface resistivity and chargeability, respectively. Depth of investigation is mainly controlled by the array geometry, but may also be limited by the received signal, which is dependent on transmitted current, and ground resistivity. The chargeability parameter is particularly susceptible to cases with a low signal-to-noise ratio.

In its standard configuration (a=100m / n=0.5-23.5) the Titan-24 surveys typically image DC resistivity to depths of 500-750m, and the IP typically images to 500-750m, in sub-vertical tabular geologic settings and up to 50% more for sub-horizontal. The differences in penetration are a function of the relative property contrasts and relative signal-to-noise levels between the two measurements. decreases or

increases proportionally to the dipole-size (i.e., 300-500m for 50m dipoles, and 1000-1500m for 200m dipoles). A detailed introduction to DC-IP is given in Telford, et al. (1976).

The primary tool for evaluating the Titan-24 data is through the inversion of the data. The goal of the inversion is to recover an earth model which acceptably reproduces field observed data. Two inverse problems have to be resolved. In the first, the DC potentials are used to recover the electrical conductivity σ, and for the second problem, the IP data are used to recover the chargeability η. An inversion model depends not only on the data collected, but also on the associated data errors in the reading and the "model norm". According to inversion theory, it is important not to fit the data precisely, as some noise contaminated data could lead to introduce inversion artefacts: Inversion models are not unique and may contain "artefacts" from the inversion process.

3.1.1.1 Data Pre-conditioning

For Titan-24 projects, the error of each data point is adjusted for the inversion process using a general error equation similar to:

$$errors\begin{pmatrix} Vp \\ IP \end{pmatrix} = \mathrm{A}\% \left| \begin{matrix} Vp \\ IP \end{matrix} \right| + B \times \mathrm{Acq\_Error} \begin{pmatrix} Vp \\ IP \end{pmatrix} + C\,(\mathrm{floor})$$

with the set of parameters $\{A, B, C\}$ adjusted (and large errors data points removed) for each dataset until we achieve convergence of the DC or IP models.

3.1.1.2 2D inversion

For Titan-24 projects, 2D inversions are carried out along each line to produce cross-sections of the resistivity and chargeability variations along the survey lines. The UBC ***DCIP2D*** (UBC-GIF) inversion suite[3] (Oldenburg & Li, 1994) is used for the 2D inversion of the DC and IP data:

1. DCINV2D: program to invert DC potentials to recover a 2D conductivity model.
2. IPINV2D: program to invert IP data to recover a 2D chargeability model.

The programs use the potential difference (voltage) and phase values as input data. Estimated errors (see §3.1.1.1) on the DC resistivity and induced polarization (IP) data are included in the inversion.

The DC data is inverted using an unconstrained 2D inversion with a homogenous half-space of average input data as starting model. The DC models are labelled as *smDC*. Two IP inversions are calculated from the same data set and parameters, but they use a different reference model[4]. The first inversion of the IP data uses the previously calculated DC model as the reference model, and is labelled the *IP_dcref* model. The second IP inversion uses a homogeneous half-space resistivity model as the reference model and is labelled IP_*hsref* model. This model is included to test the validity of chargeability anomalies, and to limit the possibility of inversion artefacts in the IP model due to the use of the DC model as a reference.

In general, the use of the DC reference IP model is considered better, but some feature on the DC model

[3] A comprehensive theory and methodology for 2D inversions for those programs is also available at www.eos.ubc.ca/ubcgif.
[4] The reference model is used to calculate the sensitivity matrix used at each iteration for the IP inversion.

might introduce 'artefacts or false anomalies' on the IP models. For example, we found the UBC code tends to add very strong IP anomaly below a very conductive overburden, while not really supported by the data: that appears just because of the strong resistivity contrast on the DC model. The HS reference IP model is not 'constraint' by any pre-defined (DC) structure, and then can be used to validate chargeability anomalies. If an anomaly is observed on the *IP_dcref* and the *IP_hsref* models, then we can be confident on the results. On the other side, if the results vary a lot between the two inversions, then the results appears to be more 'depend' on the DC reference model than the data itself, and so we can be less confident on the results.

The DC and IP inversion use the same mesh. The horizontal mesh is set as 3 cells between electrodes. The vertical mesh is designed with a cell thickness from 10 to 15m for the first hundred's metres to accommodate the topographic variation along the profile, and then it increases from 20 to 100m with depth. The inversions were generally run for a maximum of 50 iterations.

3.1.2 AUDIO-MAGNETOTELLURIC INVERSIONS

The Audio-Magnetotelluric (AMT) method is a natural source method that measures the variation of both the electric (E) and magnetic (H) field on the surface of the earth in order to determine the distribution at depth of the resistivity of the underlying rocks. A complete review of the method is presented in Vozoff (1972) and Orange (1989).

The measured MT impedance Z, defined by the ratio between the E and H fields, is a tensor of complex numbers. This tensor is generally represented by its two off-diagonal elements. In a 1D earth model, i.e. the resistivity varies only with depth, there is no strike direction and the two off-diagonal impedances are equal. In the 2D case, i.e. when the resistivity varies with depth and perpendicularly to the strike, and when the profile is set perpendicular to the strike direction, the two off-diagonal elements are not equal but reflect the variation of the resistivity along two directions, one parallel and the other perpendicular to the strike, i.e., the TE (Transverse Electric; E parallel to the strike) and the TM (Transverse Magnetic; E perpendicular to the strike) modes.

Both TE and TM impedances are represented by an apparent resistivity (a parameter proportional to the modulus of Z) and a phase (argument of Z). The variation of those parameters with frequency relates the variations of the resistivity with depth, the high frequencies sampling the sub-surface and the low frequencies the deeper part of the earth. However the apparent resistivity and the phase have an opposite behaviour. An increase of the phase indicates a more conductive zone than the host rocks, and is associated with a decrease of the apparent resistivity. The objective of the inversion of MT data is to compute a distribution of the resistivity of the surface that explains the variations of the MT parameters, i.e. the response of the model that fits the observed data. The solution however is not unique and different inversions must be performed (different programs, different conditions) in order to test and compare solutions for artefacts versus a target anomaly.

The depth of investigation is determined primarily by the frequency content of the measurement. Depth estimates from any individual sounding may easily exceed 20 km. However, the data can only be confidently interpreted when the aperture of the array is comparable to the depth of investigation.

The primary tool for evaluating the Titan MT data is 2D inversion. The inversion model is dependent on the data, but also on the associated data errors, and the model norm. The inversion models are not unique, may contain artefacts of the inversion process, and may not therefore accurately reflect all of the information apparent in the actual data. Inversion models need to be reviewed in context of the observed data, model fit, an understanding of the model norm used and if the model is geologically plausible.

For this study, 2D inversions were performed using the un-rotated data, which assumes the strike direction is perpendicular to the profile for all sites: the TM mode is then defined by the inline E-field (and cross line H-field), and the TE mode is defined by the cross line E-field (and inline H-field) data.

The MT models were calculated with the PWm code (development Quantec Geoscience; based on deLugao and Wannamaker, 1996). The inversions use the TE and TM resistivity and phase from 10 kHz to 0.1 Hz, interpolated at 6 frequencies per decade, and assume 2% error for the resistivity and 2 degrees error for the phase data.

The PWm inversion model (puth4) was derived from inverting the TE and TM apparent resistivity and phase MT data starting from a half space model of 100 Ohm-m. All the 2D inversions incorporate topography in the inversion process. This is essential in harsh terrain to accurately reproduce the subsurface anomalies with least geometrical distortions.

3.2 DISCUSSION OF RESULTS

This section presents and discusses the significant geophysical anomalies and potential targets interpreted from the final Titan-24 DC and IP inversion models.

The DC, IP and MT 2D inversions were completed along each line. Topography data along the survey line was incorporated in the inversion process in the MT, DC and IP models. In survey area, major power lines run sub-parallel to the survey lines (Figure 1-2) and data were affected by power line interferences. To reduce the effects of power lines the following tests were completed.

a. DC and IP data were inverted using UBC ***DCIP2D*** (UBC-GIF) inversion suite with different error conditioning and rejecting high error data points.

b. Pole-Dipole (PLDP) data were transformed to Dipole-Dipole (DPDP) configuration data in order to reduce the array asymmetry effects. This will help to localize the power lines interference and artefacts in inversion.

c. A set of inversions using Loke inversion code was conducted to compare with the UBC inversion results and are presented in the Appendix J.

The MT data are also noisy and phase wrapping is observed at many sites. It could be due to power line interference or extreme subsurface heterogeneity. When preparing MT data for inversions, 1D inversion model response was used to determine phase data for sites with phase wraps.

The results of the 2D inversion along each line are illustrated and the observed anomalous features are described. All sections and plan maps use a consistent and constant colour bar. The colour bars used in this interpretation are as illustrated in Figure 3-1.

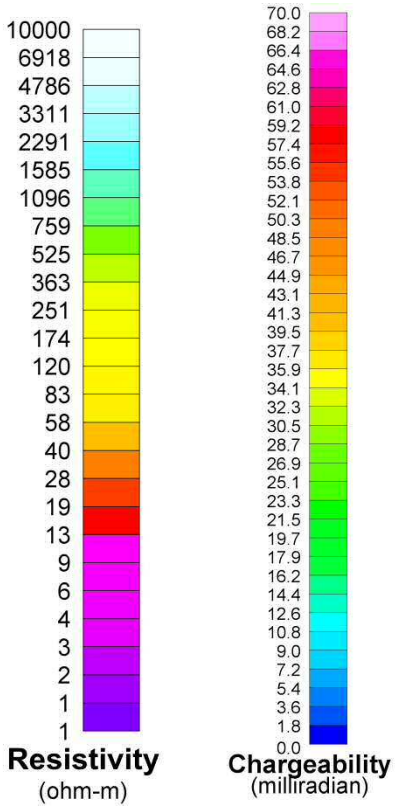

Figure 3-1. Interpretation colour bars.

Note that all of the cross-sections and plan maps are also available in Geosoft digital format and can be found in the Geosoft folder in digital archive attached to this report.

3.2.1 LINE L1E

Line L1E is the eastern N-S oriented line in the North Tisdale project. The line is a Pole-Dipole (PLDP) single spread, 2 km long profile with 80 m dipole spacing. Note that the receiver electrodes extend from station -2440 in the south to station -440 in the north.

The results of the 2D inversions of the PLDP DC data, the transformed DPDP DC data, and the MT data are displayed in Figure 3-2. The results of PLDP IP data using DC reference and half-space reference along line L1E are displayed in Figure 3-3. Also, the 2D inversions of transformed Dipole-Dipole (DPDP) IP data using DC reference and half-space reference are presented in Figure 3-4.

In DC and MT resistivity models, two conspicuous conductive anomalies with resistivity as low as 50 Ωm are observed in a resistive background (~5000 Ωm) in the southern (L1E_DC1/MT1) and northern (L1E_DC2/MT2/MT3) parts of the survey line.

The anomaly L1E_DC1 is a subvertical conductive feature resolved at station -1920. The anomaly is observed from ~75 m depth and extends to more than 600 m in depth with increases in lateral extents. In the MT model, anomaly L1E_MT1 corresponding with the location of anomaly L1E_DC1 in the DC model. The anomaly is observed from near the surface and extends down to -1300 m in depth.

In the northern part of the survey line anomaly L1E_DC2 is observed at station -800 as a subvertical conductive structure. The anomaly nearly crops out to the surface and extends down to more than 400 m in depth. In the MT resistivity model, the MT anomaly L1E_MT2 corresponds with the location of the DC anomaly L1E_DC2. The anomaly displays a resistivity variation with depth (L1E_MT3).

A near surface conductive layer with resistivity of ~300 Ωm and thickness of ~30 m is found nearly throughout the entire line L1E. The thickness of surface conductive layer displays increase in the southern part of the line (L1E_MT6).

In the central part of the MT inversion model, moderately conductive anomalies L1E_MT4 and L1E_MT5 with resistivity of ~300 Ωm are observed and appear to merge with the conductive surface layer. These anomalies are observed as minor variations in contour plot in the DC models, therefore this observation should be treated with care.

In the southern part of the survey line, the chargeability models display an elevated chargeable feature with a chargeability of ~55 mrads (L1E_IP1). The location of the chargeability structure partially corresponds with the conductive anomalies L1E_DC1 and L1E_MT1. This chargeability anomaly is resolved with different geometry in the PLDP half space reference model and the DC reference model. This anomaly is resolved in both PLDP and transformed DPDP IP inversion models; however with different depth extent. Therefore the depth extension of this anomaly must be treated with care.

The chargeability models display another IP anomaly, L1E_IP2, with chargeability of ~55 mrads in the northern part of the line, beneath station -800 at 150 m in depth. The anomaly appears to extend towards north. The shape of this anomaly varies in different chargeability models but the central part of the anomaly is reproduced in all models and is corresponding with the conductive anomaly L1E_DC2.

In the central part of the survey line shallow low chargeable (~ 12 mrads) zone is resolved in half space reference IP inversion models (L1E_IP3). This anomaly is poorly defined in the DC reference IP models as

it overlaps with anomalies L1E_IP1 and L1E_IP4.

A deep chargeability anomaly, L1E_IP4, is resolved in PLDP IP inversion models only. This anomaly is likely an inversion artefact caused by PLDP array asymmetry and should be treated with caution.

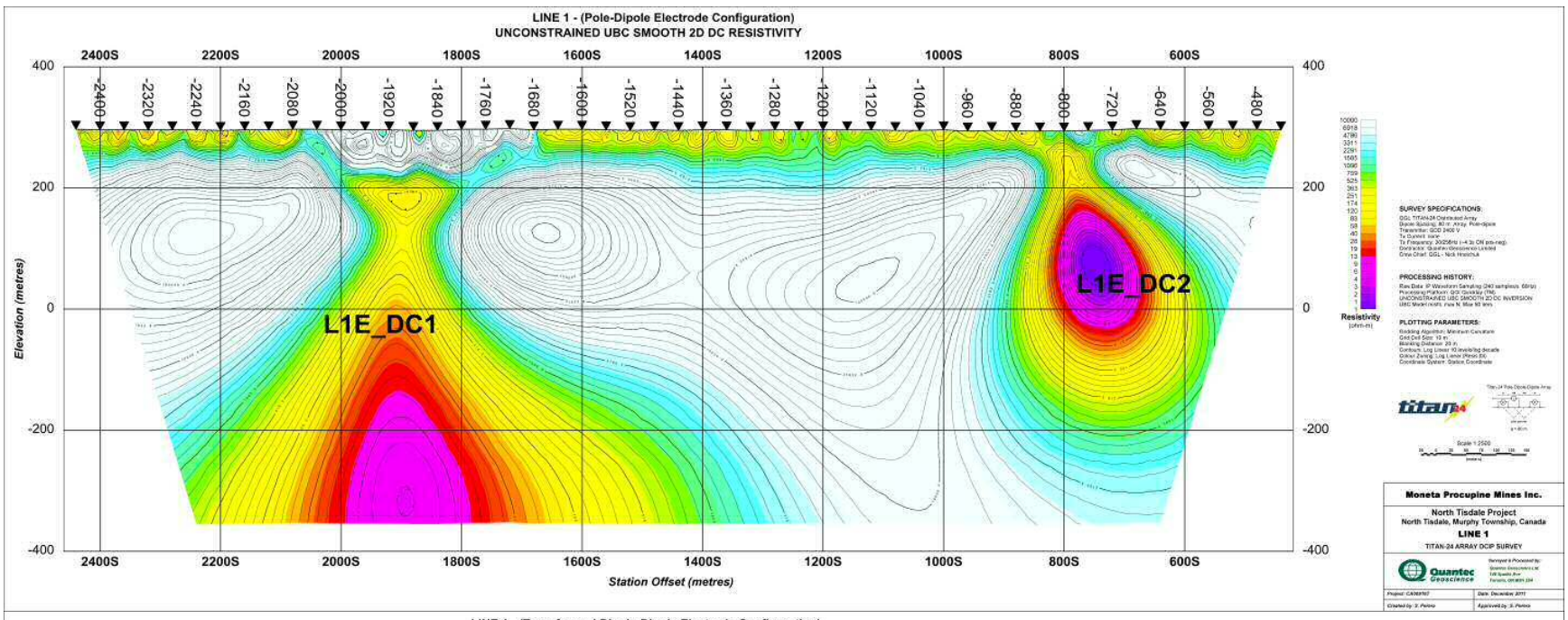

Figure 3-2.Results of the 2D inversion of PLDP DC data (top), transformed DPDP DC data (middle), MT data (bottom) along line L1E.

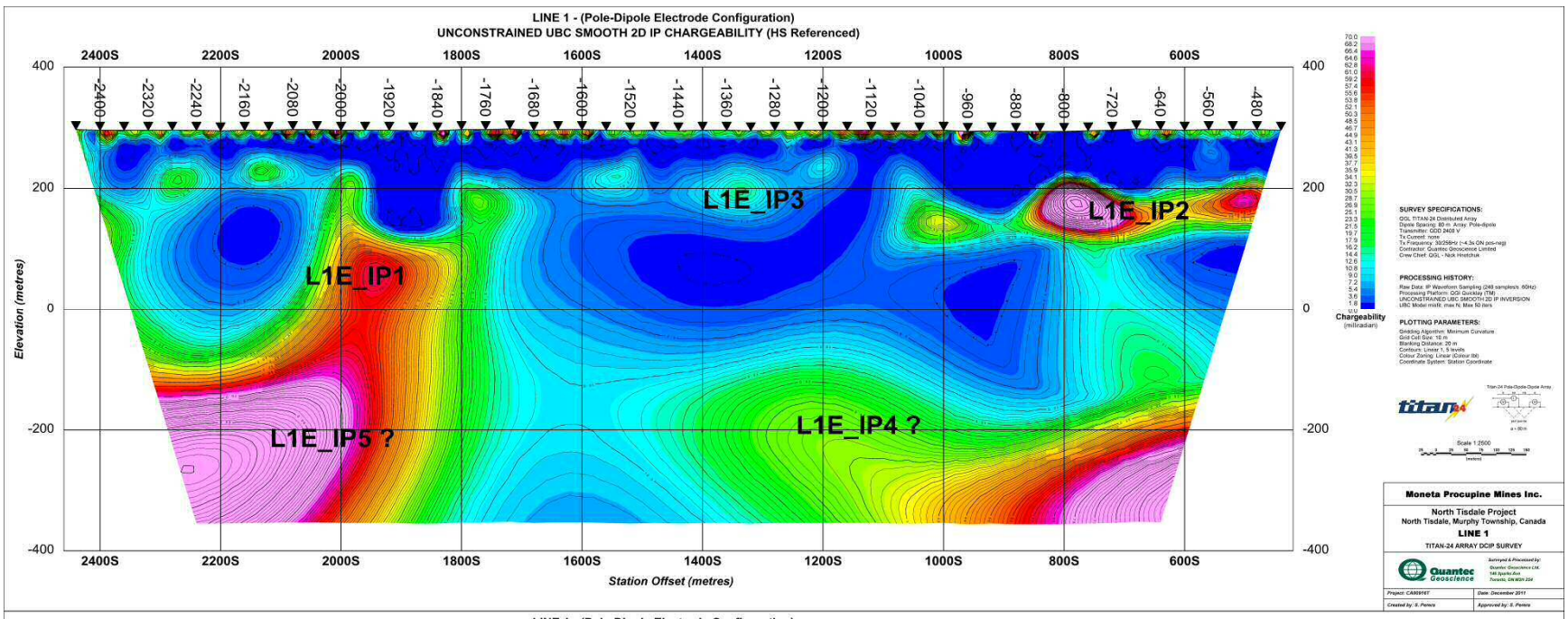

Figure 3-3.Results of the 2D inversion of PLDP IP data using half-space reference (top) and DC reference (bottom) along line L1E .

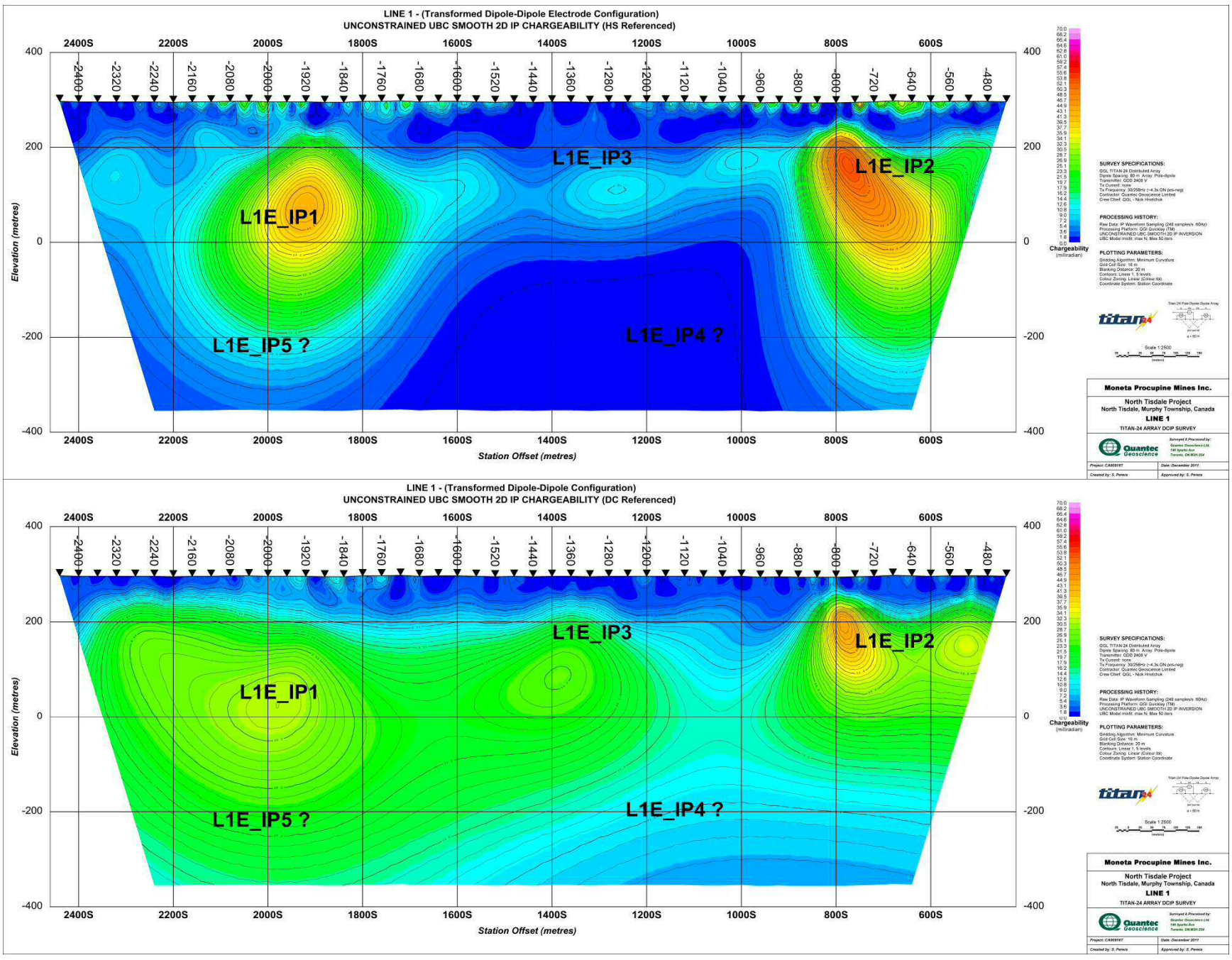

Figure 3-4.Results of the 2D inversion of transformed DPDP IP data using half-space reference (top) and DC reference (bottom) along line L1E .

3.2.2 LINE L2E

Line L2E is the western N-S oriented survey line located ~900 m west to the line L1E in the North Tisdale project. Line 2E is a Pole-Dipole electrode configuration single spread with 80 m dipole spacing. It is 2 km long profile with the receiver electrodes extend from station -2000 in the south to station 0 in the north. A set of power lines intersect the profile approximately at station -1680. The power line, however, was reported as inactive.

The results of the 2D inversions of the PLDP DC data, transformed DPDP DC data, and MT data are displayed in Figure 3-5. The results of PLDP IP data using DC reference and half-space reference along line L2E are displayed in Figure 3-6. Also, the 2D inversions of transformed Dipole-Dipole (DPDP) IP data using DC reference and half-space reference are presented in Figure 3-7.

Similar to the line L1E, two well defined sub-vertical conductive anomalies, L2E_DC1/MT1 and L2E_DC2/MT2, are resolved in a resistive background with a resistivity of ~ 5000 Ωm, in the southern and northern parts of the survey line, respectively.

Anomaly L2E_DC1 appears to be highly conductive with resistivity of less than 5 Ωm. The anomaly is observed nearly from the surface and extends down to ~600 m in depth. The MT model displays a corresponding anomaly, L2E_MT1, with similar characteristics but extends to more than 1 km in depth. Note that the conductive anomaly L2E_DC1/MT1 is resolved nearly where the power line intersects the profile at station -1680.

Another conductive anomaly, L2E_DC2, with a resistivity of ~50 Ωm is observed from near the surface and extends to great depths. The MT model displays similar conductive anomaly with resistivity ~100 Ωm, L2E_MT2, gently dipping southwards.

A thin surface conductive layer with resistivity of ~ 300 Ωm is observed, evidently in the southern half of the profile. MT anomalies L2E_MT3 and L2E_MT5 are resolved close to the surface at ~ 100 m depth and appear to merge with the conductive surface layer.

An isolated conductive anomaly, L2E_MT4, observed in the MT resistivity model is not reproduced in the DC resistivity model and cannot be confirmed.

The IP models display four anomalous zones along the survey line. The amplitude and geometry of the anomalies are resolved slightly differently in the IP models using half-space and DC reference. In the southern part of the profile IP anomaly L2E_IP1 with chargeability of ~50 mrads is resolved at station -1680. The anomaly is observed from ~50 m in depth and extends to depth of ~250 m. This chargeability anomaly corresponds to the location of the conductive anomaly L2E_DC1.

Further to the north, chargeable anomaly L2E_IP3 is resolved as northern extension of anomaly L2E_IP1. The location of the anomaly corresponds with the MT anomaly L2E_MT5.

In the northern part of the line, a moderate chargeable IP anomaly L2E_IP2 with chargeability ~ 30 mrads is observed. The anomaly extends from ~ 100m in depth to about 500 m in depth. This anomaly corresponds to the conductive anomaly L2E_DC2/MT2.

A low chargeable IP anomaly, L2E_IP4, is observed in a resistive background in the central part of the profile and merges with surrounding chargeable anomalies.

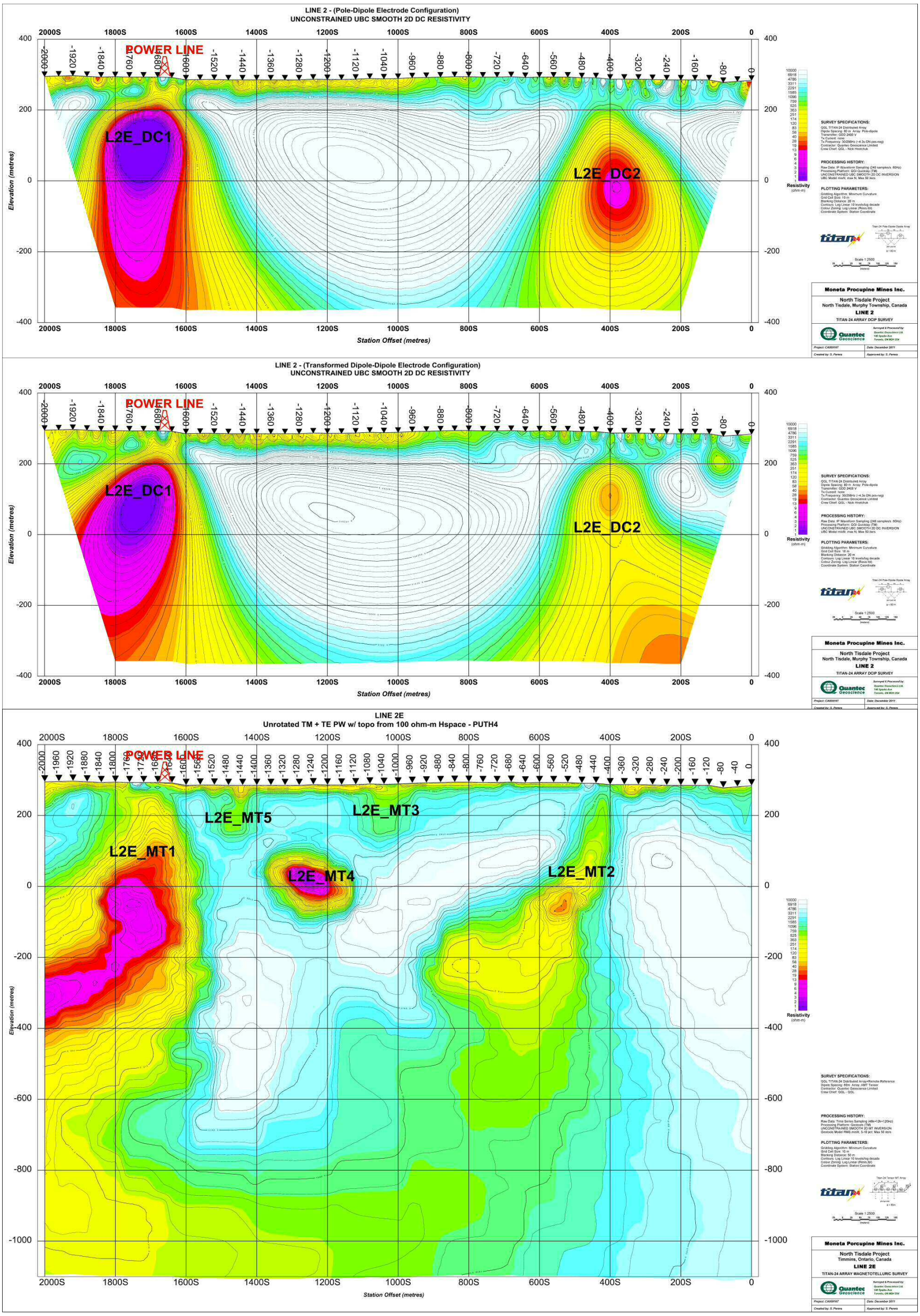

Figure 3-5.Results of the 2D inversion of PLDP DC data (top), transformed DPDP DC data (middle), MT data (bottom) along line L2E.

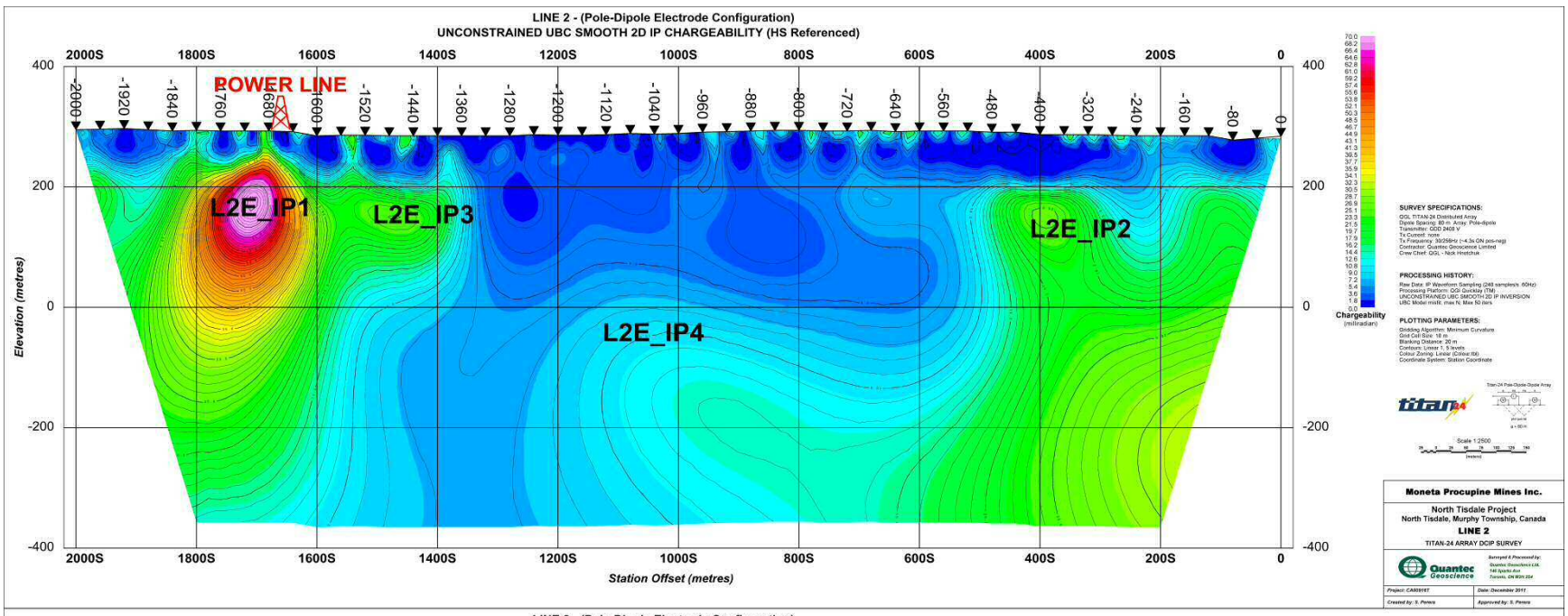

Figure 3-6.Results of the 2D inversion of PLDP DC data (top),IP data using half-space reference (middle) and DC reference (bottom) along line L2E .

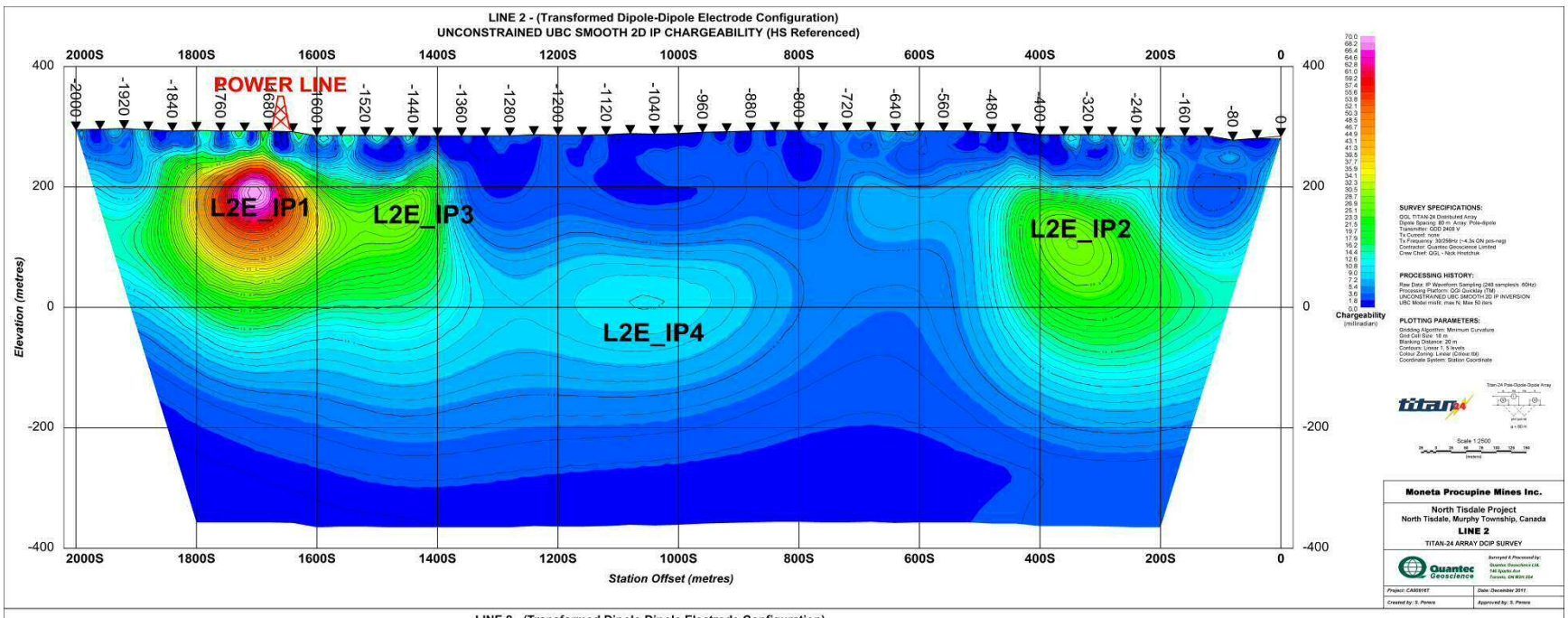

Figure 3-7.Results of the 2D inversion of transformed DPDP DC data (top),IP data using half-space reference (middle) and DC reference (bottom) along line L2E.

4 CONCLUSIONS AND RECOMMENDATIONS

This report presents the logistics and the results of the analysis of the Titan-24 DC, IP and MT data acquired over the North Tisdale Project, on behalf of Moneta Porcupine Mines Inc..

Data were acquired over 2 DC/IP/MT spreads along 2 survey lines with 80 m station interval. Two survey lines are ~900 m apart in N-S direction. A total of 4.0 km DC/IP survey line (5.6 km with current extensions) and 4 km of MT survey line were surveyed. A pole-dipole configuration was used for DC and IP measurements.

There are major power lines sub-parallel and crossing the survey lines . To reduce the possible effects of the power lines in the inversions, the data were conditioned using different error levels. Also, Pole-Dipole (PLDP) data were transformed into Dipole-Dipole (DPDP) configuration data in order to reduce array asymmetry effects. Additionally, a set of Loke's2D inversions was carried out and the results were compared with the UBC inversion results.

The DC, IP and MT inversions display two discrete conductive and chargeable anomalies in the southern (L1E_DC1/MT1, L2E_DC1/MT1 and L1E_IP1, L2E_IP1) and northern (L1E_DC2/MT2, L2E_DC2/MT2 and L1E_IP2, L2E_IP2) parts of the survey lines. Conductive anomalies with resistivity of 1-100 Ωm is observed within a highly resistive background with a resistivity of ~5000 Ωm. The IP anomalies show chargeability of 30 mrads to 70 mrads. The anomalies in the southern part of line L2E, (L2E_DC1/MT1 and L2E_IP1) are located where a power line intersects the survey line (Figure 4-1). However, the southern power line is not active (communication with the client) and therefore this anomaly is considered as a legitimate target. Also, Available geological information indicates that the conductive and chargeable anomalies observed in the southern part could be associated with the lithological contact between mafic volcanic and locally interbedded graphitic and pyritic argillite[5].The regional geological map (Figure 4-2) displays a fault zone crossing the southern part of the survey lines and that partially corresponding with the resolved anomalies.

According to the geologic map, the DC, MT and IP anomalies resolved in the northern part of the survey lines, L1E_DC2/MT2, L2E_DC2/MT2, L1E_IP2 and L2E_IP2, are appeared to be associated with the NEE-SWW striking lithological contact between mafic volcanic and greywacke. A fault zone is also observed in the northern parts of survey area in the regional geological map that is associated with the northern anomalies. The anomalies L1E_DC2 and L1E_IP2 are located near the intersection of line L1E and a surface stream. Therefore, the anomalies could be associated with a structural feature such as a fault or dike in this area.

Aeromagnetic map[6] of the first vertical derivative of the total magnetic field demonstrates a NEE-SWW oriented curvilinear magnetic signature in the southern and northern parts of the survey area (Figure 4-3). It could indicate the lithological contacts or faults in this area.

A thin surface conductive layer is observed in the area. In MT model, shallow moderately conductive areas with a resistivity of ~500 Ωm (L1E_MT5/MT6 and L2E_MT3/MT5) are merged with the conductive surface layer. Moderately chargeable IP anomalies L1E_IP3, L2E_IP3 and L2E_IP4 are resolved in the central part of the survey lines. However, no corresponding DC resistivity anomalies are observed. These IP Chargeability anomalies could associate with structural features with no conductive material.

[5] Detailed lithological boundaries provided by the client
[6] Downloaded from Geosoft DAP server

For completeness of the discussion, Figure 4-5 through Figure 4-8 display the resistivity and chargeability cross-sections superimposed by the gold grades data determined by the drilling and core samples in the survey area[7]. A good correlation is observed between the high conductivity and/or chargeability zones and high gold grade in the borehole logs.

[7] Borehole information provided by the client.

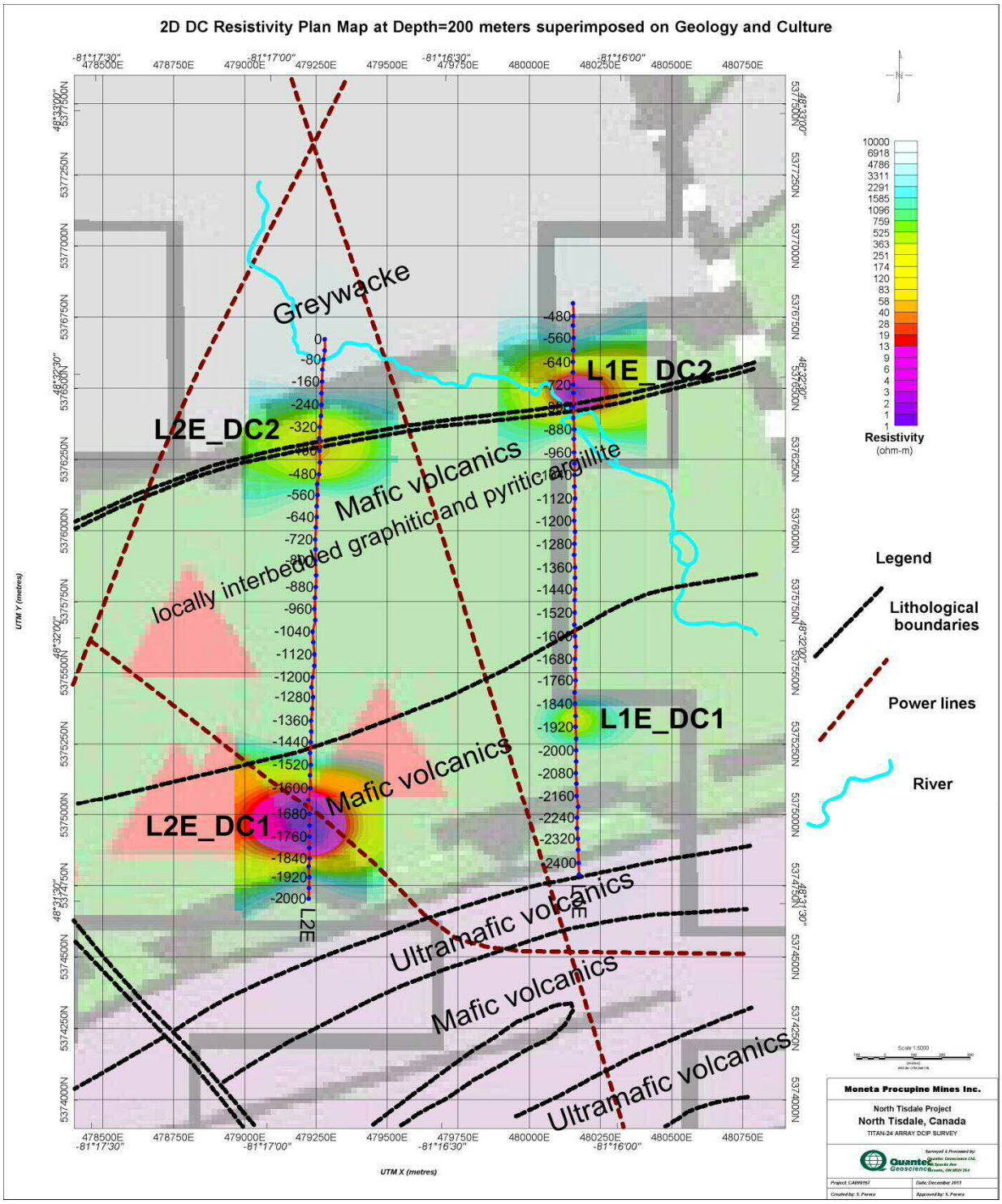

Figure 4-1.2D DC resistivity plan map at 200m depth superimposed on approximate lithological contacts and culture (Detailed lithological boundaries provided by the client and the regional geology from R. Bateman et al in Summary of Field Work and Other Activities 2004, Ontario Geological Survey, Open File Report 6145 and survey contract).

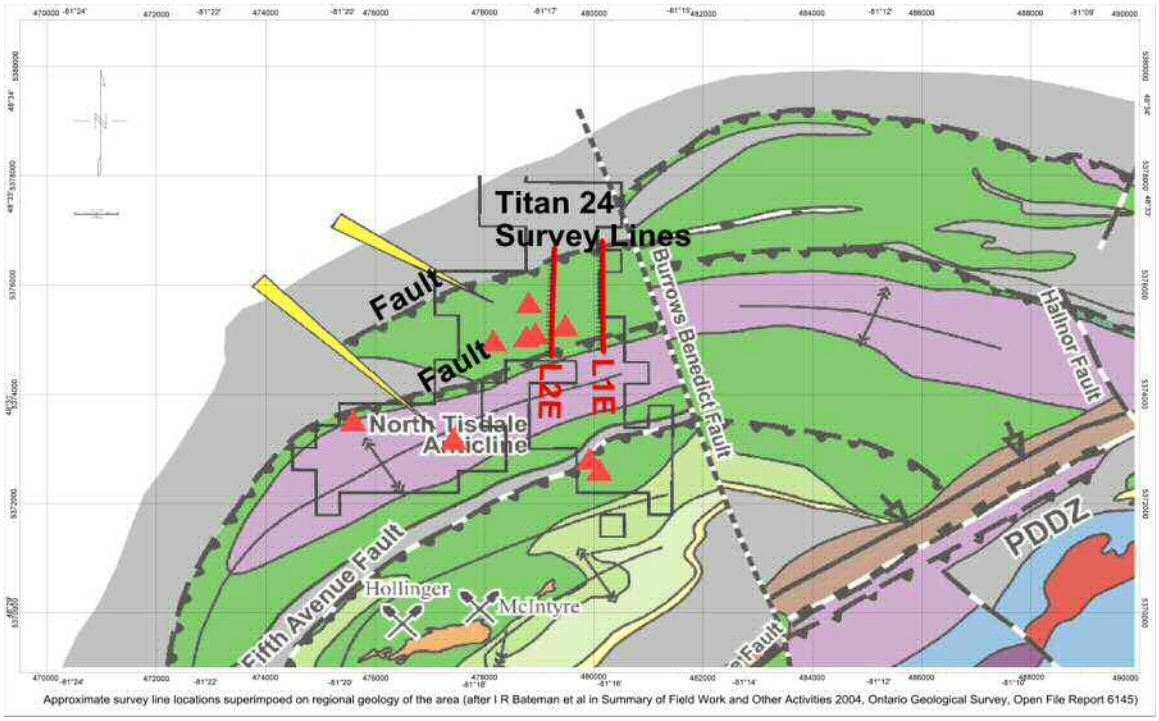

Figure 4-2. Approximate survey line locations superimposed on the regional Geology. Note two NEE-SWW faults offset northern and southern parts of survey lines (Geology map from R. Bateman et al in Summary of Field Work and Other Activities 2004, Ontario Geological Survey, Open File Report 6145 & survey contract)

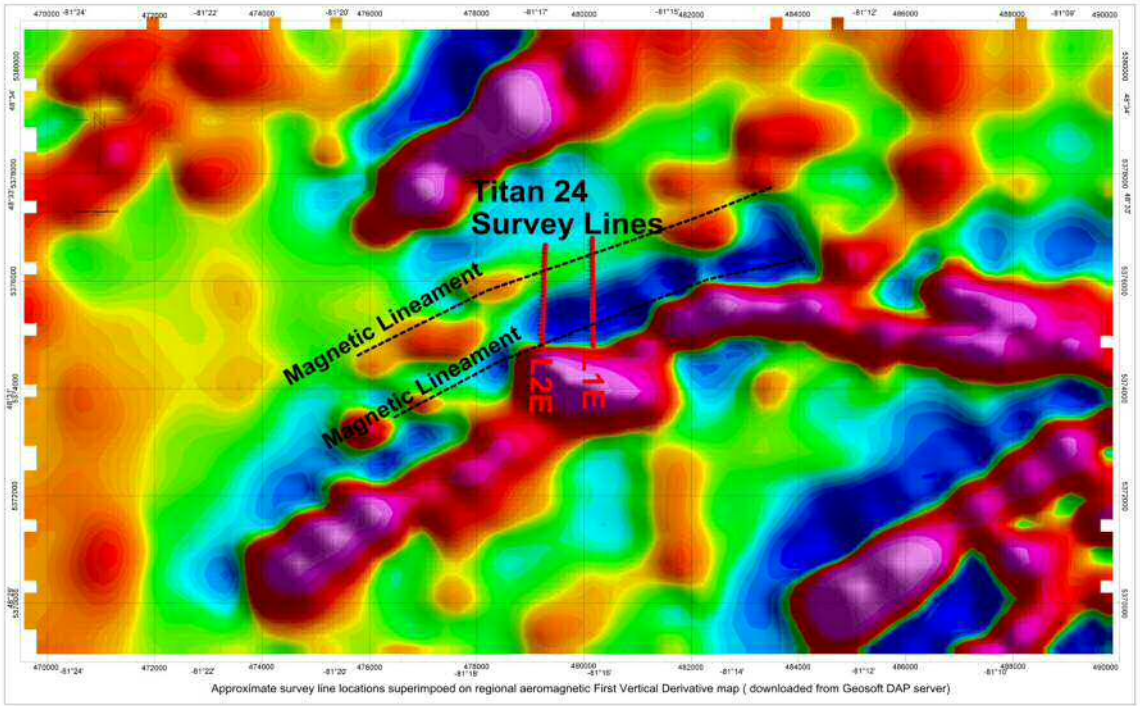

Figure 4-3. Approximate survey line locations superimposed on the regional aeromagnetic 1st vertical derivative map. (downloaded from Geosoft DAP server)

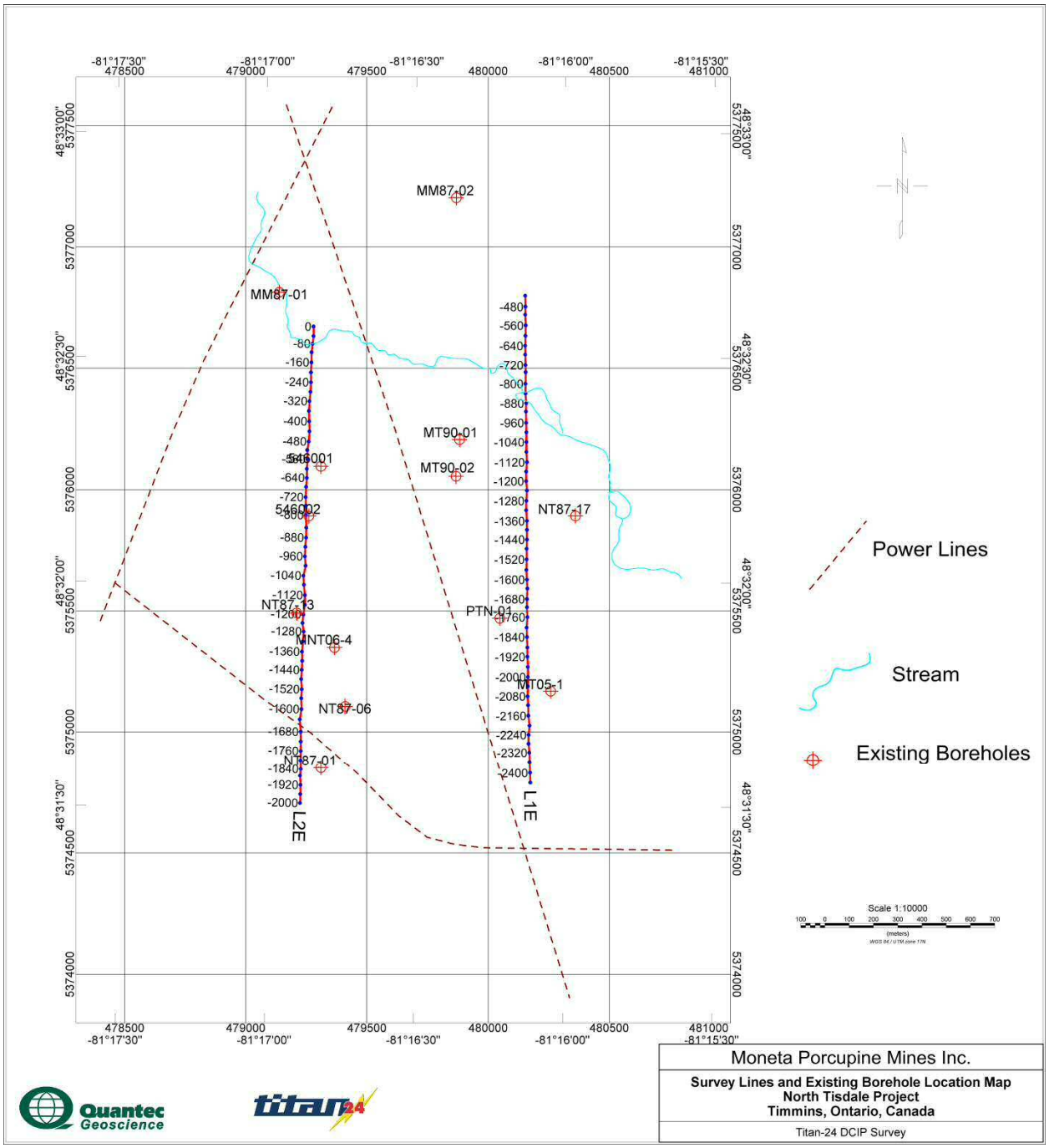

Figure 4-4. Survey lines and existing borehole Locations. (Borehole information provided by the client)

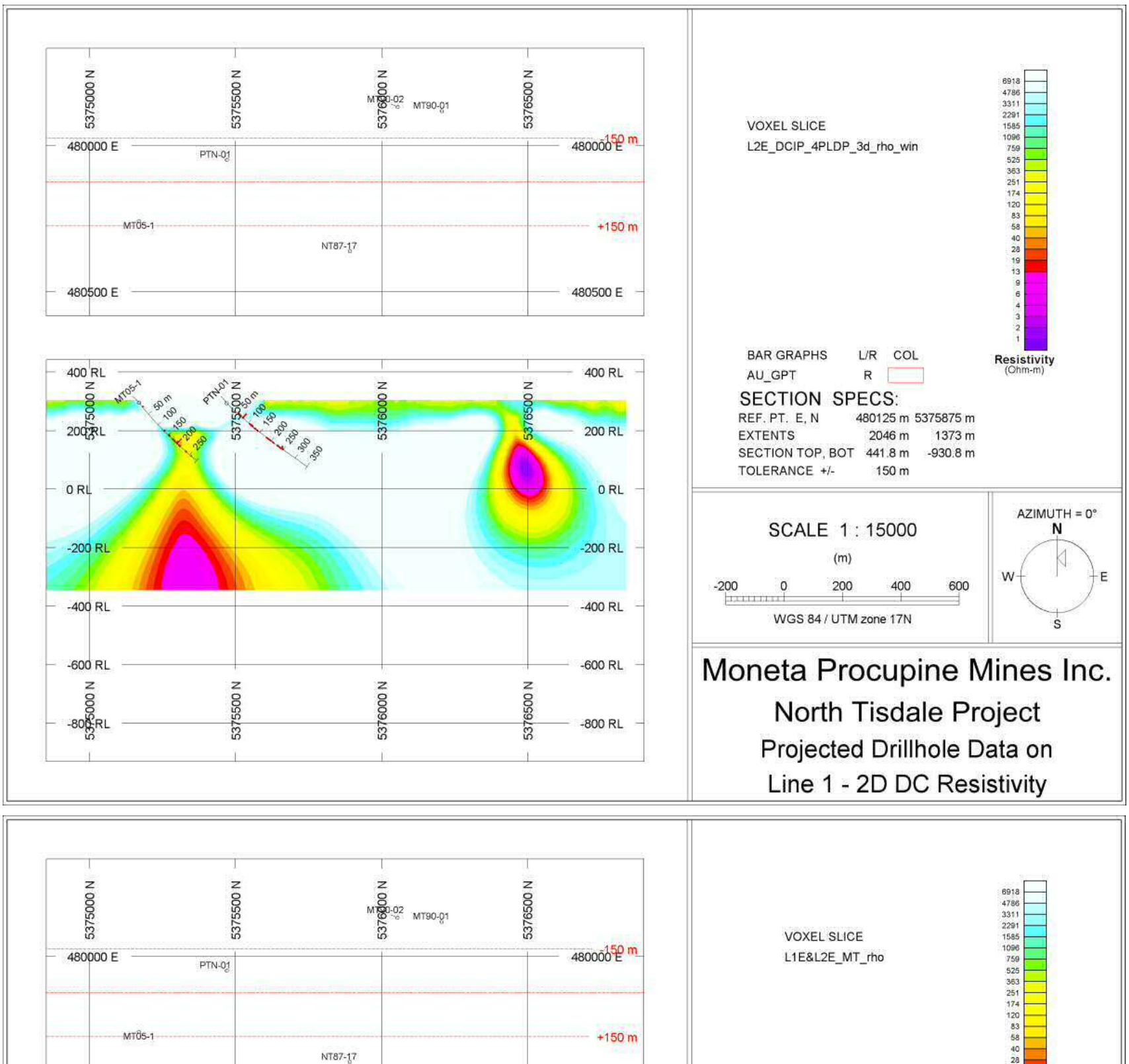

Figure 4-5. Line L1E -DC Resistivity inversion model superimposed on drillhole information (Above) and MT Resistivity inversion model superimposed on drillhole information (Below). Tolerance +/-150m from the survey line.

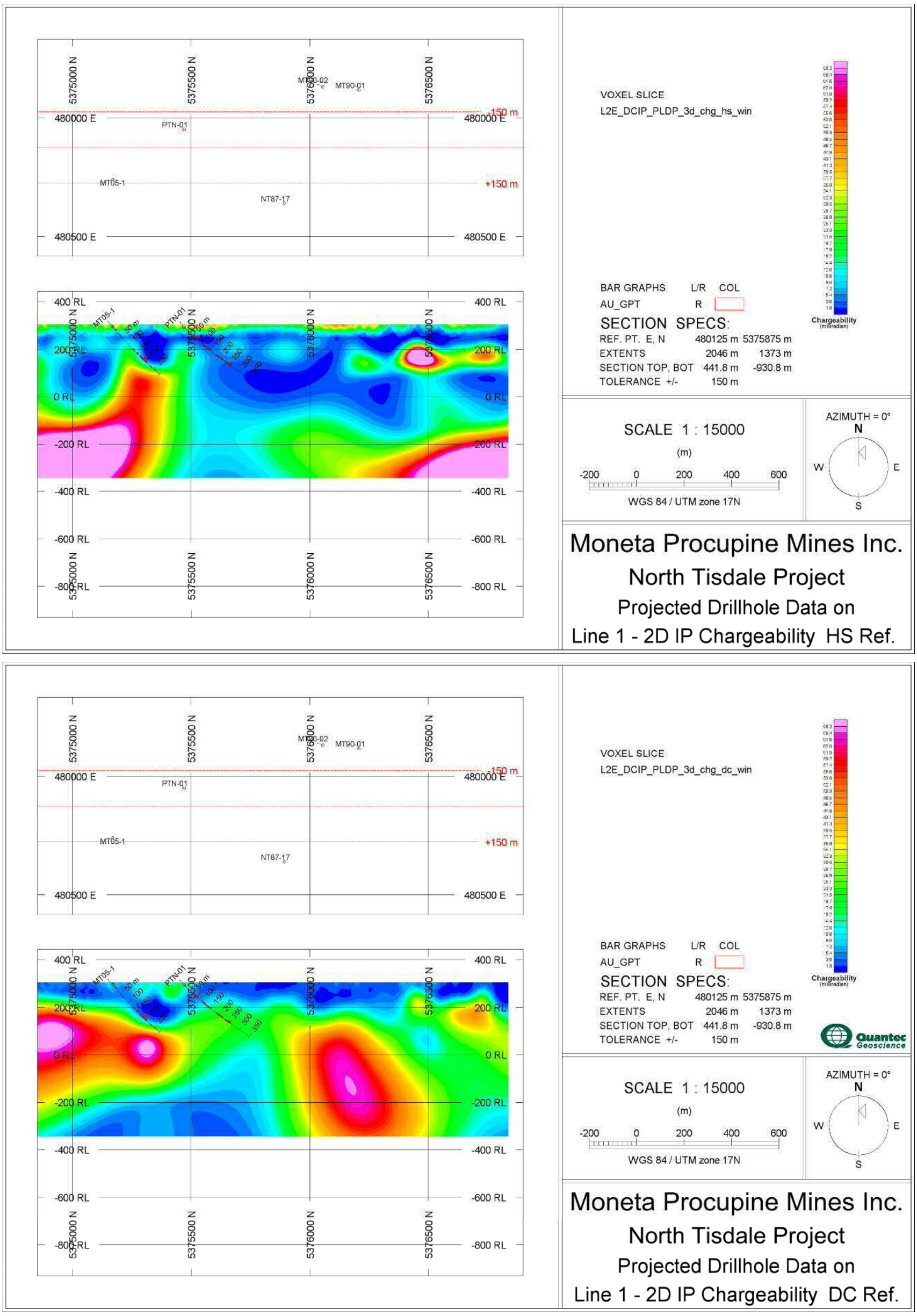

Figure 4-6. Line L1E – IP Chargeability (Half Space referenced) inversion model superimposed on drillhole information (Above) and IP Chargeability (DC referenced) inversion model superimposed on drillhole information (Below). Tolerance +/-150m from the survey line.

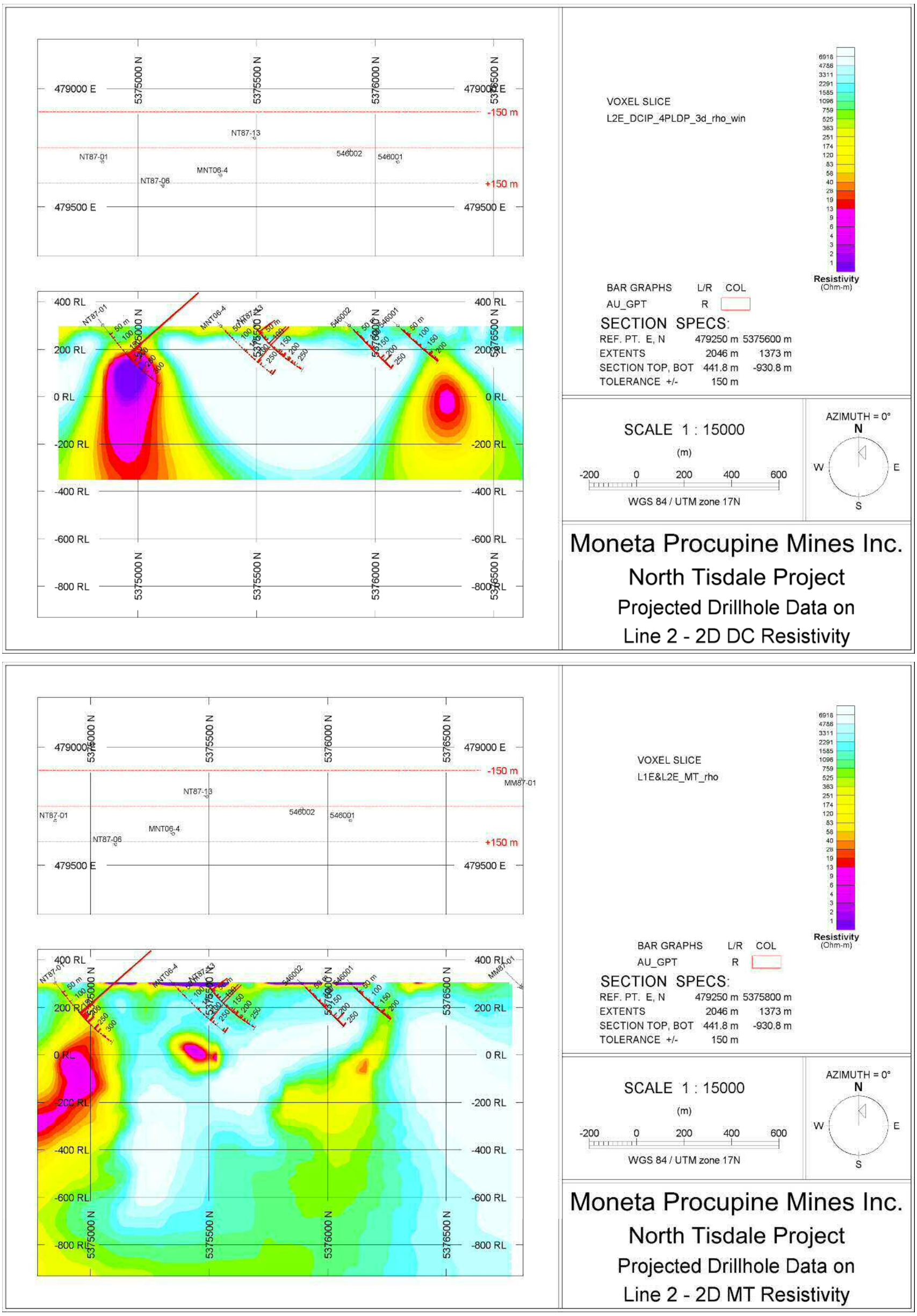

Figure 4-7. Line L2E -DC Resistivity inversion model superimposed on drillhole information (Above) and MT Resistivity inversion model superimposed on drillhole information (Below). Tolerance +/-150m from the survey line.

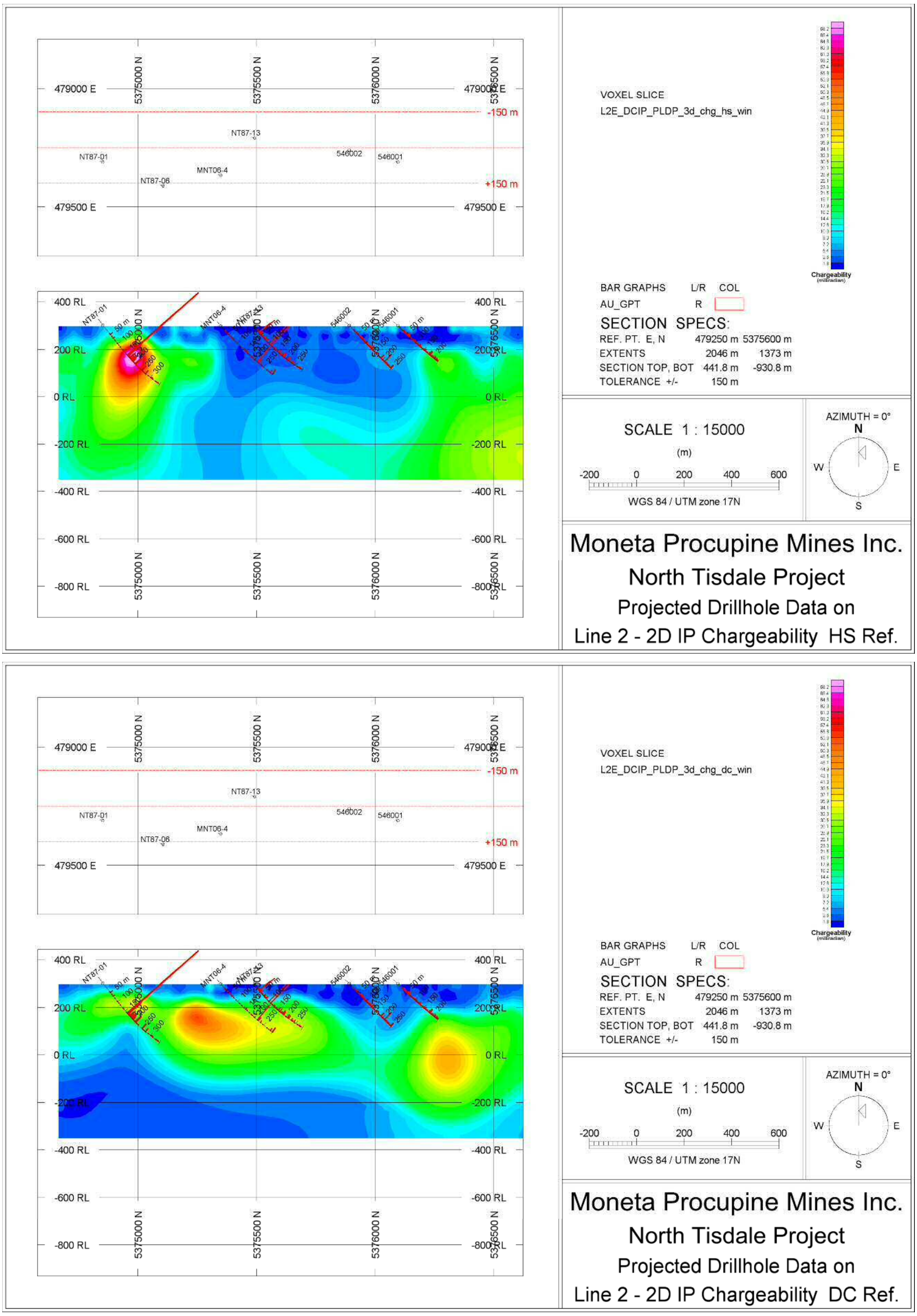

Figure 4-8. Line 2 – IP Chargeability (Half Space referenced) inversion model superimposed on drillhole information (Above) and IP Chargeability (DC referenced) inversion model superimposed on drillhole information (Below). Tolerance +/-150m from the survey line.

4.1 TARGETS OF INTEREST

Integration of resolved anomalies with available drill hole, geological information, and potential target areas, zones A to F, have been identified for future exploration in the survey area. Their specifications are illustrated and described in Figure 4-9 and Figure 4-10.

Figure 4-9 displays the MT resistivity model and IP chargeability models, PLDP half space referenced and DPDP DC referenced, along line 1E from top to bottom, respectively. Zone A is a sub-vertical high conductivity and high chargeability zone. Drill hole MT05-1 crosses the shallow part (~150 m depth) of the possible eastern extension of this zone and reported a maximum of 0.14 g/t Au assay. Zone B-1 is a moderate conductive and chargeable zone resolved close to the surface. Zone B-2 is a deep MT target and appears to be depth extension of Zone B-1.No existing drill holes are located close to these zones, making them a potential area for future exploration. Target Zone C is located in the central part of line 1E with moderate to low conductivity and chargeability. The MT model resolves a deeper anomaly in this zone whereas the IP models depict slight change in contour gradient and colour shade only. The existing drill hole, PTN-01 has not reached to the deeper part of the MT anomaly.

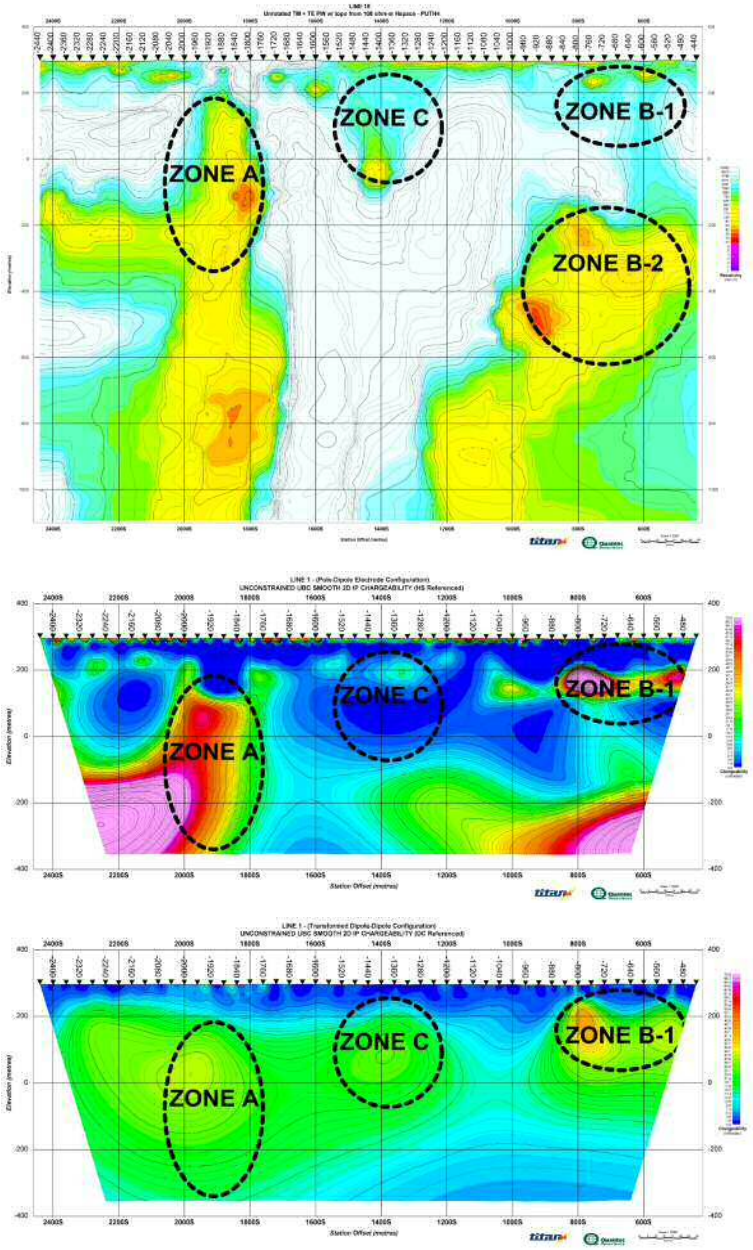

Figure 4-9. Interpreted Potential Target Zones for Line 1E: MT resistivity, PLDP half space referenced IP and DPDP DC referenced IP models from top to bottom

MT resistivity model and IP chargeability models, PLDP DC referenced and DPDP half space referenced, along line 2E are displayed in Figure 4-10. Maximum Au assay of 2.64 g/t from Drill hole NT87-01 is reported in an area with high conductivity and high chargeability (Zone D). A sub-vertical anomalous zone, Zone E, resolved in the northern part of the line is also a potential area for further exploration as the existing drill holes have not reached to the central part of this zone. In the central part of the line, Zone F has already explored with drill holes MNT06-4 and NT87-13 and reported a maximum Au assay of 0.71 g/t. However, drill holes have not reached to the deeper MT anomaly.

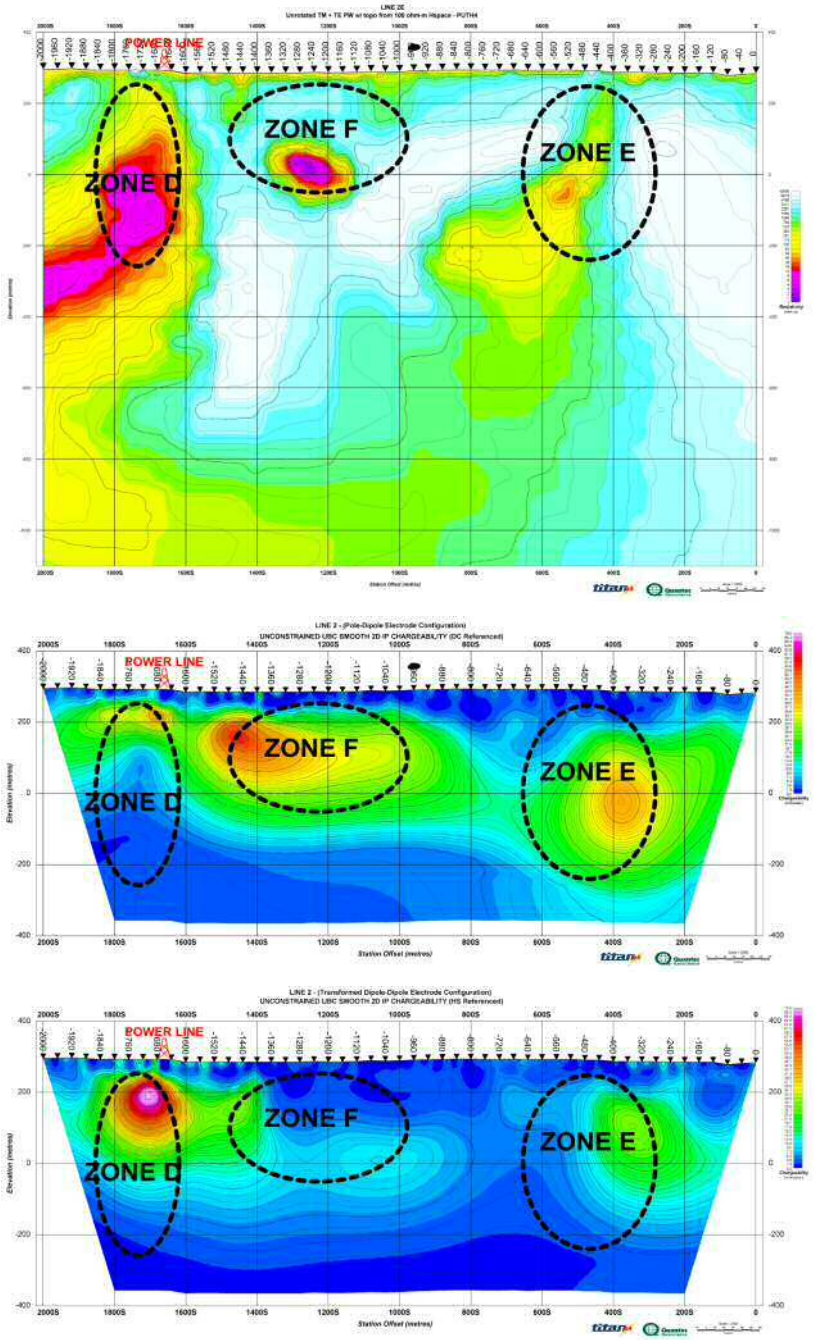

Figure 4-10. Interpreted Potential Target Zones of Line 2E: MT resistivity, PLDP DC referenced IP and DPDP half space referenced IP models from Top to Bottom,

A total of 6 anomalies with different priority levels have been resolved along the survey lines surveyed North Tisdale project are listed in the Table 1. The potential targets are prioritized as High, Moderate, or Low, and their intermediate ranges based on the category of the chargeability and conductivity of the anomalies as well as the size. The High priority anomalies are associated with large anomalies with high-moderate chargeability and high-moderate conductivity (category I). Category II denotes anomalies with high-moderate chargeability and moderate-low conductivity. A moderate-low chargeable and resistive anomaly is categorized as III.

Based on the above criteria, a total of four (4) High priority, one (1) Moderate priority and one (1) Low priority anomalies are identified.

Because of cultural interference observed in the survey area this interpretation must be validated by ground truthing. The resolved potential targets are interpreted based on the reliability and repeatability of the DC and IP inversion results. Any drilling efforts based on these interpretations must incorporate other geophysical and geological models and information to validate these results.

Table 1. List of potential targets.

Anomaly ID	Chargeability (High/Mod/Low)	DC Conductivity (High/Mod/Low)	MT Conductivity (High/Mod/Low)	Size (Large/Mid/Small)	Category	Priority	#
L1E_IP1	High	High	Mod	Large	I	High	1
L1E_IP2	High-Mod	High	Mod	Mid	I	High	2
L2E_IP1	High	High	High	Large	I	High	3
L2E_IP2	High-Mod	High	Mod	Mid	I	High	4
L2E_IP3	High-Mod	Low	Mod	Mid	II	Moderate	5
L2E_IP4	Mod-Low	Low	Low	Mid-Small	III	Low	6

Respectfully Submitted

Toronto, ON, the 17/02/2012,

Kevin Killin P. Geo

Quantec Geoscience Ltd

Saman Perera

Quantec Geoscience Ltd

Mehran Gharibi

Quantec Geoscience Ltd

5 STATEMENT OF QUALIFICATIONS

A.1 KEVIN KILLIN

I, Kevin J. Killin, declare that

I am a Professional Geophysicist with residence in Whitby, Ontario and am presently employed as the Vice President of Interpretation overseeing the interpretation group with Quantec Geoscience Ltd., Toronto, Ontario.

I obtained an Honours Bachelor of Science Degree (HBSc), in Geological Geophysics from the University of Western Ontario in London Ontario, in 1986, including a Geology degree and Geophysics degree.

I am a Professional Geophysicist, with license to practice in the Province of Ontario (APGO member # 0823).

I am a member of the Prospectors and Developers Association of Canada, the Canadian Exploration Geophysics Society (KEGS), and the American Geophysical Union (AGU).

I have no interest, nor do I expect to receive any interest in the properties or securities of **Moneta Porcupine Mines Inc.**, its subsidiaries or its joint-venture partners;

I am the Professional Geophysicist responsible for supervising the interpretation and reporting of this project and have reviewed this Geophysical dataset. This includes reviewing the survey results, logistics , processing and inversion results contained in the interpretation report.

I can attest that these accurately and faithfully reflect the data acquired on site to the best of my knowledge.

The statements made in this report represent my professional opinion in consideration of the information available to me at the time of writing this report.

Toronto, Ontario

February, 2012

Kevin Killin, H.BSc. P.Geo.

Quantec Geoscience Ltd.

A.2 SAMAN PERERA

I, A. G. Saman. Perera, declare that:

I am a consultant with residence in North York, Ontario and am presently employed with Quantec Geoscience Ltd., Toronto, Ontario;

I obtained a Bachelor's Degree in Geology, Physics and Chemistry at University of Peradeniya in Sri Lanka, in 1990, and a Master Degree in Exploration Geophysics with Distinction (M.Sc) at the ITC in Delft, The Netherlands, in 1997.

I have practiced my profession continuously since February, 1990 in Sri Lanka, The Netherlands, Australia, China, United Kingdom and Canada.

I have no interest, nor do I expect to receive any interest in the properties or securities of **Moneta Porcupine Mines Inc.**, its subsidiaries or its joint-venture partners;

I have undertaken the 2D inversions and compiled this report and can attest that these accurately and faithfully reflect the data acquired on site. The statements made in this report represent my professional opinion based on my consideration of the information available to me at the time of writing this report.

Toronto, Ontario

February, 2012

A.G. Saman Perera M.Sc.

Quantec Geoscience Ltd.

A.3 MEHRAN GHARIBI

I, Mehran Gharibi, declare that

I am a Geophysicist with residence in Toronto, Ontario and am presently employed in this capacity with Quantec Geoscience Ltd., Toronto, Ontario.

I obtained a Bachelor of Science Degree (B.Sc.), Nuclear Physics, from the University of Shiraz, Iran in 1986, a Master of Science Degree (M.Sc.), Geophysics, Seismic Methods, from Tehran University, Iran in 1991, and a Doctor of Philosophy Degree (Ph.D.), Geophysics, Electromagnetic Methods, from the University of Uppsala, Sweden in 2000.

I have practiced my profession continuously since 1991 in Middle- East, Europe, and Canada.

I have no interest, nor do I expect to receive any interest in the properties or securities of **Moneta Porcupine Mines Inc.**, its subsidiaries or its joint-venture partners;

I was in charge of data acquisition quality control; I have reviewed the survey results and can attest that these accurately and faithfully reflect the data acquired on site; I oversaw the 2D DC/IP and MT inversions and have reviewed this report, and the statements made in this report represent my professional opinion in consideration of the information available to me at the time of writing this report.

Toronto, Ontario

February, 2012

Mehran Gharibi, Ph.D

Quantec Geoscience Ltd.

A.4 MOJTABA DANESHVAR

I, Mojtaba Daneshvar, declare that:

I am a data processor with residence in Toronto, Ontario and am presently employed in this capacity with Quantec Geoscience Ltd., Toronto, Ontario;

I obtained a Bachelor of Science Degree (B.Sc.), with Honours, in Earth Science/Geophysics Specialization in 2010 from the University of Waterloo, Waterloo, Ontario.

I have practiced my profession continuously since Sep, 2010 in Canada;

I have no interest, nor do I expect to receive any interest in the properties or securities of **Moneta Porcupine Mines Inc.**, its subsidiaries or its joint-venture partners;

I was a data processor on site, responsible for the quality control of data acquired throughout the survey. I compiled and edited the logistics report. The statements made in this report represent my professional opinion based on my consideration of the information available to me at the time of writing this report.

Toronto, Ontario

February, 2012

Mojtaba Daneshvar, B.Sc.

Quantec Geoscience Ltd.

A.5 CHRIS FUREY

I, Chris Furey, declare that:

I am a data processor with residence in Mount Pearl, Newfoundland and am presently employed in this capacity with Quantec Geoscience Ltd., Toronto, Ontario;

I obtained a Bachelor of Science Degree (B.Sc), Majoring in Geology/Geophysics with a Minor in Geography (Geographic Information Sciences), from Memorial University in St. John's, Newfoundland in 2011.

I have practiced my profession continuously since April, 2011 in North America and Europe.

I have no interest, nor do I expect to receive any interest in the properties or securities of **Moneta Porcupine Mines Inc.**, its subsidiaries or its joint-venture partners;

I was a data processor on site, responsible for the quality control of data acquired throughout the survey. The statements made in this report represent my professional opinion based on my consideration of the information available to me at the time of writing this report.

Toronto, Ontario

February, 2012

Chris Furey, B.Sc

Quantec Geoscience Ltd.

6 DIGITAL ARCHIVE

The DVD attached to this report contains a copy of all the inversion results, final processed data, including the survey files, the daily processing (and field) notes, and an electronic copy of this report (with all appendices).

Folder	Sub level 1	Sub level 2	Description
NorthTisdaleProject	Misc	Contract Processing Notes PrelimReport Images_PNGs	Contract, Processing Notes Prelim Report Images_PNGs
NorthTisdaleProject	Data	DCIP MT	Final field results CSV, EDI,
NorthTisdaleProject	Survey Files		Survey Files
NorthTisdaleProject	Geosoft		Geosoft Files
		Location Map	Base maps, location, etc
		Sections_drillholeplot	DDH geosoft db
		DCIP	DCIP 2D sections
		MT	MT 2D sections
		DiffrentColourScale	DC maps with different colour Scale to focus on the central part (as requested by the client)
NorthTisdaleProject	Inversion_Results_TS_XYZ		Inversion results TS files and xyz files
			DC IP inversion
NorthTisdaleProject	invDCIP	UBC_DPDP	Transformed Dipole dipole configuration raw data and error conditioning
		UBC_PLDP	Pole dipole configuration raw data and error conditioning
		LOKE	LOKE inversions
			MT inversions
NorthTisdaleProject	invMT		Geotools database

A PRODUCTION SUMMARY

DATE	FIELD ACTIVITIES AND OBSERVATIONS	PROCESSOR COMMENTS AND OBSERVATIONS	LINE SPREAD	LINE START	LINE END	TX STAR T	TX END	READ (km)			COMPLETED SPREAD	TOTAL CHARGE (Survey + Interp)
								MT	IP	IP CURRENT EXTENSIONS		
Moneta Porcupine Gold - North Tisdale Project CA00916T - Production Summary												
06/12/2011	Mob to Timmins, Ontario											
07/12/2011	Setup Line 1E. Line Infinite is done and GPS Points were taken.		**Line 1 E**	**440s**	**2440s**	**0s**	**2880s**	**0**	**0**	**0.88**	**0**	
08/12/2011	Finished setup of Line 1E. Ran a few test shots of IP at the line. PST was completed. Remote site was set up but not completed.		**Line 1 E**	**440s**	**2440s**	**0s**	**2880s**	**0**	**0**	**0**	**0**	
09/12/2011	Read 400m partial IP. PST and Remote site was completed and tested.		**Line 1 E**	**440s**	**2440s**	**0s**	**2880s**	**0.4**	**0**	**0.88**	**0**	
10/12/2011	Finished IP on line 1E, Partial MT data was acquired over the night.		**Line 1 E**	**440s**	**2440s**	**0s**	**2880s**	**1.6**	**2**	**0**	**1**	
11/12/2011	Moved to Line 2E. MT could not be acquired because many contacts were left above 50,000ohms. Processed a full IP and MT run for line 1.		**Line 2 E**	**0s**	**2000s**	**440n**	**2440s**	**0**	**0**	**0**	**0**	
12/12/2011	Surveyed IP and MT on Line 2E. Completed a full process run of line 2 IP data.		**Line 2 E**	**0s**	**2000s**	**440n**	**2440s**	**2**	**2**	**0.88**	**1**	
13/12/2011	Pick up all equipment and finalized inventory. Full MT data was acquired. Completed a full process run of line 2 MT dada.											
14/12/2011	Mob to Toronto.											
	TOTAL SURVEY COVERAGE (KM) AND CHARGE							**4**	**4**	**1.76**	**2**	**$ -**

B SURVEY LOGISTICS

B.1 ACCESS

Base of Operation: Hobo Lodge
100 Laforest Rd,
Timmins, ON P4N 7C3

Mode of Access to Grid: Trucks

Mode of Access to Lines: Quad, Walking

B.2 SURVEY GRID AREA

Established by: Moneta Porcupine Mines

Coordinate Reference System: Grid referenced to UTM Coordinates

Datum & Projection: WGS84/Zone 17U

Grid Azimuth: 0^{o}

Magnetic Declination: $10W^{o}$

Station Interval: 80m

Method of Chaining: Metric, slope distance, pickets GPS surveyed

Surveyed Line-start and -end point coordinates.

Line	Grid Coordinate		UTM Coordinate Start		UTM Coordinate End	
	Start	End	Easting	Northing	Easting	Northing
L1 E	440	2440	480153	5377208	480174	5374789
L2 E	440	2440S	479290	5377112	479228	5374311

B.3 PRODUCTION AND COVERAGE

Survey Period/days: December 6th to December, 14th, 2010
9 days

Survey Days (read time): 7 days

Mob/Demob: 2 days

Safety Inductions: 0 days

Parallel Sensor Test: 1 day

Weather/Down Days: 0 days

Number of Lines surveyed: 2 Lines

DCIP Survey Coverage: 4 km

MT Survey Coverage: 4 km

Max and Min Pole (Tx) and Potential (P1-P2) Electrode Position.

Line	Setup	Min P1	Max P2	Min Tx	Max Tx	Coverage (km)
L 1 E	1	440S	2440S	0S	2800S	2 km (2.8 km with extension)
L 2 E	1	440S	2440S	0S	2800S	2 km (2.8 km with extension)
					TOTAL	**4 km (5.6 km with extension)**

MT Survey Coverage (Electrode to Electrode).

Line	Setup	Min Extent (m)	Max Extent (m)	Coverage (km)
L 1 E	1	440S	2440S	2 km
L 2 E	1	440S	2440S	2 km
			TOTAL	**4 km**

B.4 PERSONNEL

Project Manager:	Kevin Blackshaw
Responsible Geophysicist:	Mehran Gharibi Saman Perera
Data Processing (in field):	Mojtaba Daneshvar, Chris Furey
Crew Chief:	Nick Hnotchuk
IP operator:	Nick Hnotchuk
MT operator:	Ryan Foyle
Remote Operator:	Mojtaba Daneshvar Chris Furey
Field Technicians:	Chad Commanda Eric Hotvedt Luc Lafond Shawn Jones Carmen Vucko Ryan Foyle

B.5 INSTRUMENTATION

Receiver System: Quantec Distributed Array Acquisition System:
- 61 channels max. per system (55ch operationally
with
internal A/D conversion (24bit @120db / dual
speed
@120-48kHz), and buffer memory (6Mb).
24 x 2-channel Acquisition Modules (AMs)
13 x 1-channel Acquisition Modules (AMs)
AM data transmission using LAN cabling
- 2 Central Recording Units (CRU; 140 Gb data
storage)
at base & at MT remote reference (MT survey)
- 2 GPS synchronization clocks
(10nsec precision /12.3MHz clock-speed),
at base & at MT remote reference (MT survey)
- 2 PC-based Central Processing Units (CPU)
at base & at MT remote reference (MT survey)

Transmitter (DCIP Surveys): GDD (5kW) with frequency/waveform control, using CRU and Current Monitor (CM)

Power Supply (DCIP Surveys): Honda 6500W generator

Transmit Electrodes 4 x 1.2cm diameter 1 meter long stainless steel rods

Receiver Electrodes: Ground contacts using stainless steel rods

Receiver Coils (MT Surveys): Low Frequency Range (0.0001Hz to 1kHz):
4 Magnetometers (P50 or BF-4 model)
{2 at base & 2 at remote}
Mid to High Frequency Range (1Hz to 25kHz)
4 Magnetometers (P30 or BF-6 model)
{2 at base & 2 at remote}

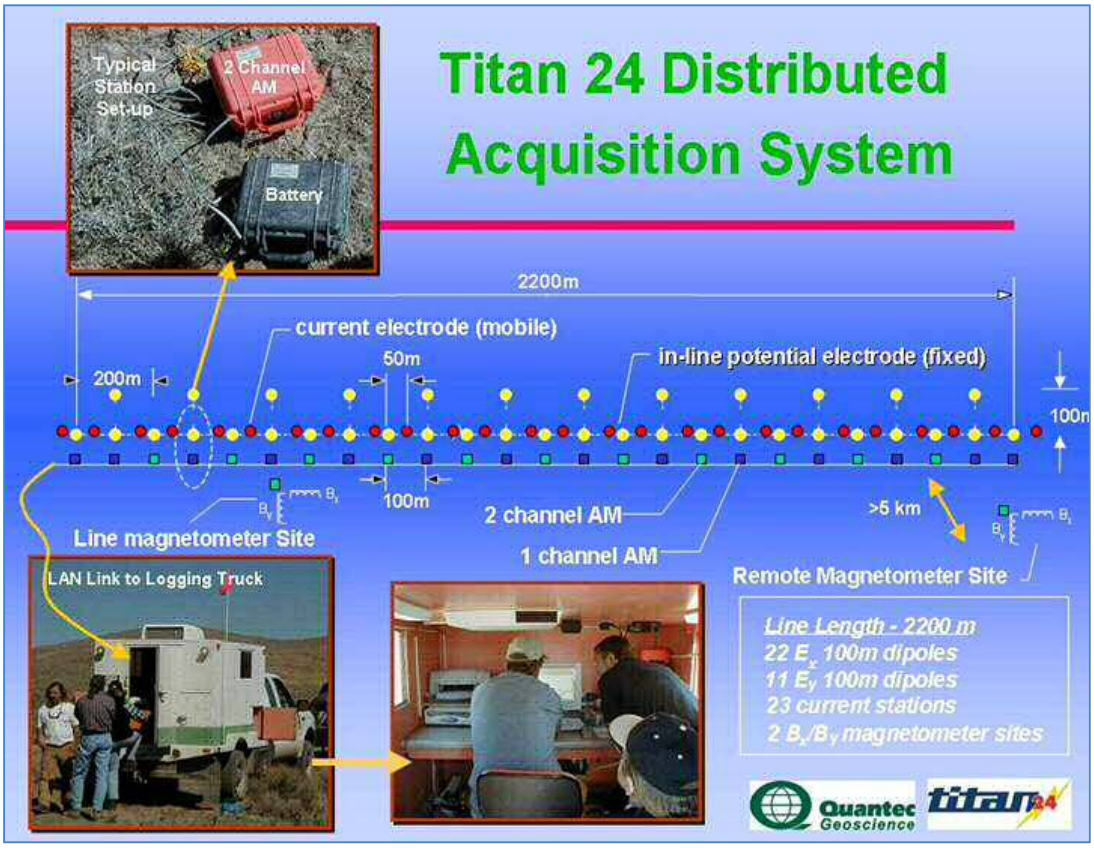

Titan-24 DCIP and MT Schematic Survey Layout.

B.6 DCIP SURVEY SPECIFICATION

B.6.1 GEOMETRY

Survey Array:	Dipole-Pole-Dipole Array
Receiver Configuration:	23-24 Ex = Continuous In-line voltages, 12-13 Ey = Alternating (2-stations) cross-line voltages[8].
Array Length:	2 km
Number of Arrays/line:	1
Dipole length:	Ex = 80 metres Ey = 80 metres
Sampling Interval:	Ex = 80 metres
Rx-Tx Separation:	N-spacing (Pn-Cn min)[9] = 0.5 to 29.5
Infinite Pole Location:	485951m E, 5374073m N (WGS84/Zone 17) (Grid Coordinate: 5798.00 E, 3152.00 S)

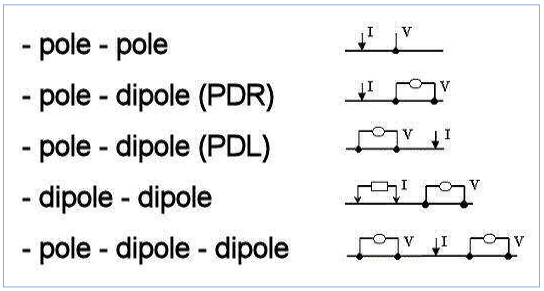

Common DCIP Survey Layouts.

B.6.2 ACQUISITION & PROCESSING

Spectral Domain:	Tx = Frequency-domain square-wave current Rx = Full waveform time-series acquisition Data processing/output in frequency-domain.
Spectral Chargeability Model[10]:	Halverson-Wait
Transmitter Waveform:	30/256 Hz square waves at 100% duty cycle (~4sec Pos./Neg.)
Transmitter Output Current:	min ~0.33 Amperes to max ~5.71 Amperes
Receiver Sampling Speed:	240 samples/second (24 bit A/D @ 120 db dynamic range)
Tx-Rx Synchronization:	using current monitor (10 μsec time-accuracy)

[8] Note: Cross-Line (Ey) voltages obtained for future reference purposes – not presented in cross-sectional plots.
[9] Current electrodes at midpoints between potential electrodes.
[10] The Halverson-Wait model chargeability (Halverson et al., 1981) is similar to and improves upon the frequency-domain Cole-Cole model (Pelton et el., 1978) described in the time-domain by Johnson (1984).

Time-Series Stacking:	20 cycles (full-waveform)
Read Time:	approx 3.0 minutes per event
Time-Domain Decay Window:	
	Integration Start Time: T_O = 0.8 seconds
	Integration End Time: T_F = 1.9 seconds
Post-Processing:	using Quantec proprietary QuickLay v.2.30.14 1) Time-series stacking 2) Robust statistics 3) Current waveform deconvolution 4) Digital filtering (60Hz + harmonics) 5) Spectral model decay-curve fitting

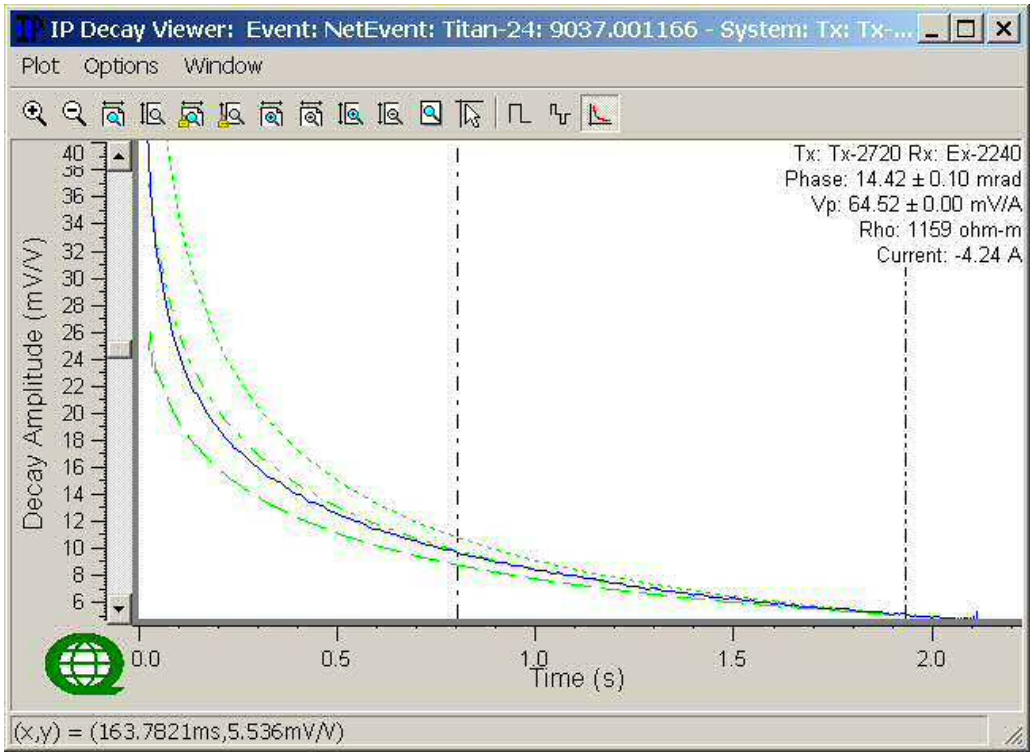

Spectral Chargeability Model and Calculated Halverson-Wait Decays[11].

[11] Halverson-Wait (HW) model parameters calculated in frequency domain, with hatched green lines corresponding to theoretical HW decay with spectral r-factors of 0.1, 1.0 (default) & 10, k-factor of 0.2 (default).

B.6.3 DATA PRESENTATION

Accuracy and Repeatability Measured Data average error (from CSV files) using Halverson-Wait model calculation:

Voltage Errors	0.00141mV/V (average)
Phase Errors	71.1% less than 1.0 mrad

Pseudo-Section Plots: In-line[12] DC Resistivity and IP Chargeability pseudo sections, posted, contoured (equal area zoning) and plotted in ground units using QuickLay viewer.

Raw Data (digital): (external Hard Drive) Raw Event Log File Folders (eg. Eventxxxx.dat). Also contains AU.txt and Event.log files which contain information on the location and time of the event in QuickLay digital format (Raw data output to Matlab format upon request).

Processed Data (digital): DC/IP Data in ASCII CSV (comma delimited) file format from QuickLay, containing final processed voltage and phase data.

CSV File Format:

Line 1:	Column headings
Column 1	Event name/number (e.g., Eventxxxx)
Column 2:	Transmitter site ID (e.g., Tx150)
Column 3:	Receiver site ID (e.g., Rx150)
Column 4-11:	C1-C2/P1-P2 positions in X and Y (m)
Column 12:	Current (Amperes)
Column 13:	Current error (Amperes)
Column 14:	Normalized voltage (Volts/Ampere)
Column 15:	Voltage error (Volts/Ampere)
Column 16:	Phase (milliradians)
Column 17:	Phase error (milliradians)
Column 18:	Apparent resistivity (Ohm-m)[13]

B.6.4 DATA QA/QC COMMENTS

Low amplitude signals and relatively noisy signals dominate most of the data.

[12] Cross-line (Ey) values not shown for presentation purposes.

[13] Apparent resistivity's are calculated in 2D space using the 4 electrodes general array configuration (as per XY electrode positioning in columns 4-11 of CSV file) – not based on pole-dipole calculations (K. Nurse, QGL, pers. comm., 07-2004).

B.7 MT SURVEY SPECIFICATION

B.7.1 GEOMETRY

Technique: Tensor soundings, remote-referenced

Line Configuration:
23-24 Ex = Continuous In-line voltages,
12-13 Ey = Alternating (2-stations) cross-line E-fields
1 pair Low Frequency coils
1 pair High Frequency coils

Remote Configuration:
1 Ex = in line E-fields
1 Ey = cross-line E fields
1 pair Low Frequency coils
1 pair High Frequency coils

Array Length: 2

Number of Arrays/line: 2

Dipole size:
Ex = 80 metres
Ey = 80 metres

Sampling Interval:
Ex = 80 metres
Ey = 160 metres

Ex/Ey sampling Ratio 2/1

E/H sampling Ratio
Ex: 23-24/2
Ey: 12-13/2

Remote Reference Position:
565102m E, 5388934m N (WGS84/Zone 17)
(Grid Coordinate: 84947.00 E, 11697.00 S)

B.7.2 ACQUISITION & PROCESSING

Data Acquisition:
Full-waveform time-series acquisition
Data processing/output in frequency-domain.

Remote-Base Synchronization: GPS clocks (10μsec time-accuracy)

Frequency Bandwidth:
Operating: 0.01 to 48000 Hz
Effective: 0.1 to 20000 Hz

Time-series Sampling:
High Range: 48000 samples/sec
Mid-Range: 12000 samples/sec
Low Range: 120 samples/sec

Time-Series Stacking:
High Range: 1,534,999 samples
Mid-Range: 2^{20} (1,048,576) samples
Low Range: 2^{19} (524,288) samples

Sample/Record Time:
High Range: min. 2 events @ 30 seconds per event
Mid Range: min. 2 events @ 2.0 minutes per event
Low Range: 1.5 - 3 events @ 80 minutes for a full event (total recording and retrieving time approx. 7 hrs)

Post-Processing: using Quantec proprietary QuickLay v.4.00.41
1) Coherent noise rejection using remote-reference
2) Proprietary digital filtering (scrubbing)
3) Coherency sorting
4) Impedance estimate stacking

B.7.3 DATA PRESENTATION

Parallel Sensor Test: Result of the test of the equipment (PST) is presented in detail in Appendix Parallel Sensor Test.

Data Error: Apparent Resistivity = <1/20TH decade average.
Phase = <3 degrees average

Sounding Curves: Apparent resistivity and phase (XY and YX) sounding curves versus the frequency (8 pts. per decade) using Geotools™ viewer.

Pseudo-Section Plots: MT Apparent Resistivity and Phase Pseudo-Sections (XY, and YX) posted, contoured (equal area zoning) and plotted in grid units using Geotools™ viewer.

Raw Data (digital): (external Hard Drive)
Base and Remote Raw Event Log File Folders
(i.e. Base-Eventxxx.dat; Remote-Eventxxxx.dat).
Also contains AU.txt and Event.log files, which contain information on the location and time of the event in QuickLay digital format (external Hard Drive).
(Raw data output to Matlab format upon request)

Processed Data (digital): MT DATA in EDI (Electronic Data Interchange) file created in Geotools™ containing Auto and Cross-power Spectral estimates for individual stations (sites) and profiles (site-sets);
Spectra are in Right Hand positive down co-ordinate system, and for profiles, EDI files are created with X as the profile direction.

For this study, final EDI have X at 0 deg (ROTSPEC= 0)

EDI is a format conforming to SEG standard for the storage of magnetotelluric (MT) data
(Wight, D. E., 1987).

B.7.4 DATA QA/QC COMMENTS

MT data has poor quality and contains a lot of noise due to the extreme culture in the area.

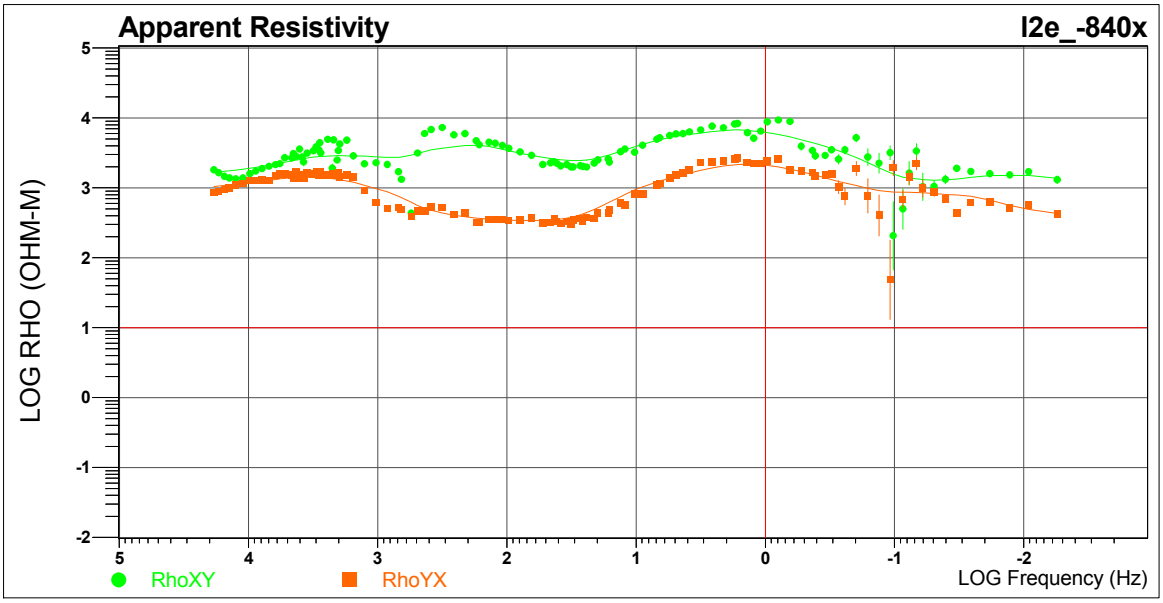

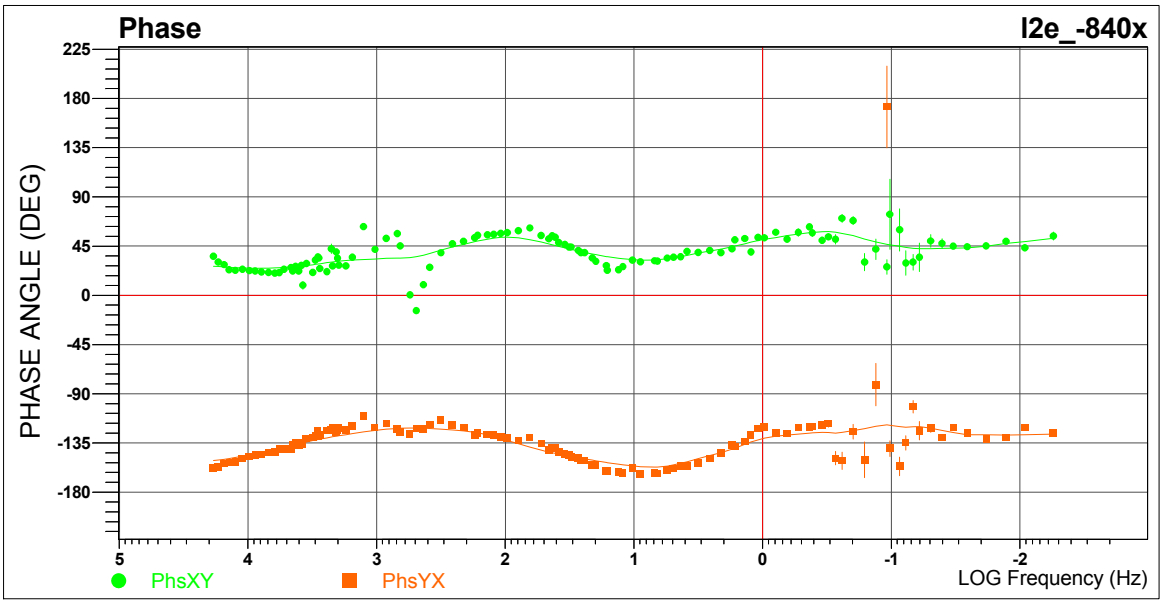

Example of Apparent Resistivity and Phase (XY and YX) Sounding Curves.

C DC – IP PSEUDO-SECTIONS OF FINAL PROCESSED DATA

C.1 LINE 1 E

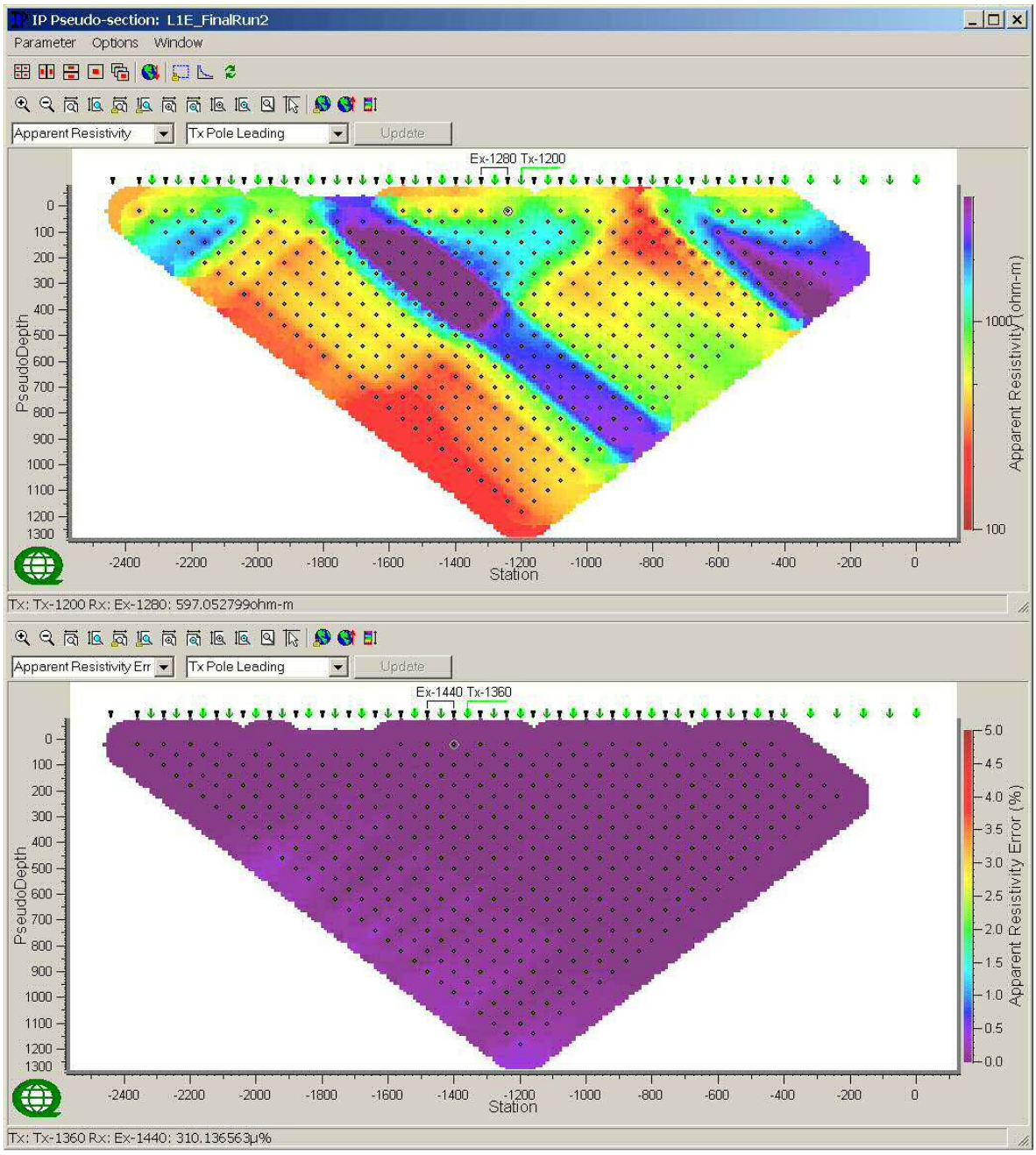

Line 1E – Observed Apparent Resistivity Raw Data (Ohm.m) & Voltage Errors (%)- Tx Pole Leading.

☐ Tx with more than one event

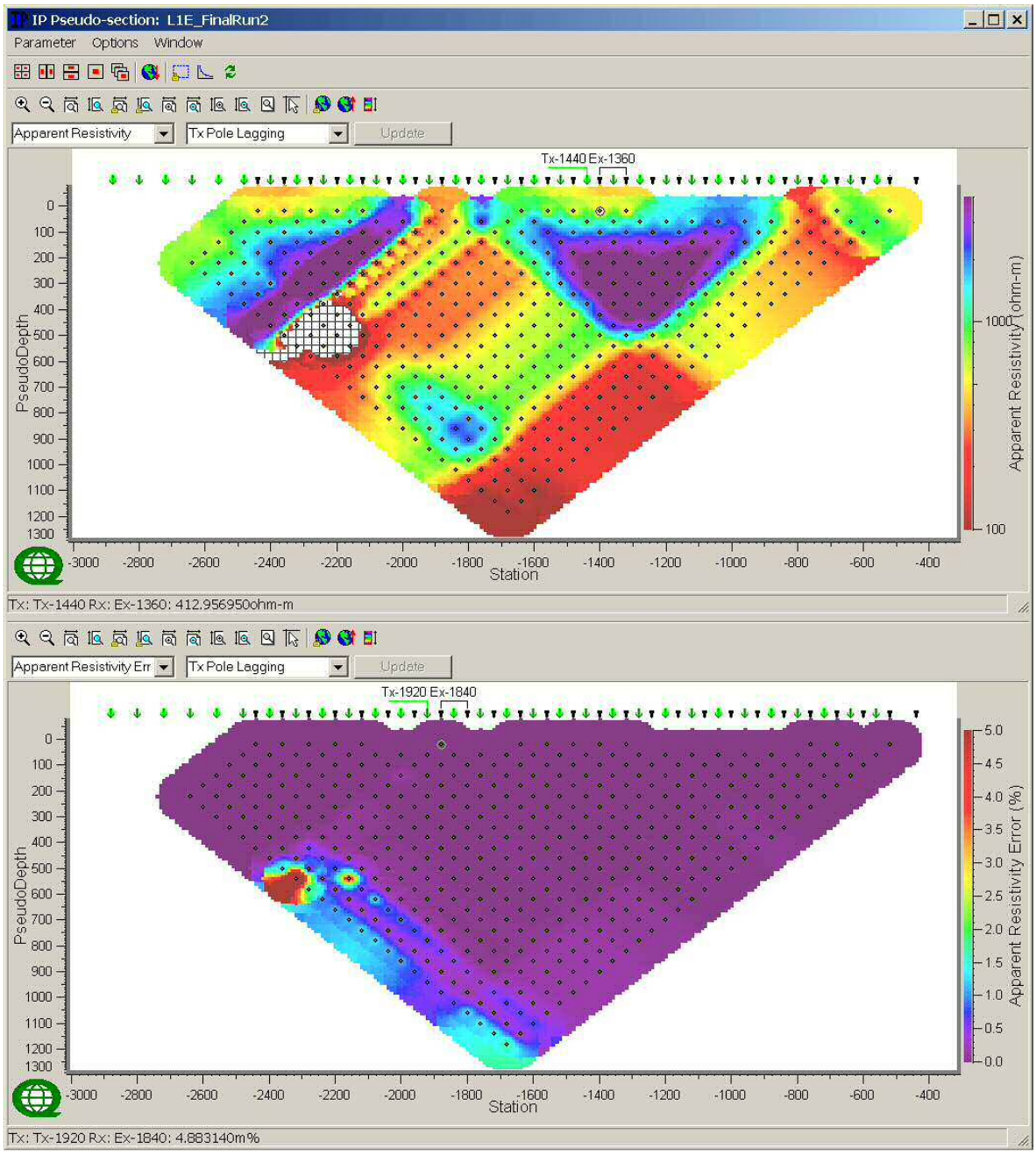

Line 1 E – Observed Apparent Resistivity Raw Data (Ohm.m) & Voltage Errors (%)- Tx Pole Lagging.

☐ Tx with more than one event

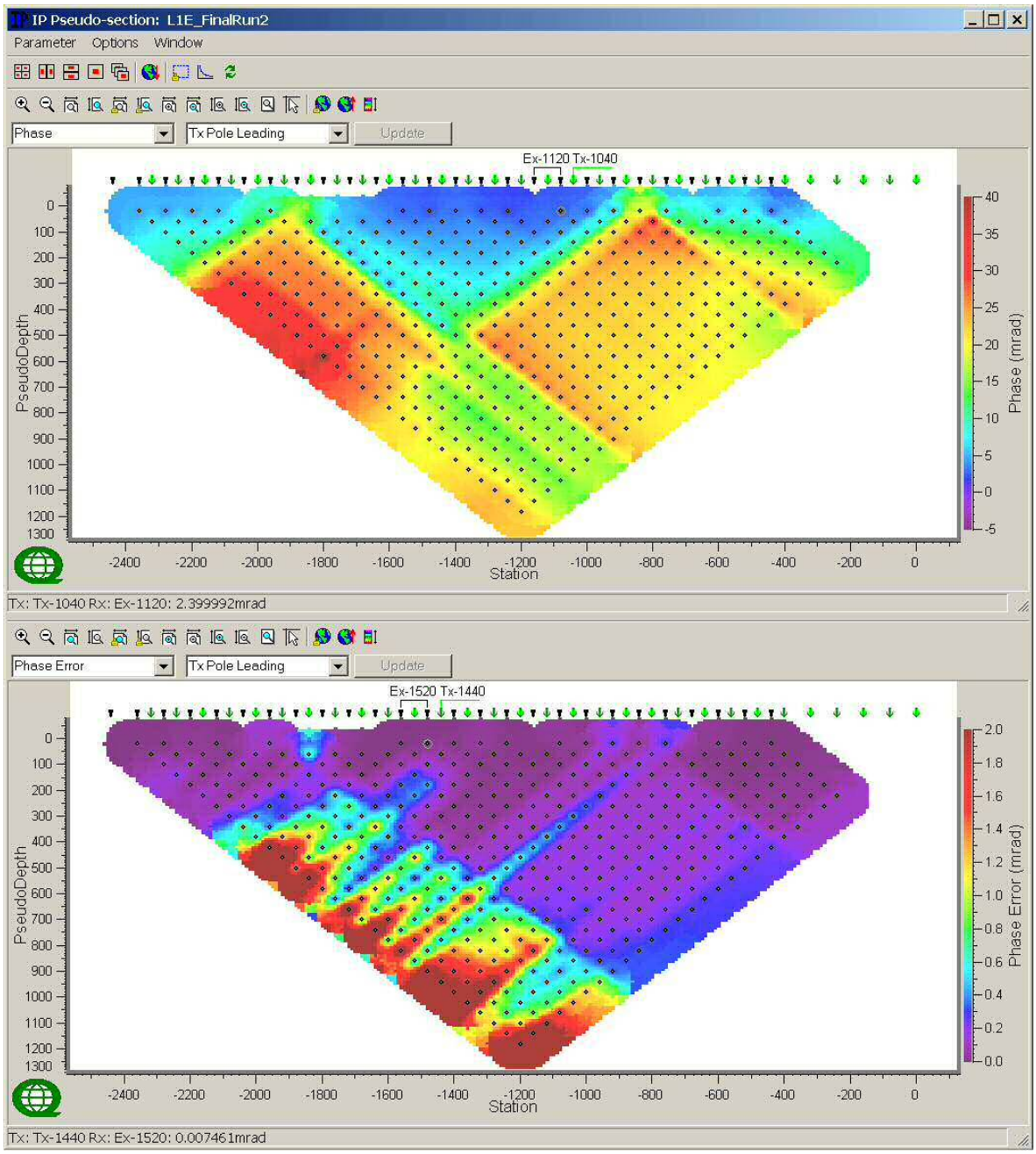

Line 1 E – Observed IP Raw Data (mrad) & IP Errors (mrads)-Tx Pole Leading.

☐ Tx with more than one event

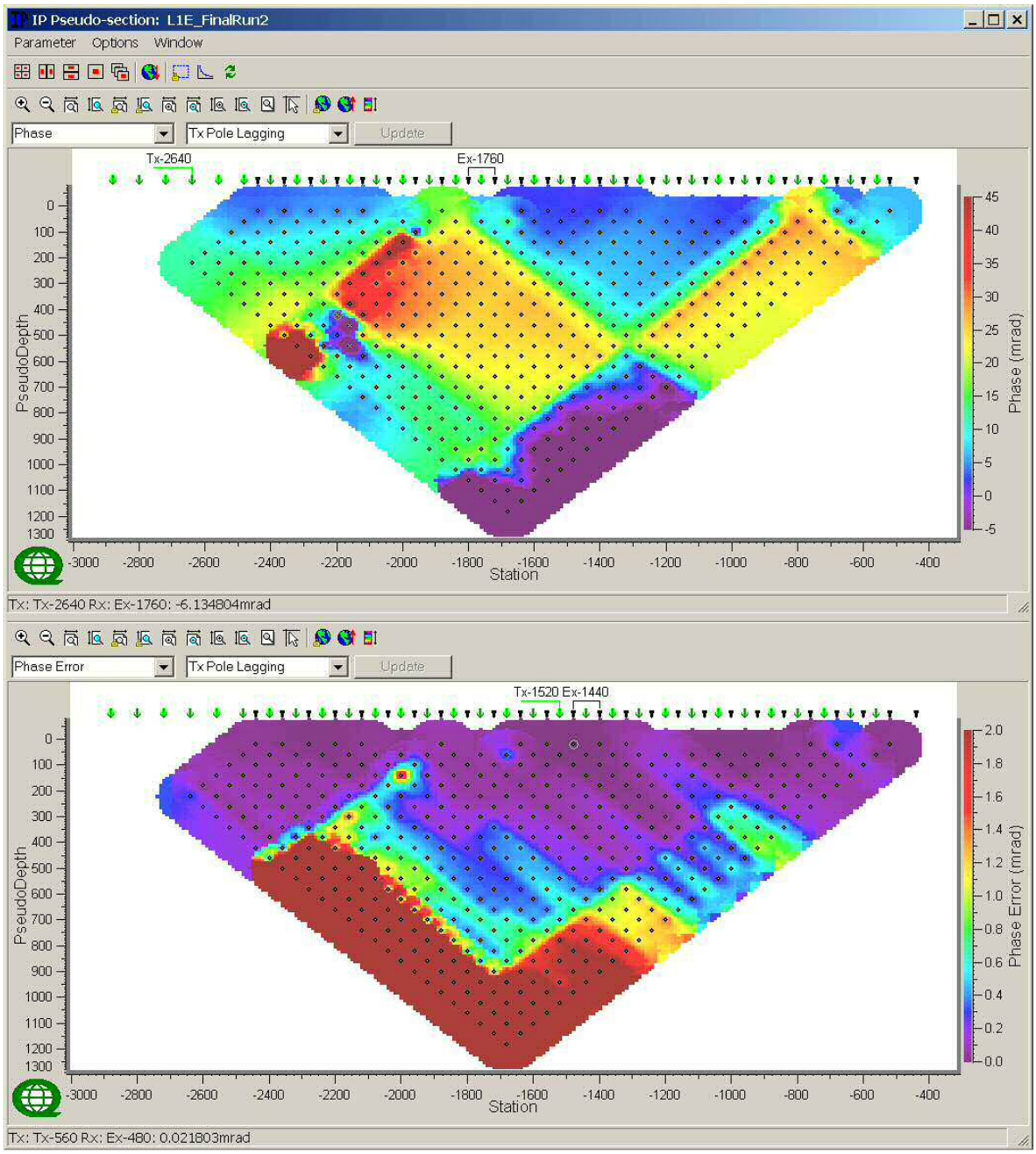

Line 1 E – Observed IP Raw Data (mrad) & IP Errors (mrads)-Tx Pole Lagging.

☐ Tx with more than one event

C.2 LINE 2 E

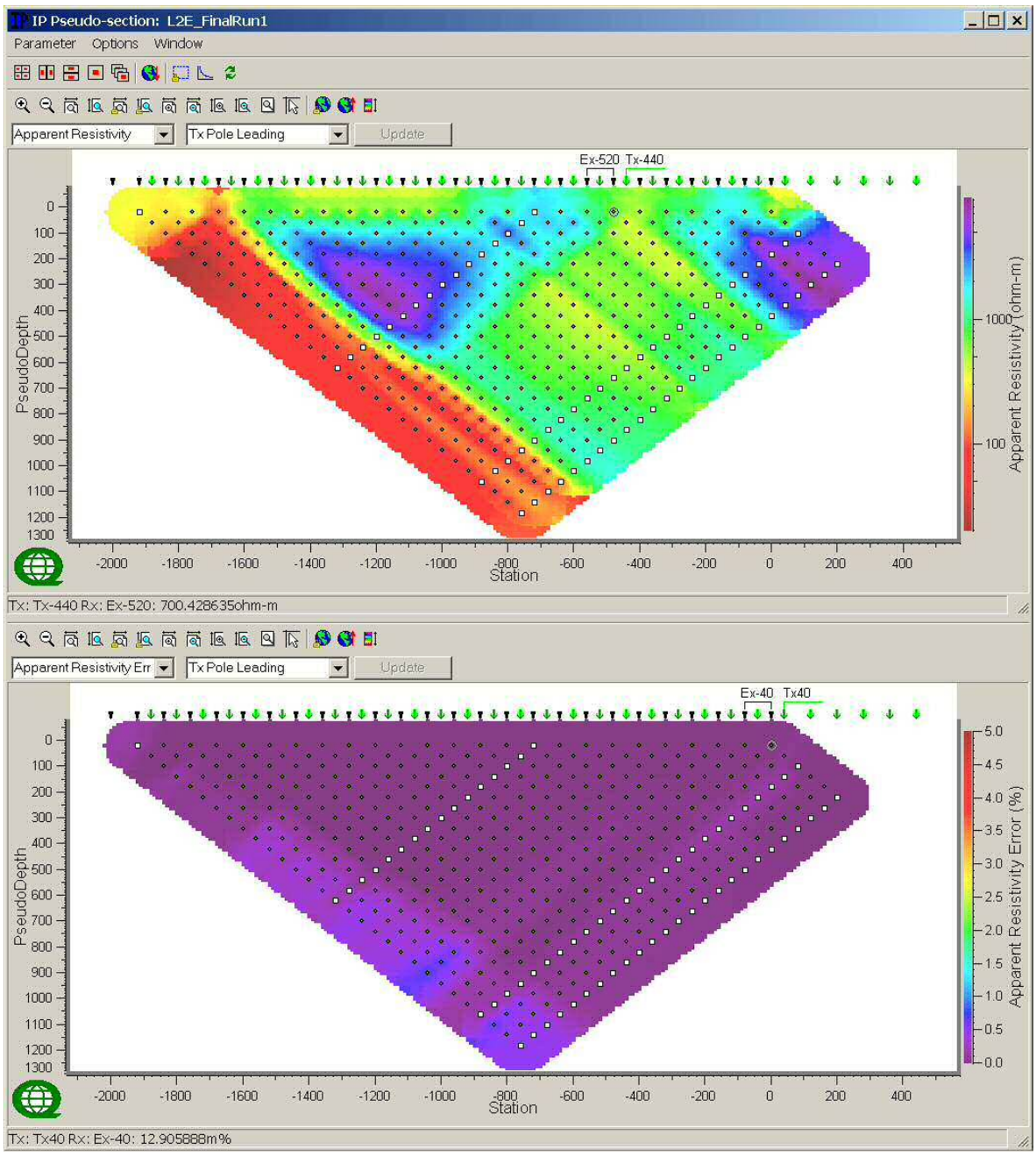

Line 2 E – Observed Apparent Resistivity Raw Data (Ohm.m) & Voltage Errors (%)- Tx Pole Leading.

☐ Tx with more than one event

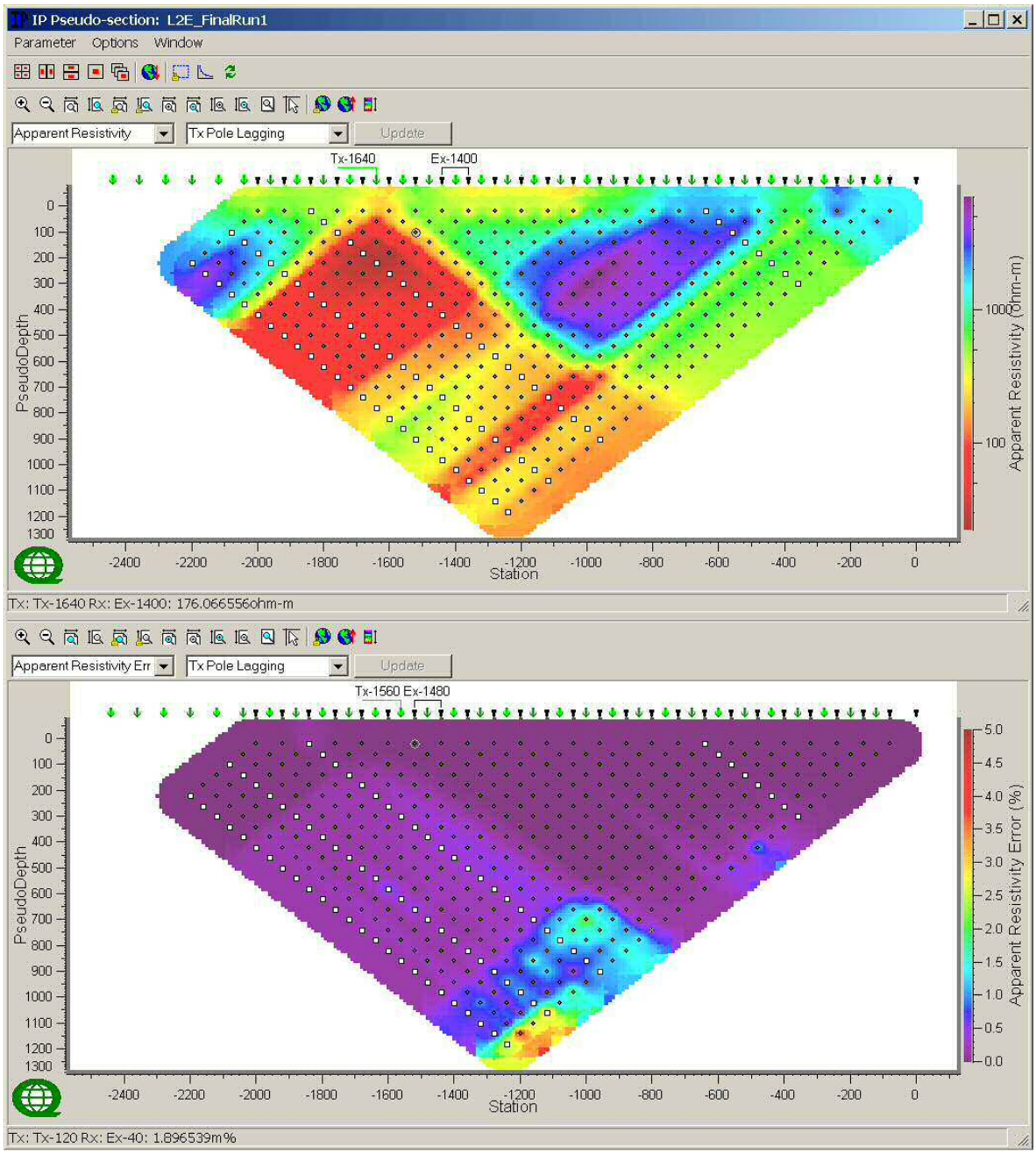

Line 2 E – Observed Apparent Resistivity Raw Data (Ohm.m) & Voltage Errors (%)- Tx Pole Lagging.

☐ Tx with more than one event

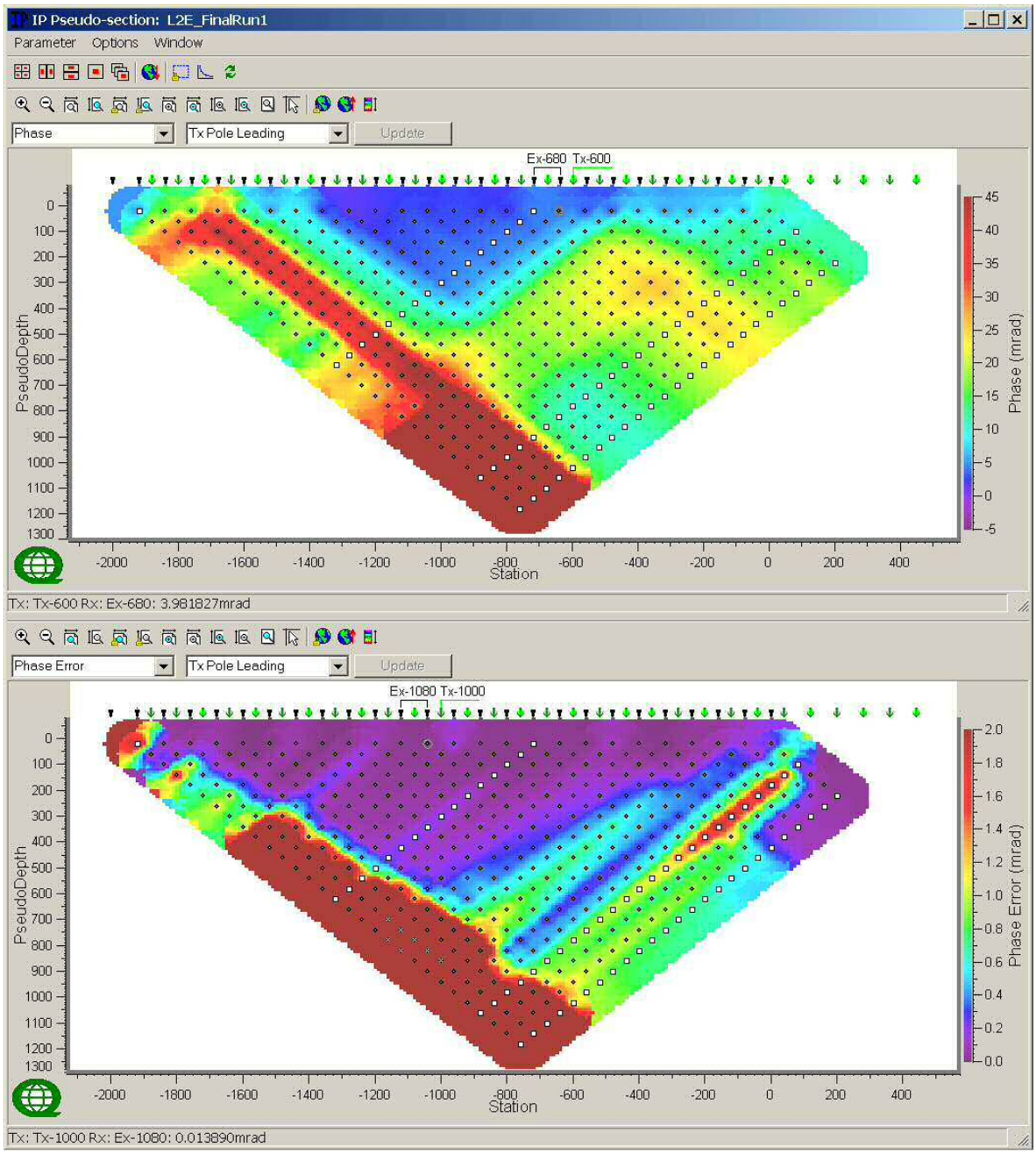

Line 2 E – Observed IP Raw Data (mrad) & IP Errors (mrads)-Tx Pole Leading.

☐ Tx with more than one event

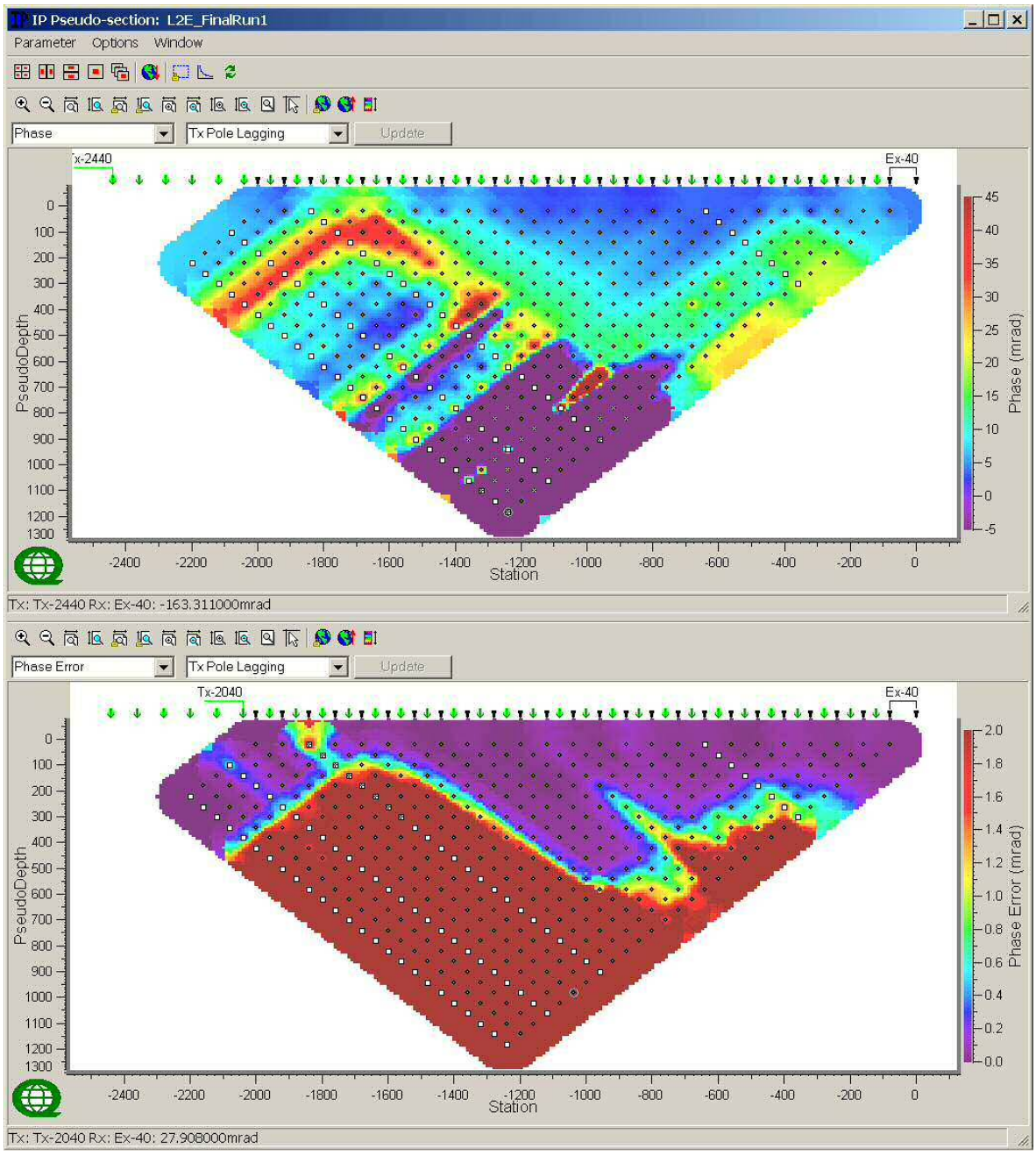

Line 2 E – Observed IP Raw Data (mrad) & IP Errors (mrads)-Tx Pole Lagging.

☐ Tx with more than one event

D MT SOUNDINGS CURVES OF FINAL PROCESSED DATA

D.1 LINE 1E

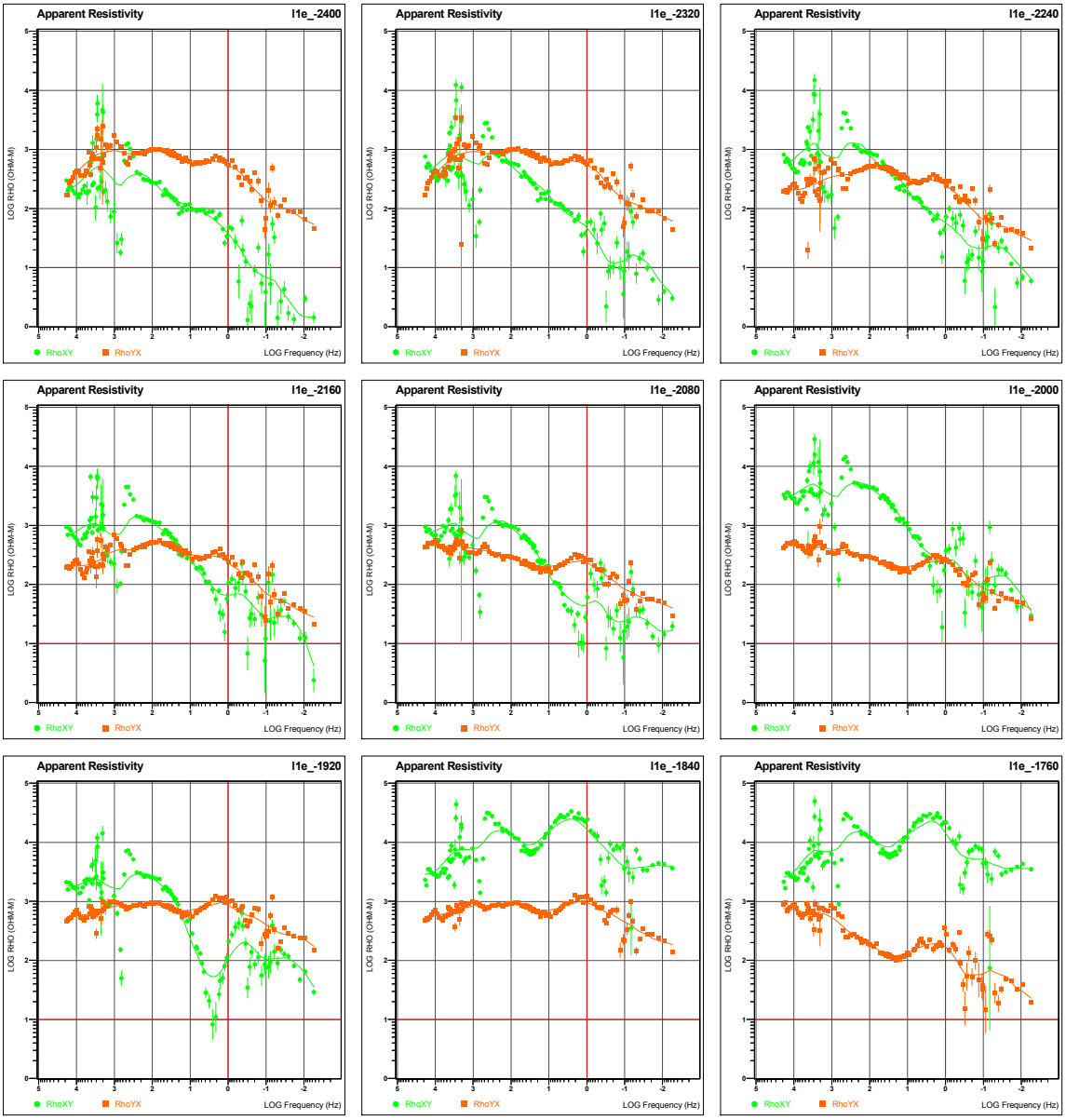

Line 1E – Apparent Resistivity Sounding Curves vs Frequency (1 of 3).

MODE XY (GREEN) DENOTES ELECTRICAL (**EX**) FIELD AND ORTHOGONAL MAGNETIC (**HY**) FIELD (=EX/HY)
MODE YX (ORANGE) DENOTES ELECTRICAL (**EY**) FIELD AND ORTHOGONAL MAGNETIC (**HX**) FIELD (=EY/HX)

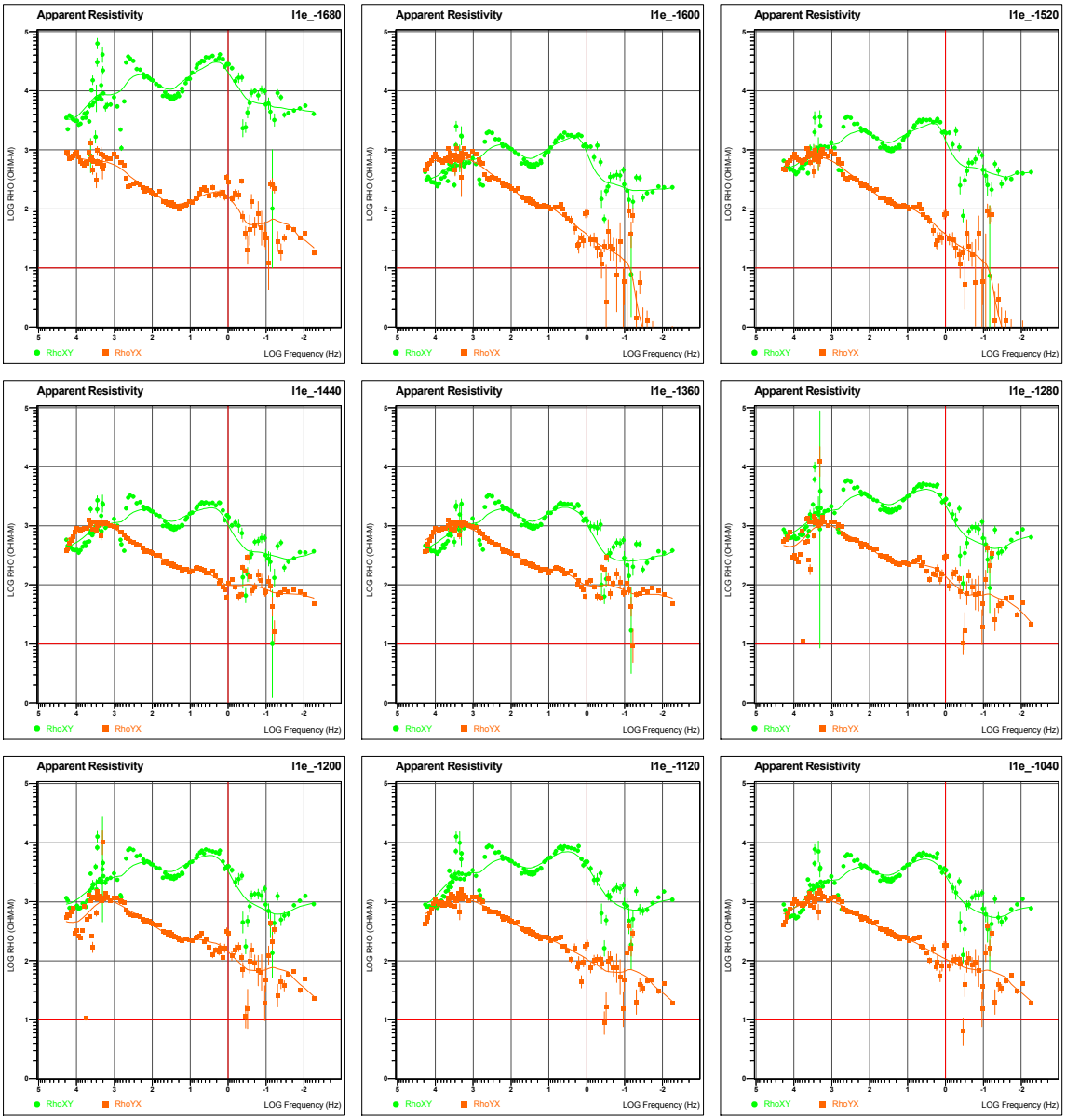

Line 1E – Apparent Resistivity Sounding Curves vs Frequency (2 of 3).

MODE XY (GREEN) DENOTES ELECTRICAL (**EX**) FIELD AND ORTHOGONAL MAGNETIC (**HY**) FIELD (=EX/HY)
MODE YX (ORANGE) DENOTES ELECTRICAL (**EY**) FIELD AND ORTHOGONAL MAGNETIC (**HX**) FIELD (=EY/HX)

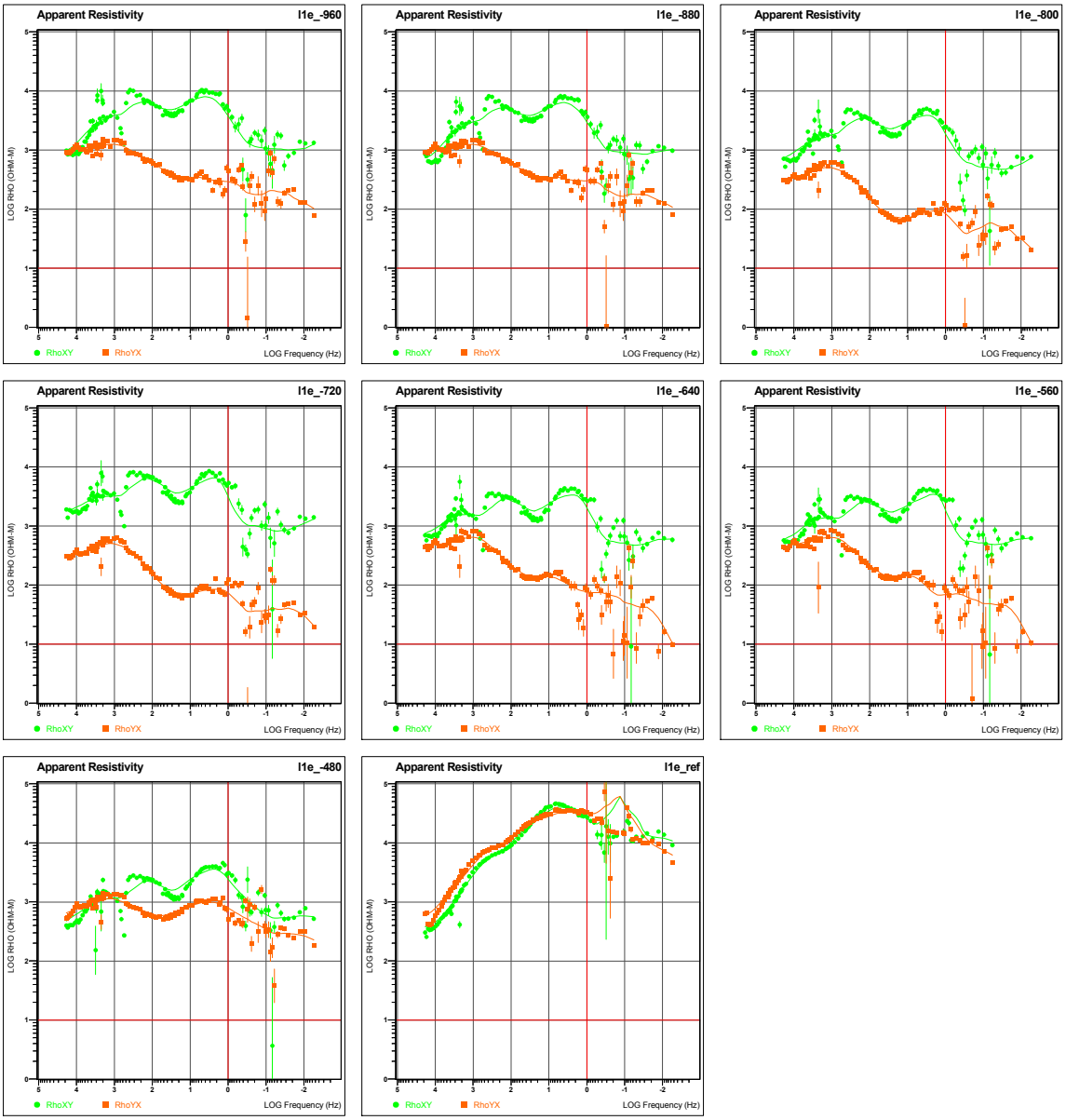

Line 1E – Apparent Resistivity Sounding Curves vs Frequency (3 of 3).

MODE XY (GREEN) DENOTES ELECTRICAL (**EX**) FIELD AND ORTHOGONAL MAGNETIC (**HY**) FIELD (=EX/HY)
MODE YX (ORANGE) DENOTES ELECTRICAL (**EY**) FIELD AND ORTHOGONAL MAGNETIC (**HX**) FIELD (=EY/HX)

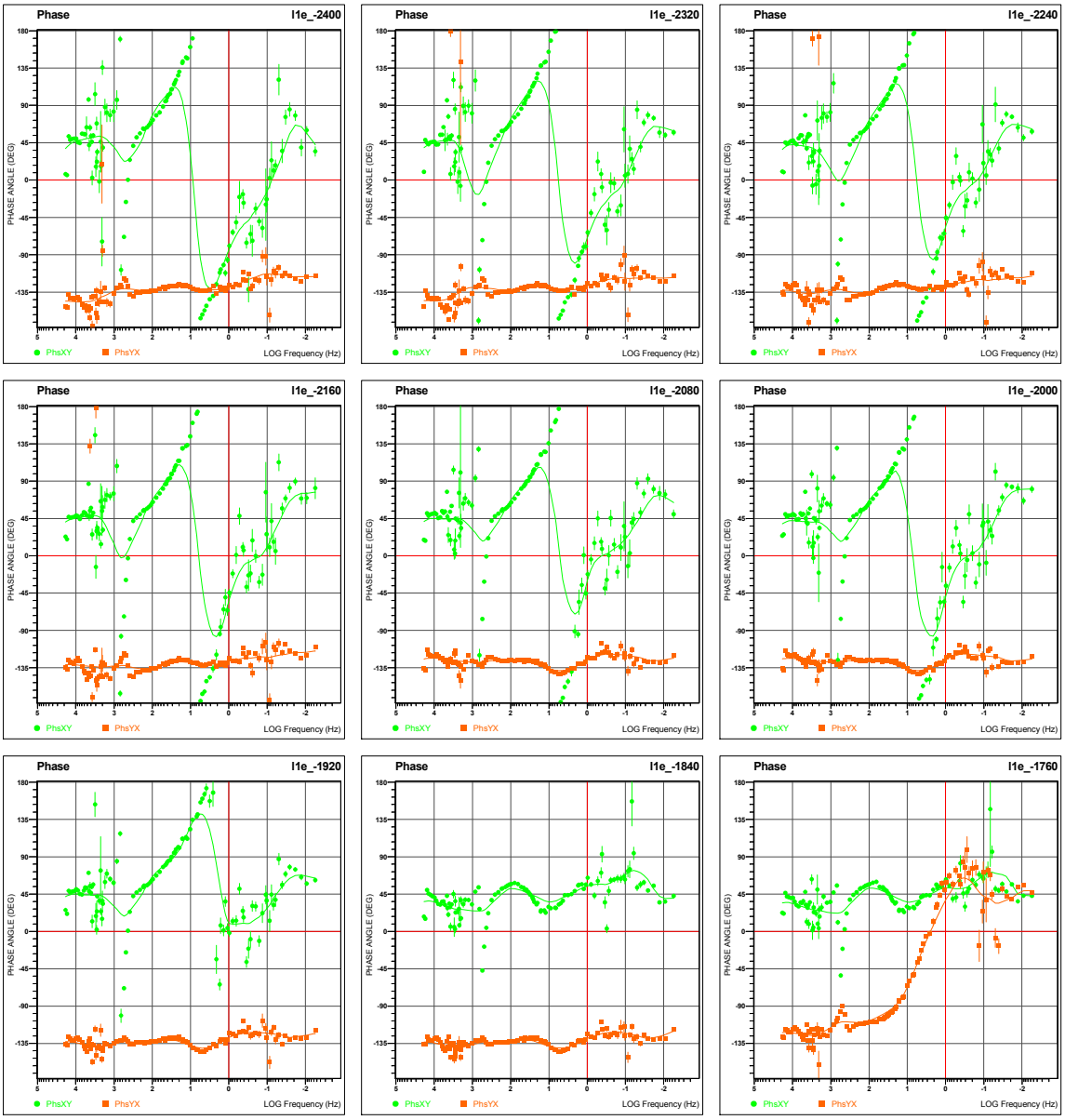

Line 1E – Phase Sounding Curves vs Frequency (1 of 3).

MODE XY (GREEN) DENOTES ELECTRICAL (**EX**) FIELD AND ORTHOGONAL MAGNETIC (**HY**) FIELD (=EX/HY)
MODE YX (ORANGE) DENOTES ELECTRICAL (**EY**) FIELD AND ORTHOGONAL MAGNETIC (**HX**) FIELD (=EY/HX)

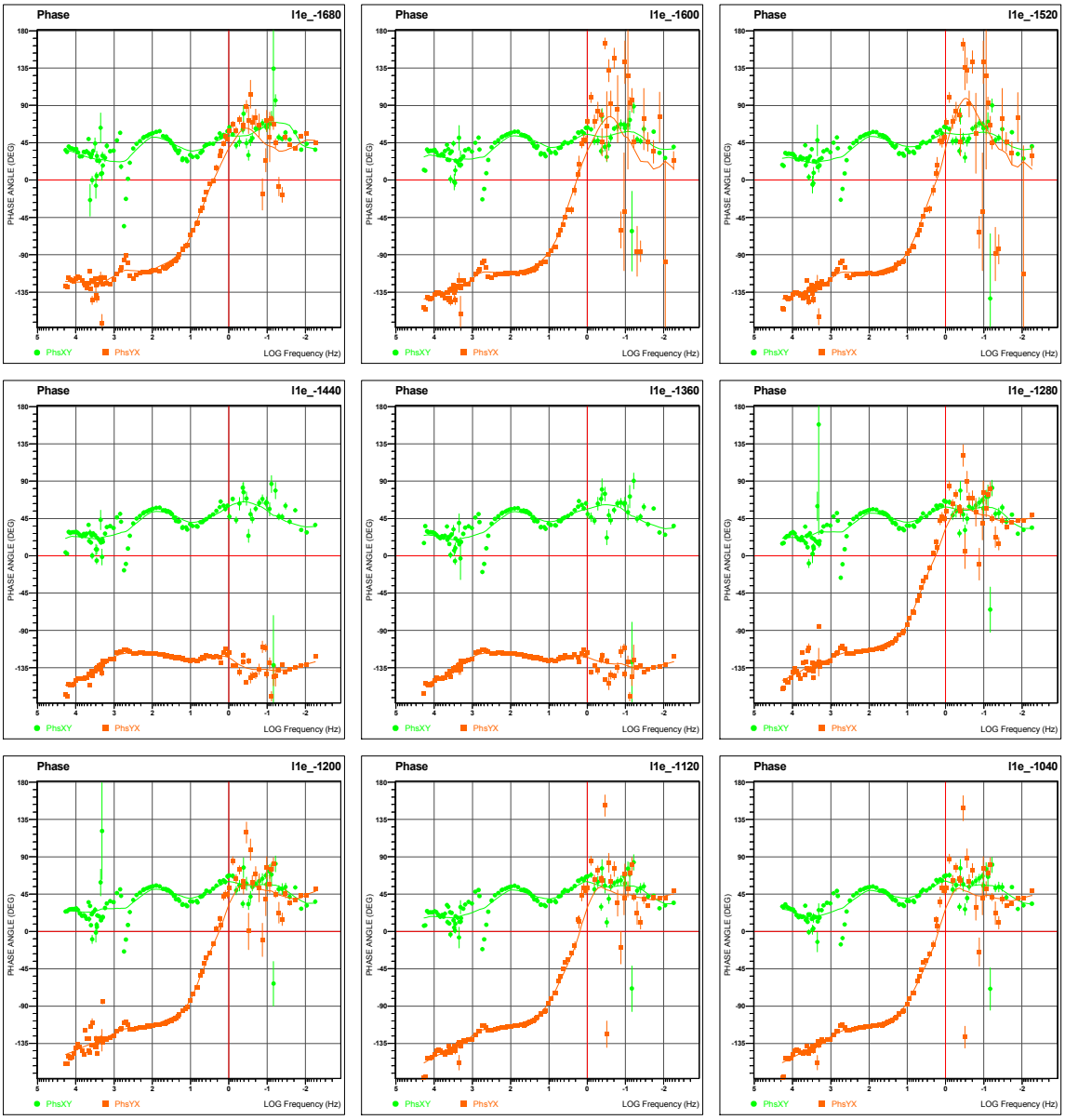

Line 1E – Phase Sounding Curves vs Frequency (2 of 3).

MODE XY (GREEN) DENOTES ELECTRICAL (**EX**) FIELD AND ORTHOGONAL MAGNETIC (**HY**) FIELD (=EX/HY)
MODE YX (ORANGE) DENOTES ELECTRICAL (**EY**) FIELD AND ORTHOGONAL MAGNETIC (**HX**) FIELD (=EY/HX)

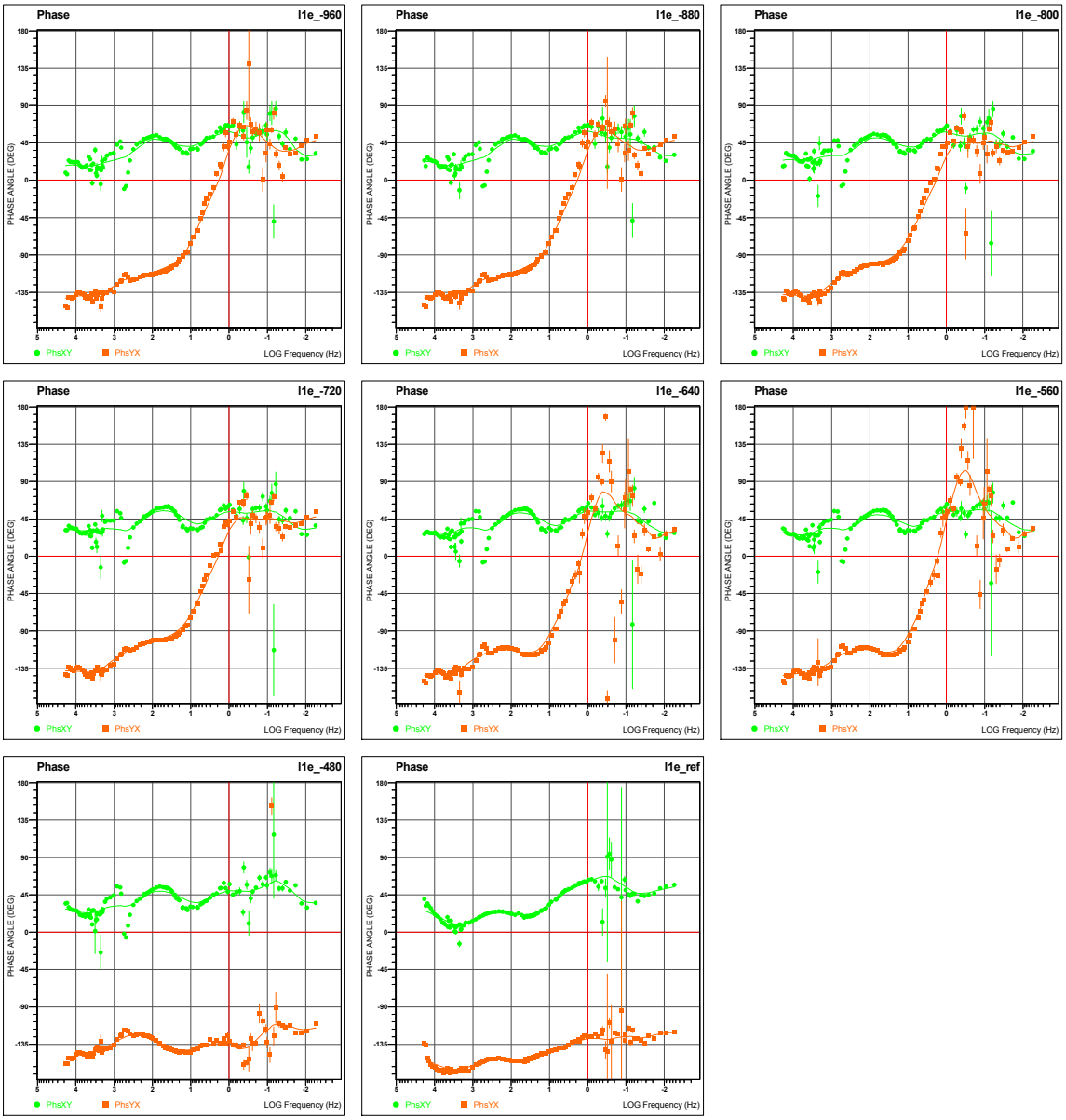

Line 1E – Phase Sounding Curves vs Frequency (3 of 3).

MODE XY (GREEN) DENOTES ELECTRICAL (**EX**) FIELD AND ORTHOGONAL MAGNETIC (**HY**) FIELD (=EX/HY)
MODE YX (ORANGE) DENOTES ELECTRICAL (**EY**) FIELD AND ORTHOGONAL MAGNETIC (**HX**) FIELD (=EY/HX)

D.2 LINE 2E

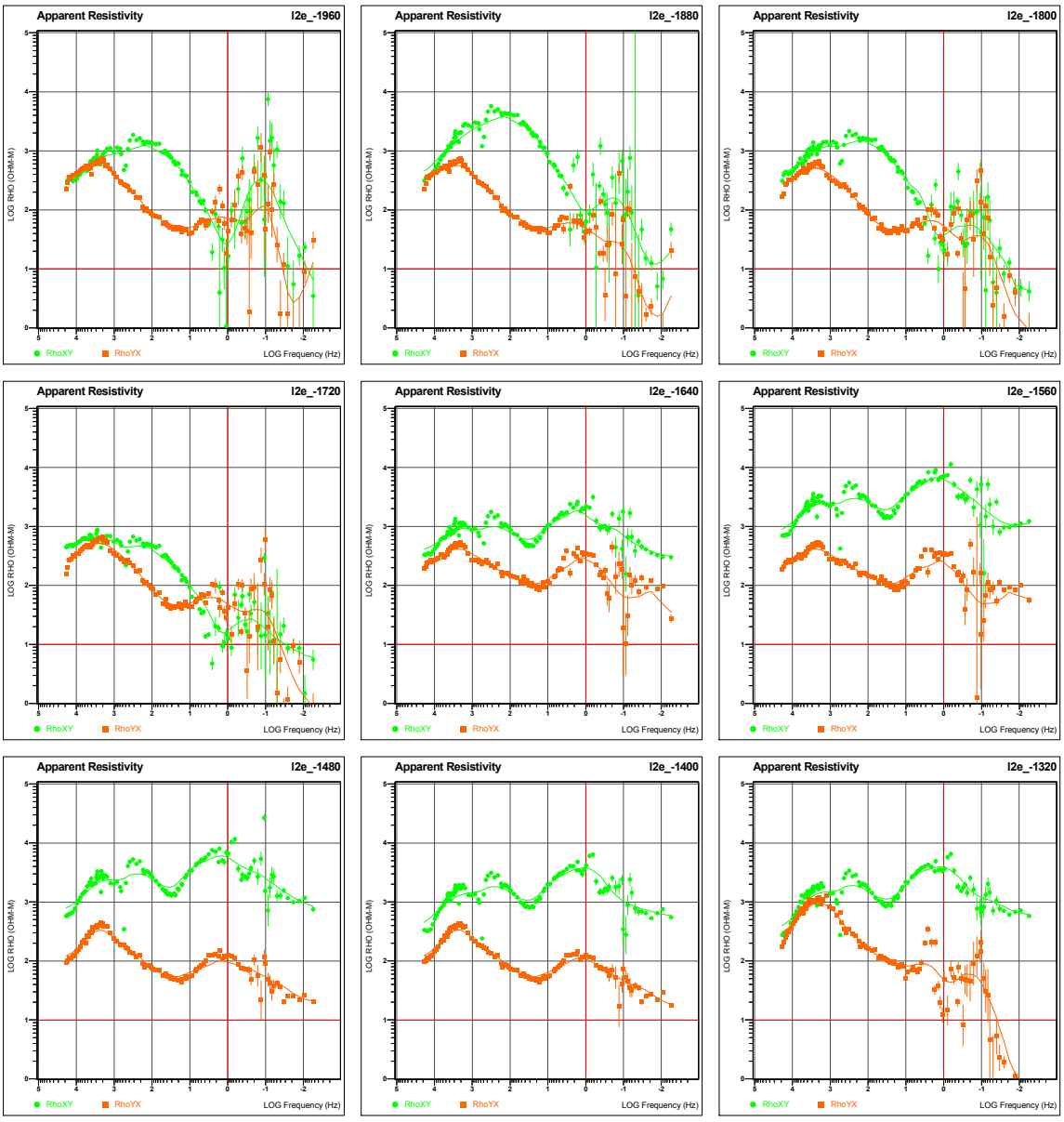

Line 2E – Apparent Resistivity Sounding Curves vs Frequency (1 of 3).

MODE XY (GREEN) DENOTES ELECTRICAL (**EX**) FIELD AND ORTHOGONAL MAGNETIC (**HY**) FIELD (=EX/HY)
MODE YX (ORANGE) DENOTES ELECTRICAL (**EY**) FIELD AND ORTHOGONAL MAGNETIC (**HX**) FIELD (=EY/HX)

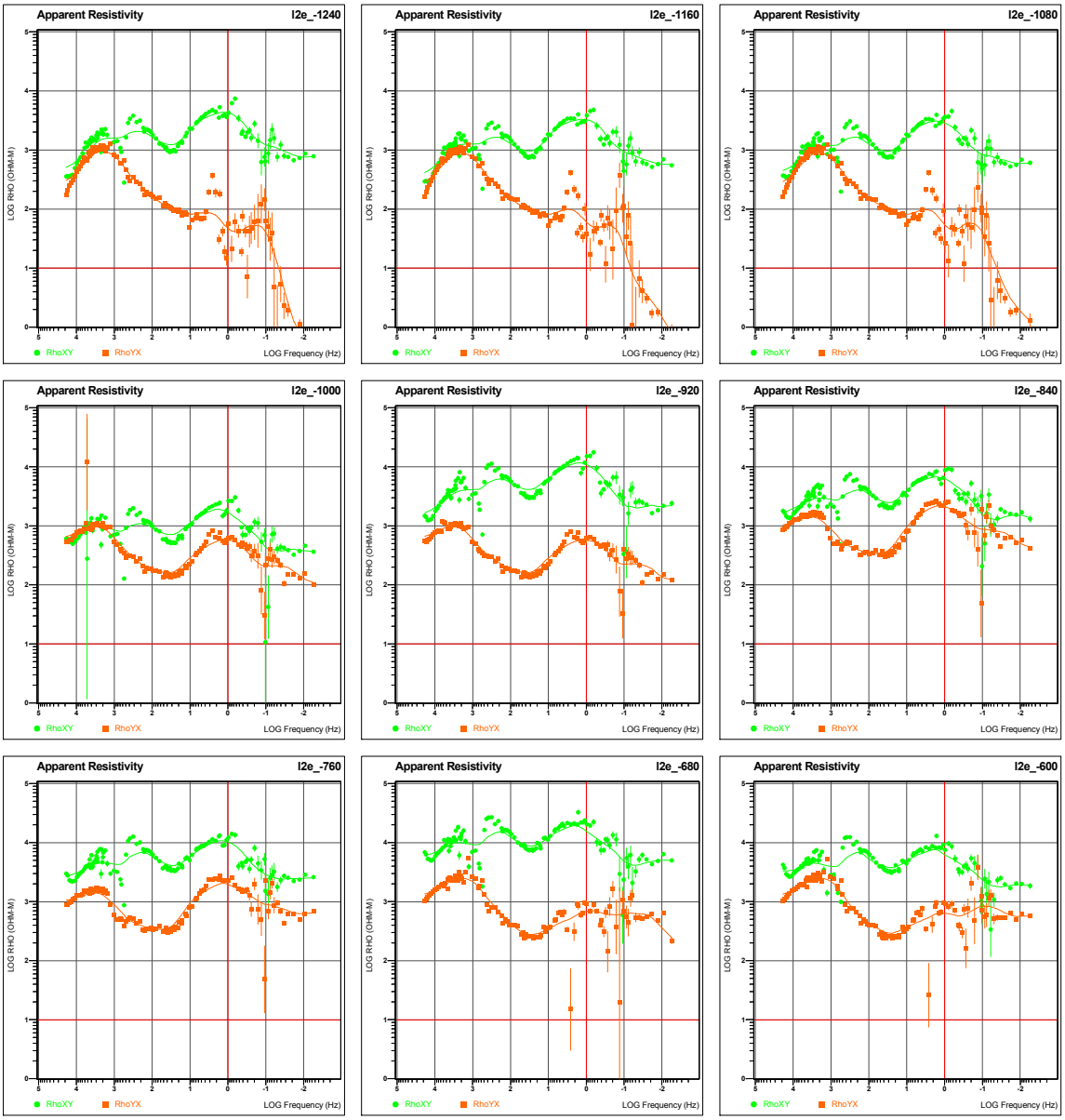

Line 2E – Apparent Resistivity Sounding Curves vs Frequency (2 of 3).

MODE XY (GREEN) DENOTES ELECTRICAL (**EX**) FIELD AND ORTHOGONAL MAGNETIC (**HY**) FIELD (=EX/HY)
MODE YX (ORANGE) DENOTES ELECTRICAL (**EY**) FIELD AND ORTHOGONAL MAGNETIC (**HX**) FIELD (=EY/HX)

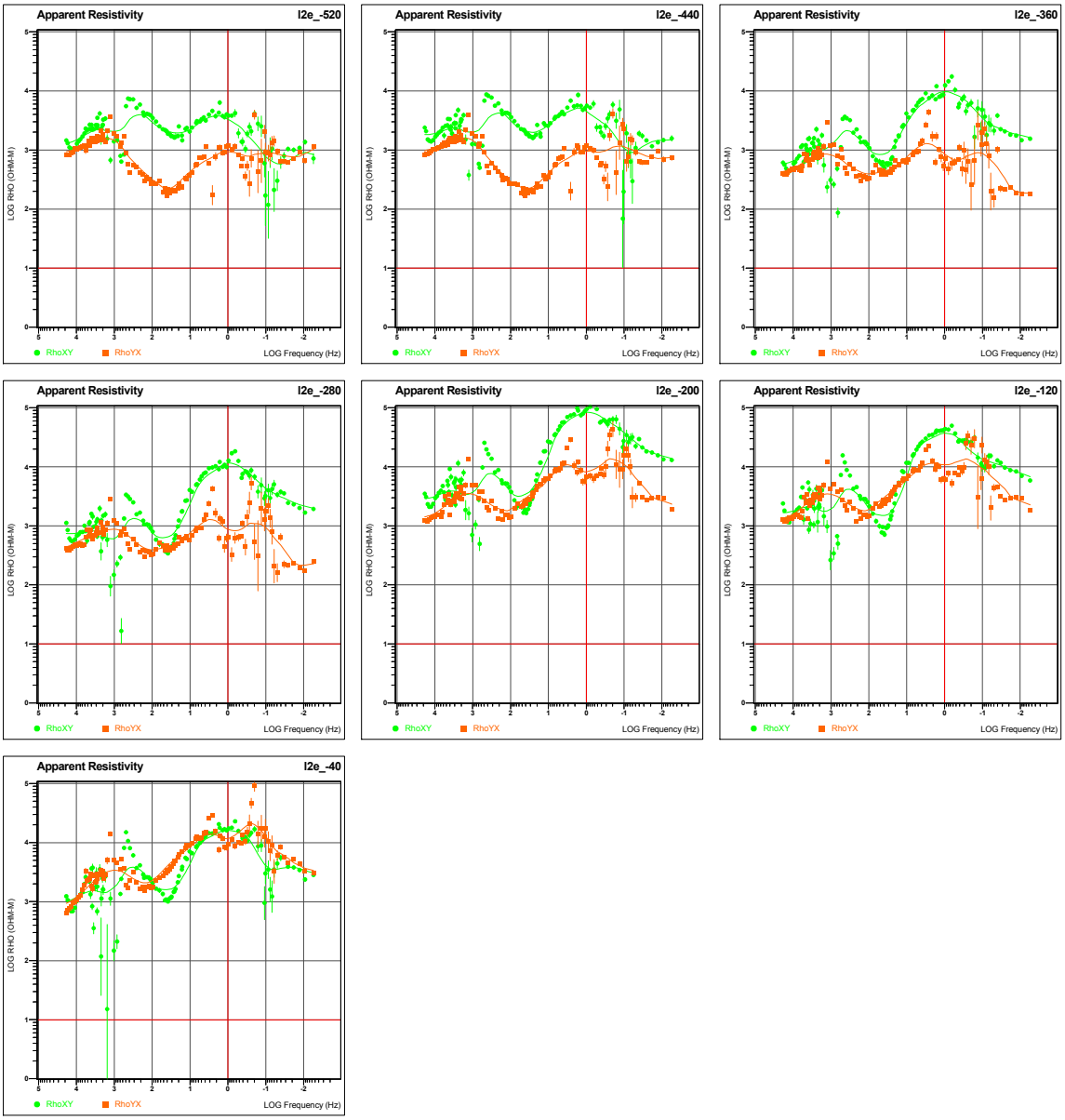

Line 2E – Apparent Resistivity Sounding Curves vs Frequency (3 of 3).

MODE XY (GREEN) DENOTES ELECTRICAL (**EX**) FIELD AND ORTHOGONAL MAGNETIC (**HY**) FIELD (=EX/HY)
MODE YX (ORANGE) DENOTES ELECTRICAL (**EY**) FIELD AND ORTHOGONAL MAGNETIC (**HX**) FIELD (=EY/HX)

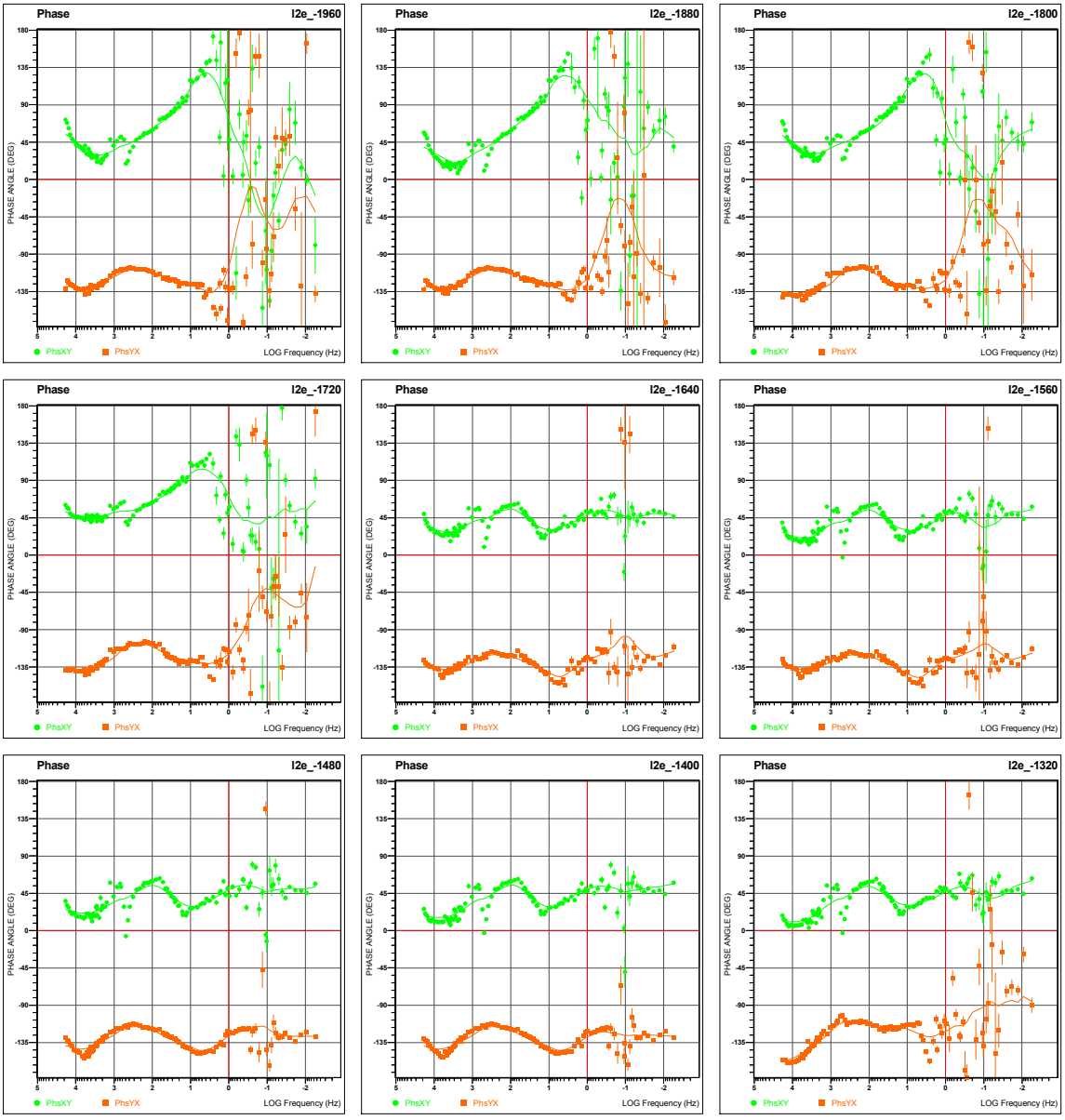

Line 2E – Apparent Resistivity Sounding Curves vs Frequency (1 of 3).

MODE XY (GREEN) DENOTES ELECTRICAL (**EX**) FIELD AND ORTHOGONAL MAGNETIC (**HY**) FIELD (=EX/HY)
MODE YX (ORANGE) DENOTES ELECTRICAL (**EY**) FIELD AND ORTHOGONAL MAGNETIC (**HX**) FIELD (=EY/HX)

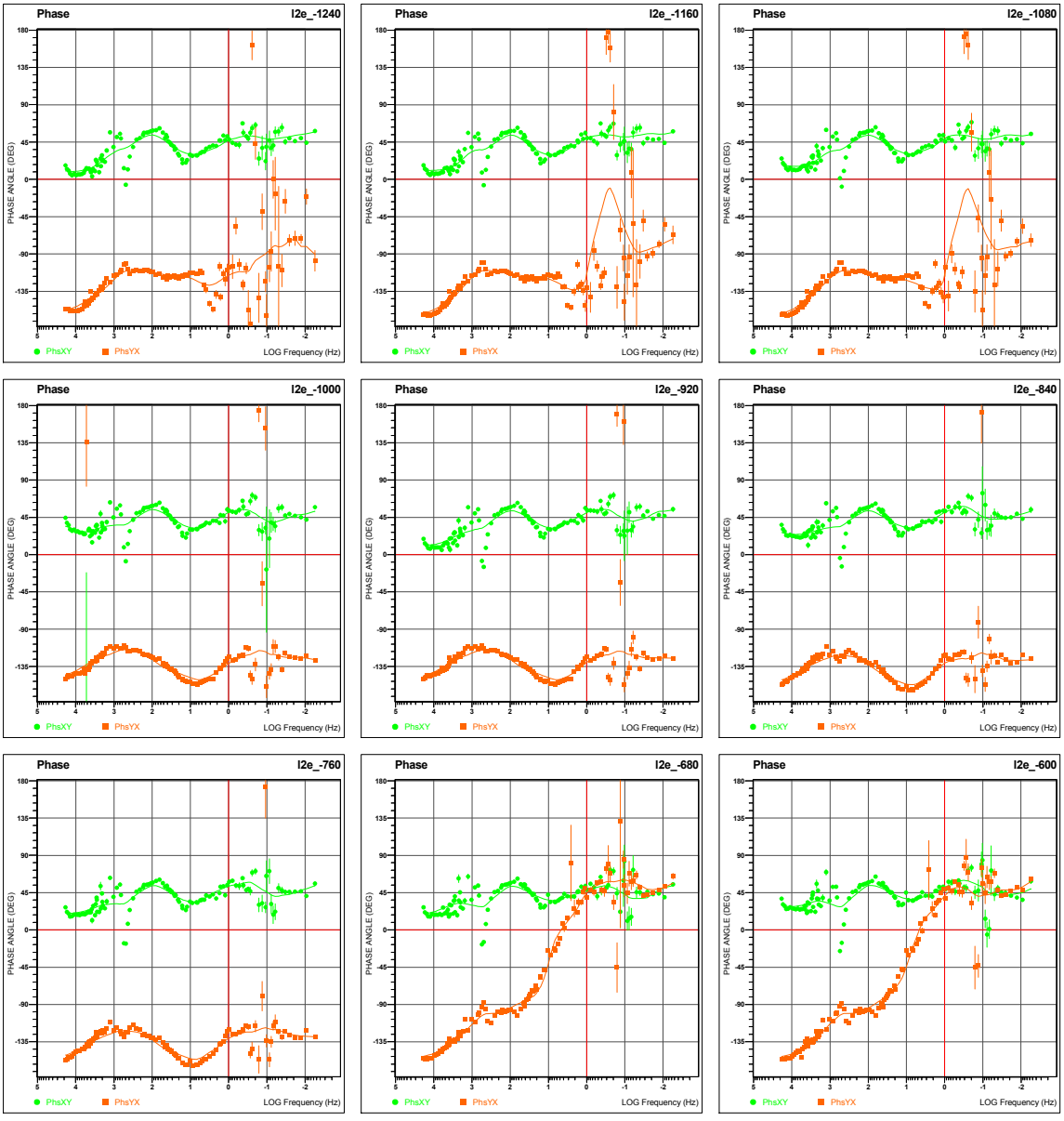

Line 2E – Apparent Resistivity Sounding Curves vs Frequency (2 of 3).

MODE XY (GREEN) DENOTES ELECTRICAL (**EX**) FIELD AND ORTHOGONAL MAGNETIC (**HY**) FIELD (=EX/HY)
MODE YX (ORANGE) DENOTES ELECTRICAL (**EY**) FIELD AND ORTHOGONAL MAGNETIC (**HX**) FIELD (=EY/HX)

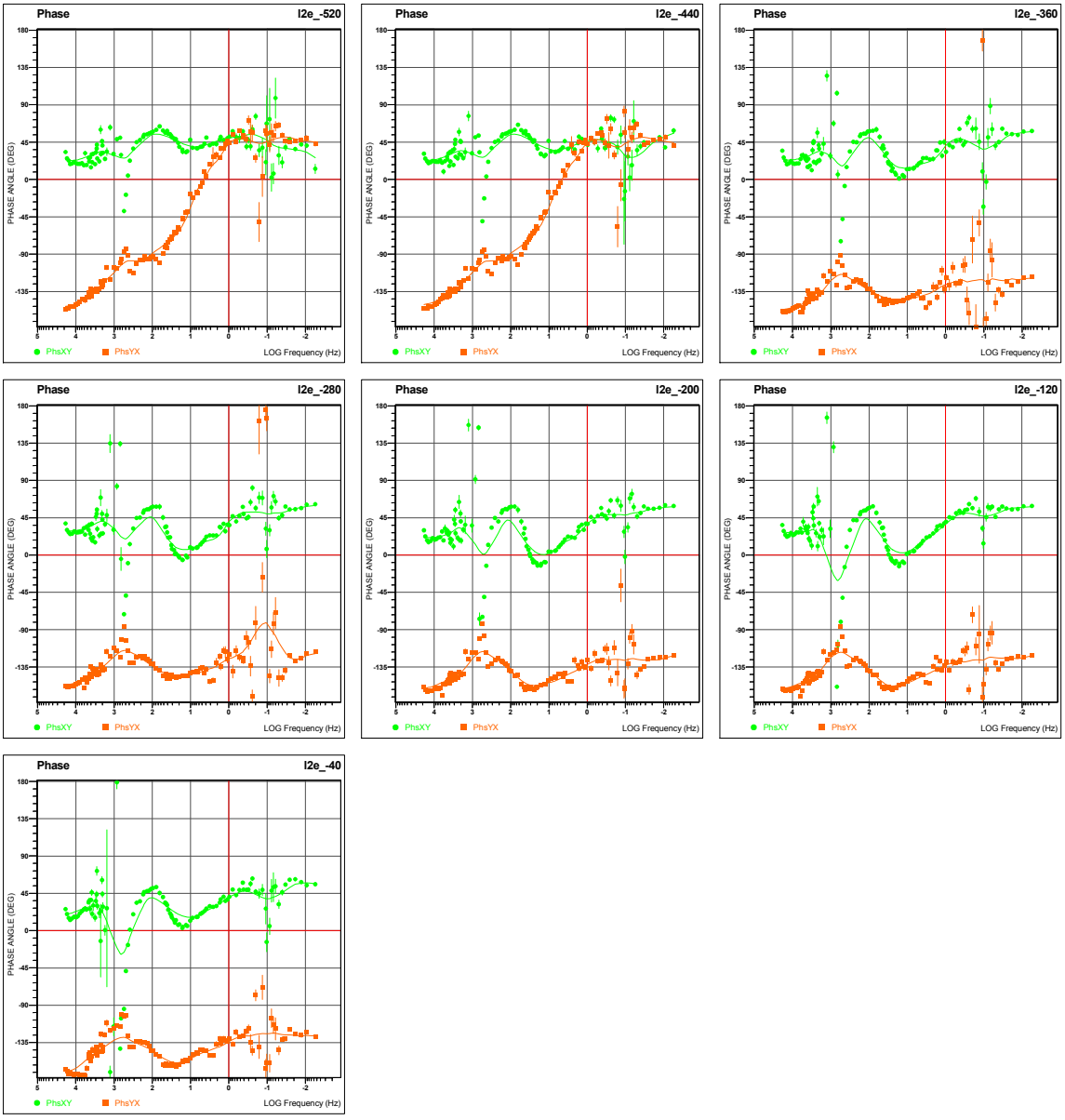

Line 2E – Apparent Resistivity Sounding Curves vs Frequency (3 of 3).

MODE XY (GREEN) DENOTES ELECTRICAL (**EX**) FIELD AND ORTHOGONAL MAGNETIC (**HY**) FIELD (=EX/HY)
MODE YX (ORANGE) DENOTES ELECTRICAL (**EY**) FIELD AND ORTHOGONAL MAGNETIC (**HX**) FIELD (=EY/HX)

E MT PSEUDO-SECTIONS OF FINAL PROCESSED DATA

E.1 LINE 1 E

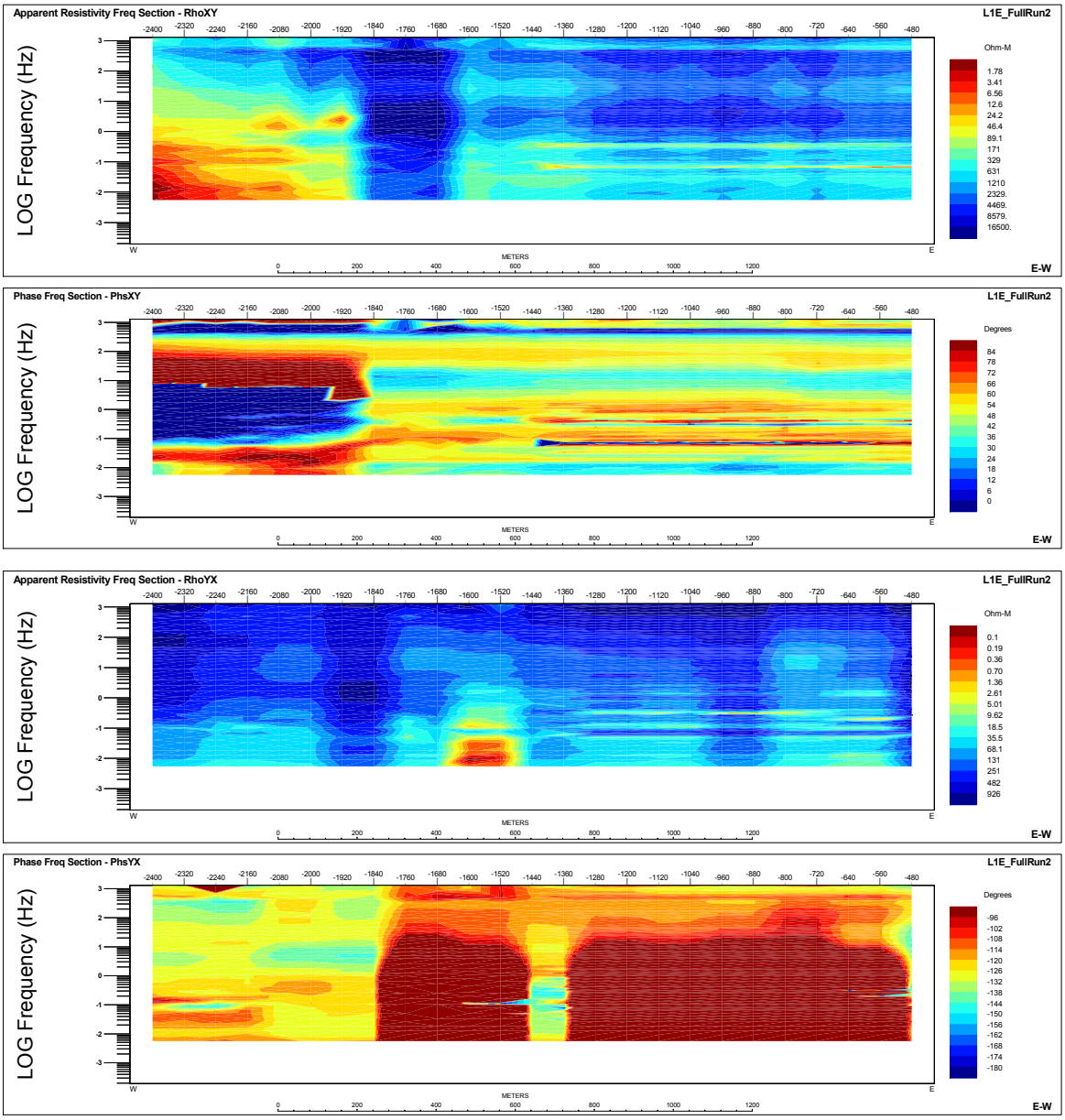

Line 0E – Apparent Resistivity and Phase (XY & YX) Pseudo-Section.

STRIP 1 (TOP): RHO XY – STRIP 2: PHASE XY – STRIP 3: RHO YX – STRIP 4 (BOTTOM): PHASE YX
WHERE XY DENOTES ELECTRICAL (**EX**) FIELD AND ORTHOGONAL MAGNETIC (**HY**) FIELD (=EX/HY)
AND YX DENOTES ELECTRICAL (**EY**) FIELD AND ORTHOGONAL MAGNETIC (**HX**) FIELD (=EY/HX)

E.2 LINE 2 E

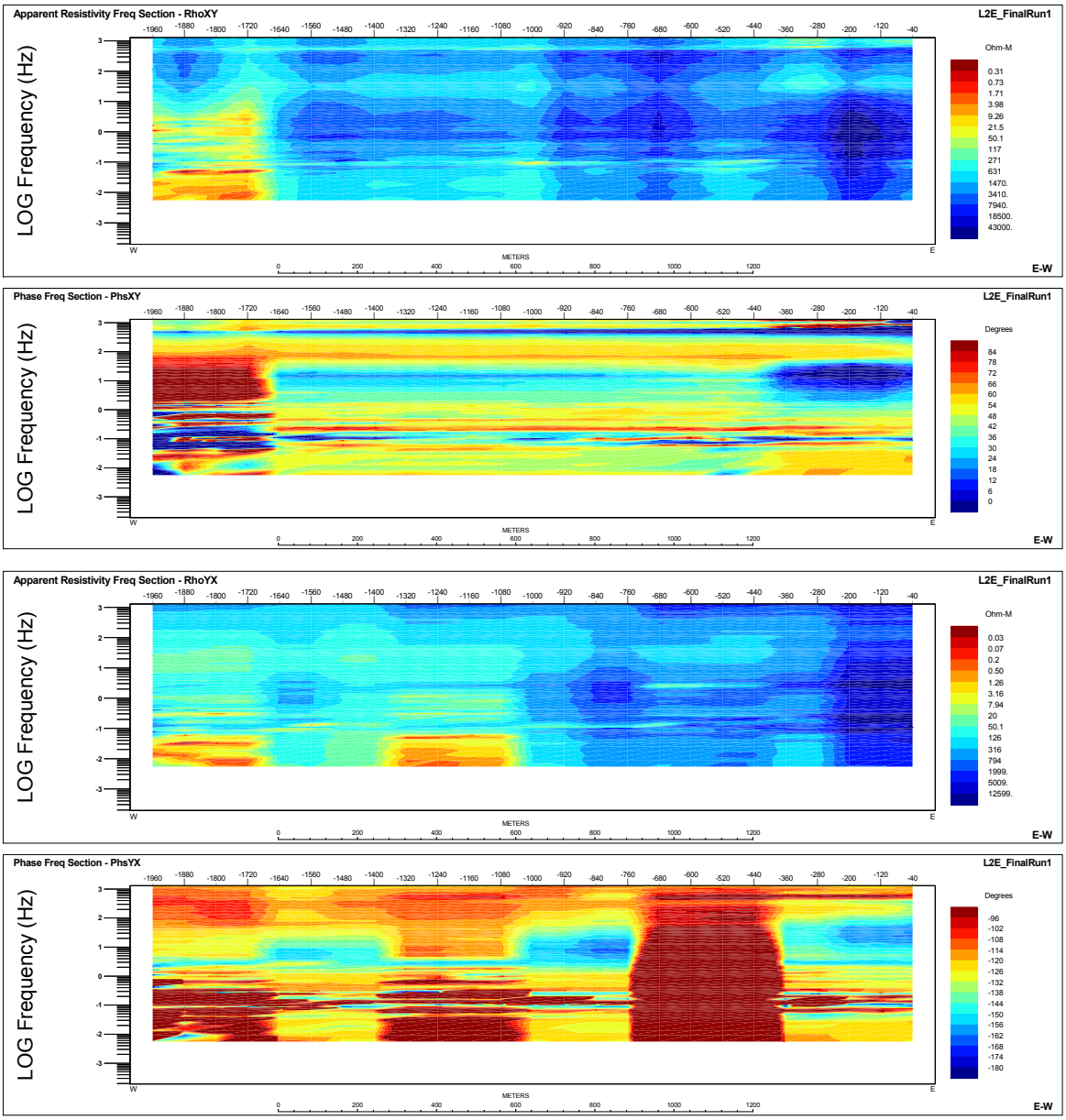

Line 2 E – Apparent Resistivity and Phase (XY & YX) Pseudo-Section.

STRIP 1 (TOP): RHO XY – STRIP 2: PHASE XY – STRIP 3: RHO YX – STRIP 4 (BOTTOM): PHASE YX
WHERE XY DENOTES ELECTRICAL (**EX**) FIELD AND ORTHOGONAL MAGNETIC (**HY**) FIELD (=EX/HY)
AND YX DENOTES ELECTRICAL (**EY**) FIELD AND ORTHOGONAL MAGNETIC (**HX**) FIELD (=EY/HX)

F PARALLEL SENSOR TEST

Project	CA00916T
Date:	December 9th, 2011
Report by:	Chris Furey
Staff:	Roger Sharpe Mojtaba Daneshvar
QuickLay Version	4.00.010
Common folder	V1.52
Datum:	UTM NAD 83 / Zone 17U
Station:	565102mE / 5388934mN
Coil Azimuth:	60° Magnetic
Magnetic Declination	10W

Results:

BF6-6276:	Poor coherency and higher phase
P30-1939:	Weak performance – coherency

F.1 LOW FREQUENCY COILS

Available Coils.

TS Strip	Manufacture	Serial #	Task for
1	Phoenix	P50-1963	Line Hx
2	Phoenix	P50-1969	Line Hy
3	Phoenix	P50-2114	Remote Hx
4	Phoenix	P50-2130	Line Spare
5	Phoenix	P50-2131	Remote Hy
6	Phoenix	P50-9501	Remote Spare

Processing Parameters.

Parameters	Values
PSD Method	Welch
Window	Hanning
Window Length	2048
Segment Overlap	50%

F.1.1 TEST RESULTS: 120SPS

NetEvent:	9039.000011
Sample Rate:	120sps
TS Length:	72 000 Samples (10 minutes)

Results:

All Coils Seem to be tracking consistently but not as coherently as I would have expected

Time Series

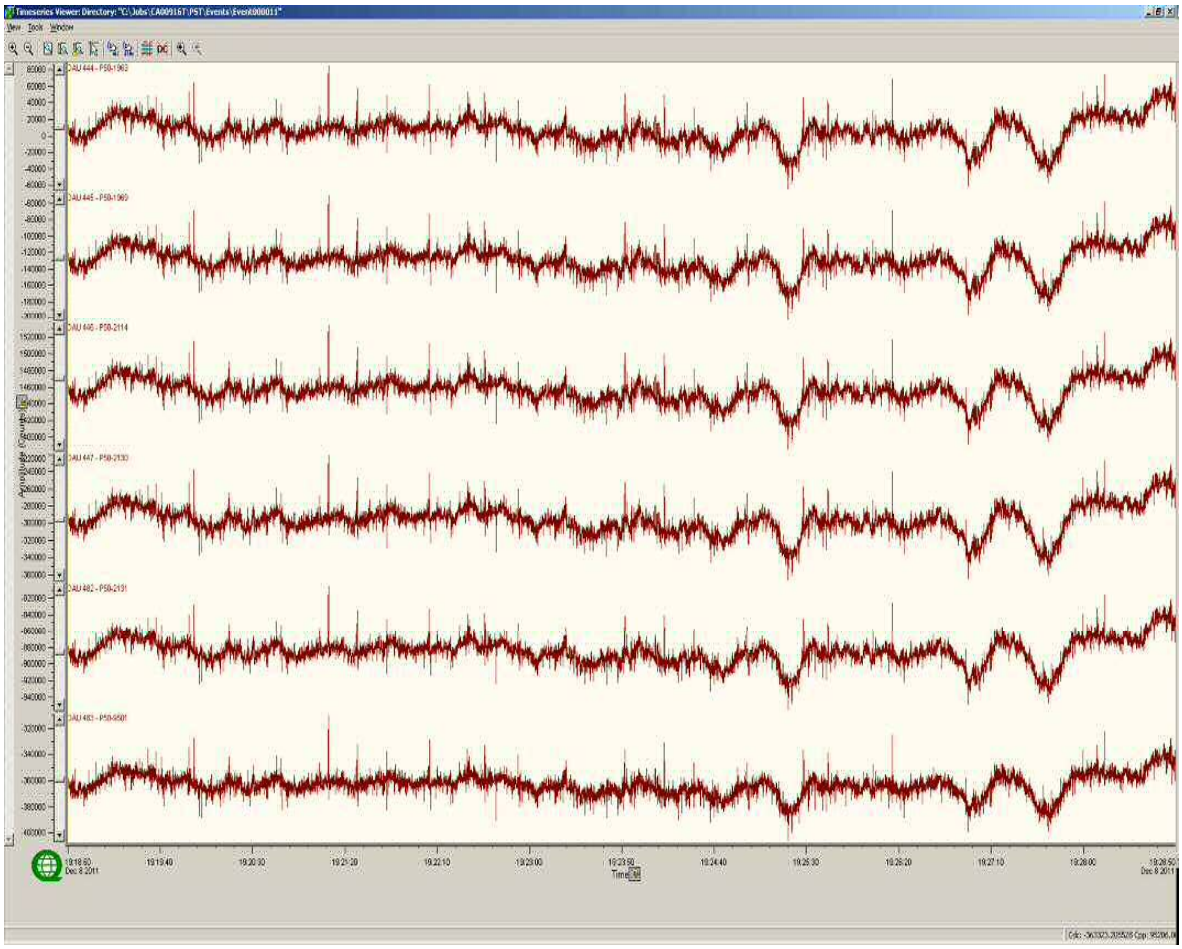

Complete time series @ 120sps.

Low Frequency Coil Results **Coherency to P50-1963(Blue)**

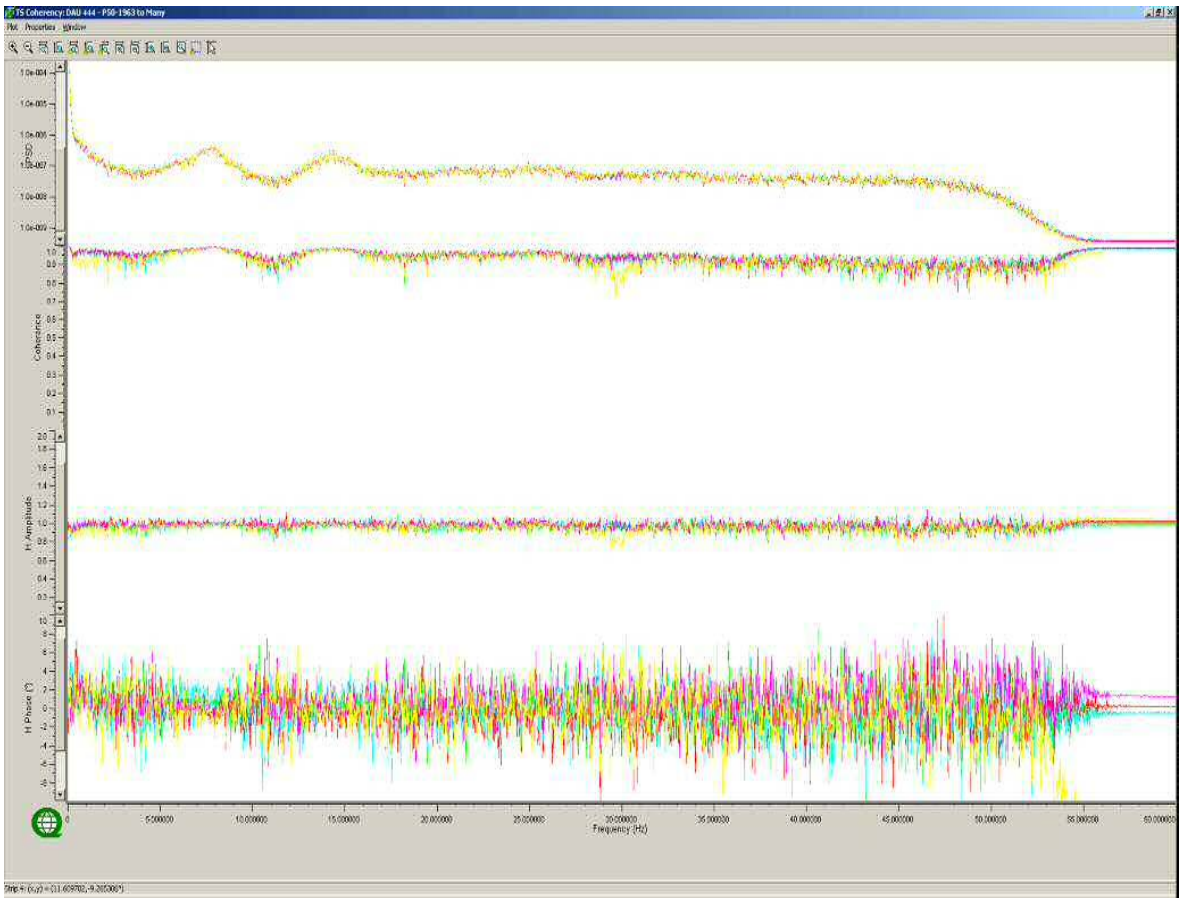

From top to bottom: PSD of channels and Coherency and Response Function (Amplitude and Phase) compared to Reference Channel – Linear frequency scale.

Colour	Channel	Notes
Blue	P50-1963	
Green	P50-1969	
Red	P50-2114	
Cyan	P50-2130	Cyan appears to be slightly off compared to the other coils and shows a comparatively low coherency, this will be used as the line spare
Magenta	P50-2131	
Yellow	P50-9501	Shows the lowest coherency especially ~30Hz where it dips from the other coils, will be used as spare for remote

Low Frequency Coil Results (continued) **Coherency to P50-1963(Blue)**

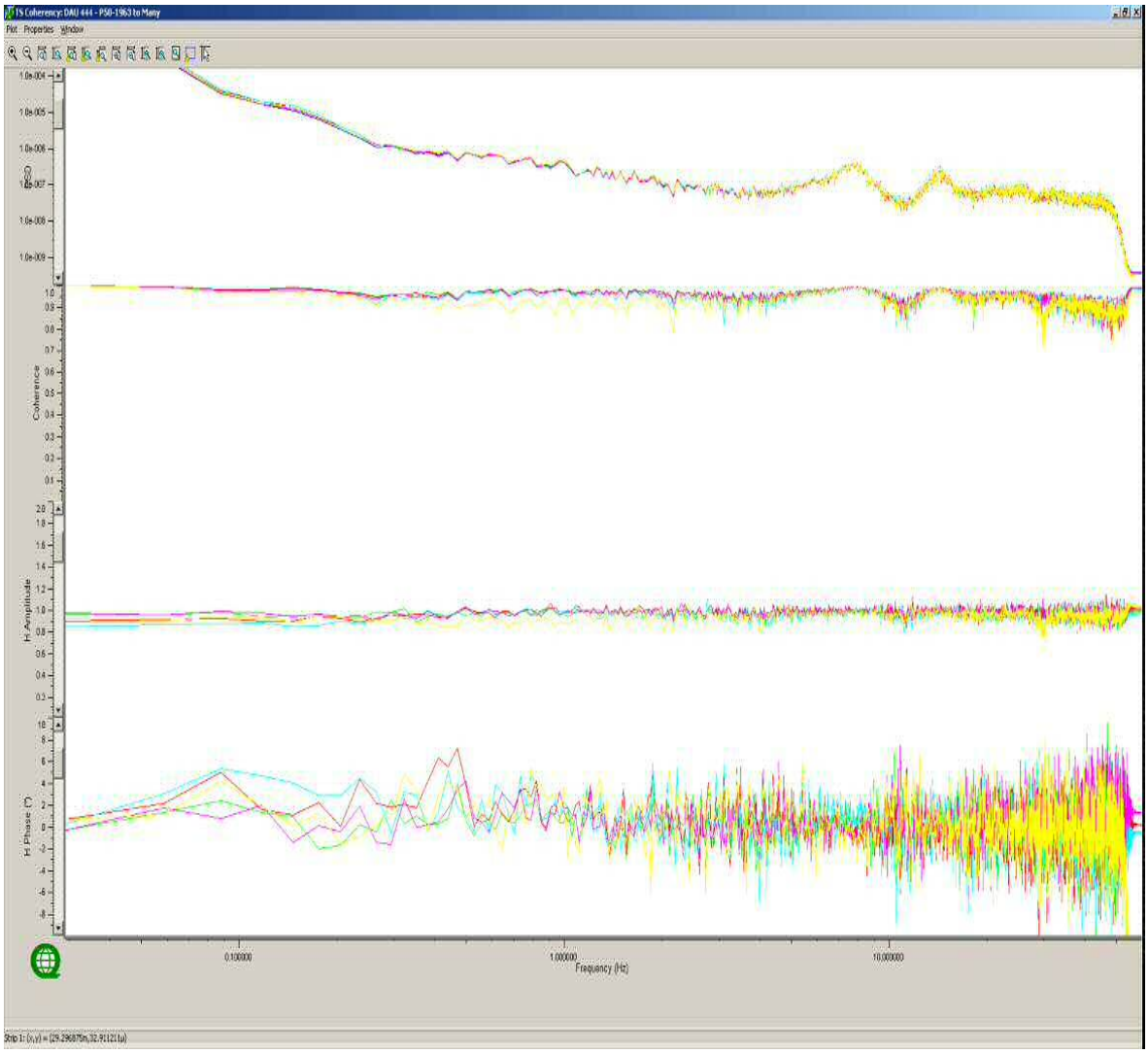

From top to bottom: PSD of channels and Coherency and Response Function (Amplitude and Phase) compared to Reference Channel – Logarithmic frequency scale.

Colour	Channel	Notes
Blue	P50-1963	
Green	P50-1969	
Red	P50-2114	
Cyan	P50-2130	
Magenta	P50-2131	
Yellow	P50-9501	

F.2 HIGH FREQUENCY COILS

Available Coils.

TS Strip	Manufacture	Serial #	Task for
1	EMI	BF6-0110	Line Hx
2	Phoenix	P30-1939	Ln Spare
3	Phoenix	P30-1971	Line Hy
4	Phoenix	P30-1972	Remote Hx
5	Phoenix	P30-1973	Remote Hy
6	EMI	BF6-6276	Rm Spare

Processing Parameters.

Parameters	Values
PSD Method	Welch
Window	Hanning
Window Length	2048
Segment Overlap	50%

F.2.1 TEST RESULTS: 48KSPS

NetEvent:	9039.000014
Sample Rate:	48ksps
TS Length:	1 500 000 samples (~31s)

Results:

Noticeable variations from the trend seen in BF6-6276 and P30-1939, these coils will be reserved as spares with the EMI to be used last or at the remote.

Time Series

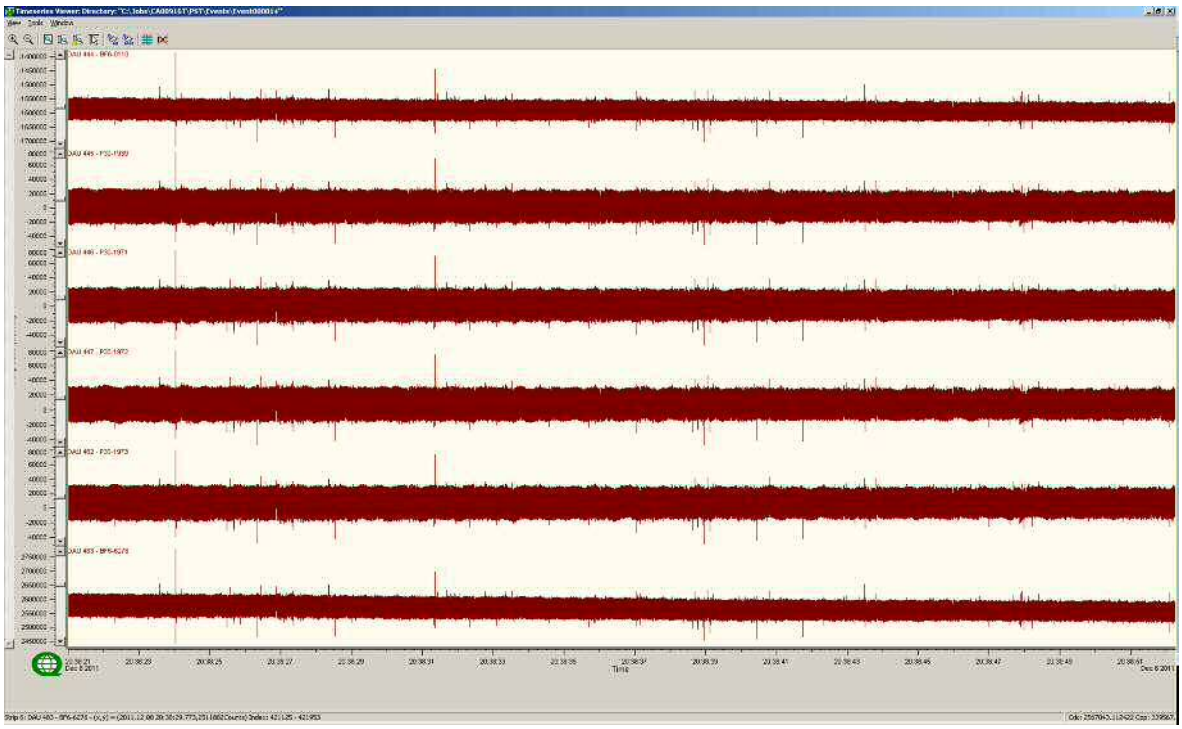

Complete time series at 48ksps.

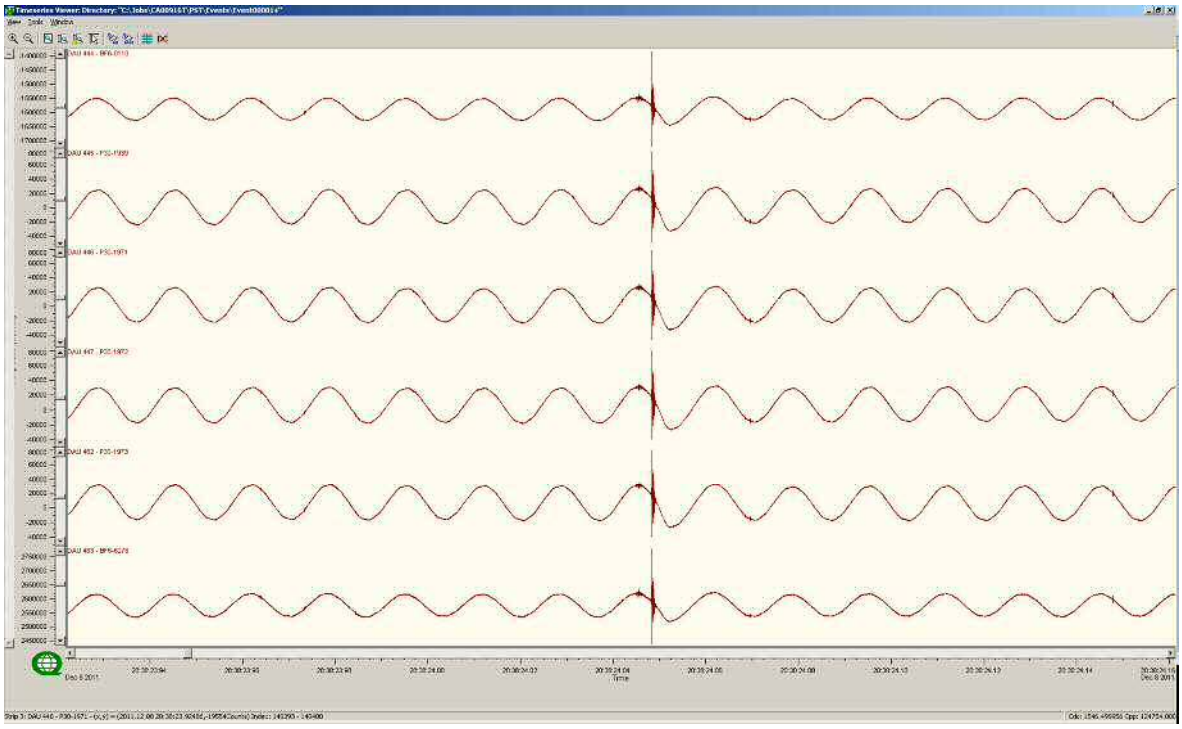

Time series focused in on ~1s at 48ksps.

High Frequency (48k) Coil Results **Coherency to BF6-0110 (Blue)**

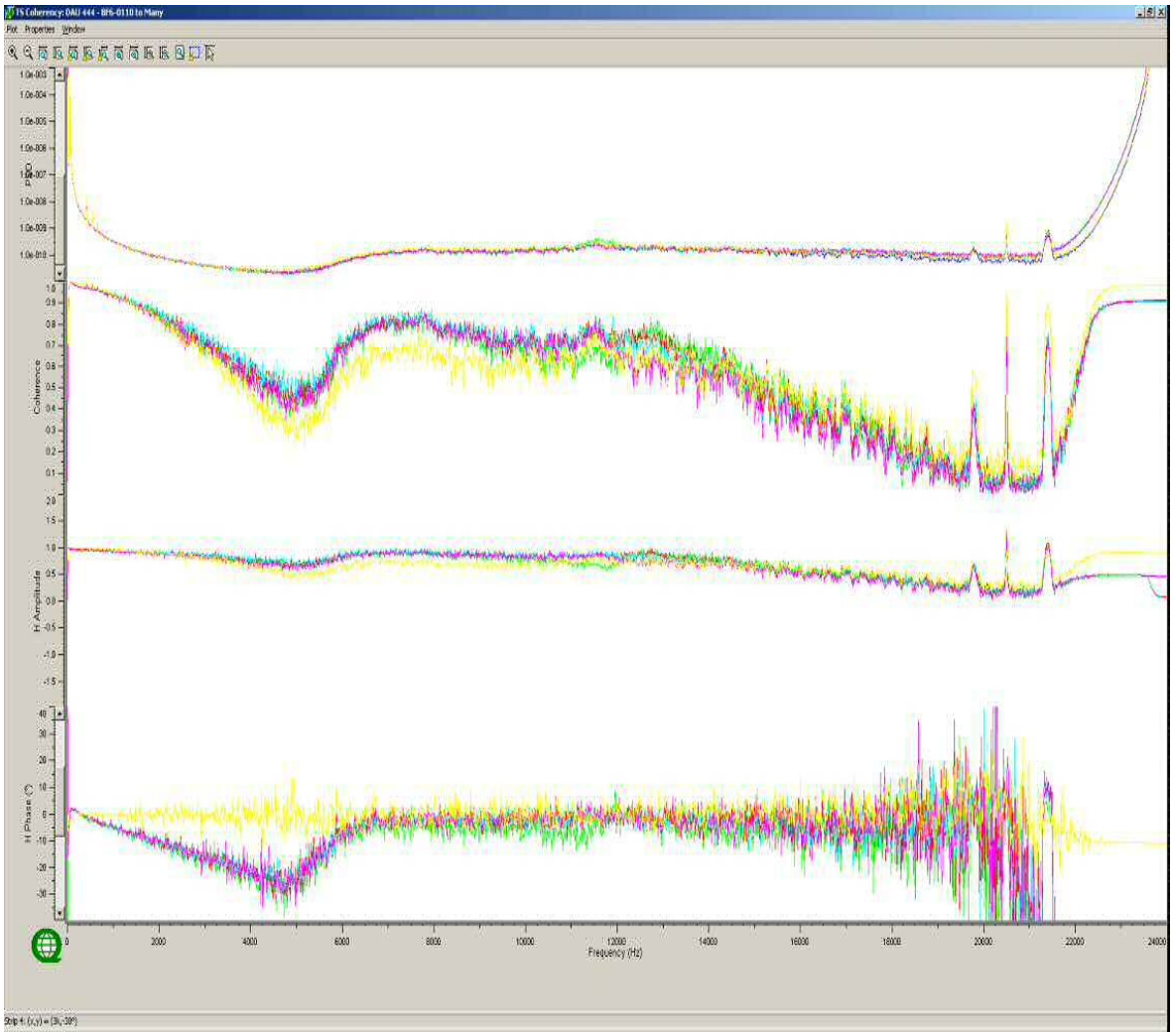

From top to bottom: PSD of channels and Coherency and Response Function (Amplitude and Phase) compared to Reference Channel – Linear frequency scale.

Colour	Channel	Notes
Blue	BF6-0110	
Green	P30-1939	Less coherent, shift in coherency ~1200Hz
Red	P30-1971	
Cyan	P30-1972	
Magenta	P30-1973	
Yellow	BF6-6276	Less coherent, dropping off ~400Hz

High Frequency (48k) Coil Results (Continued) **Coherency to BF6-0110 (Blue)**

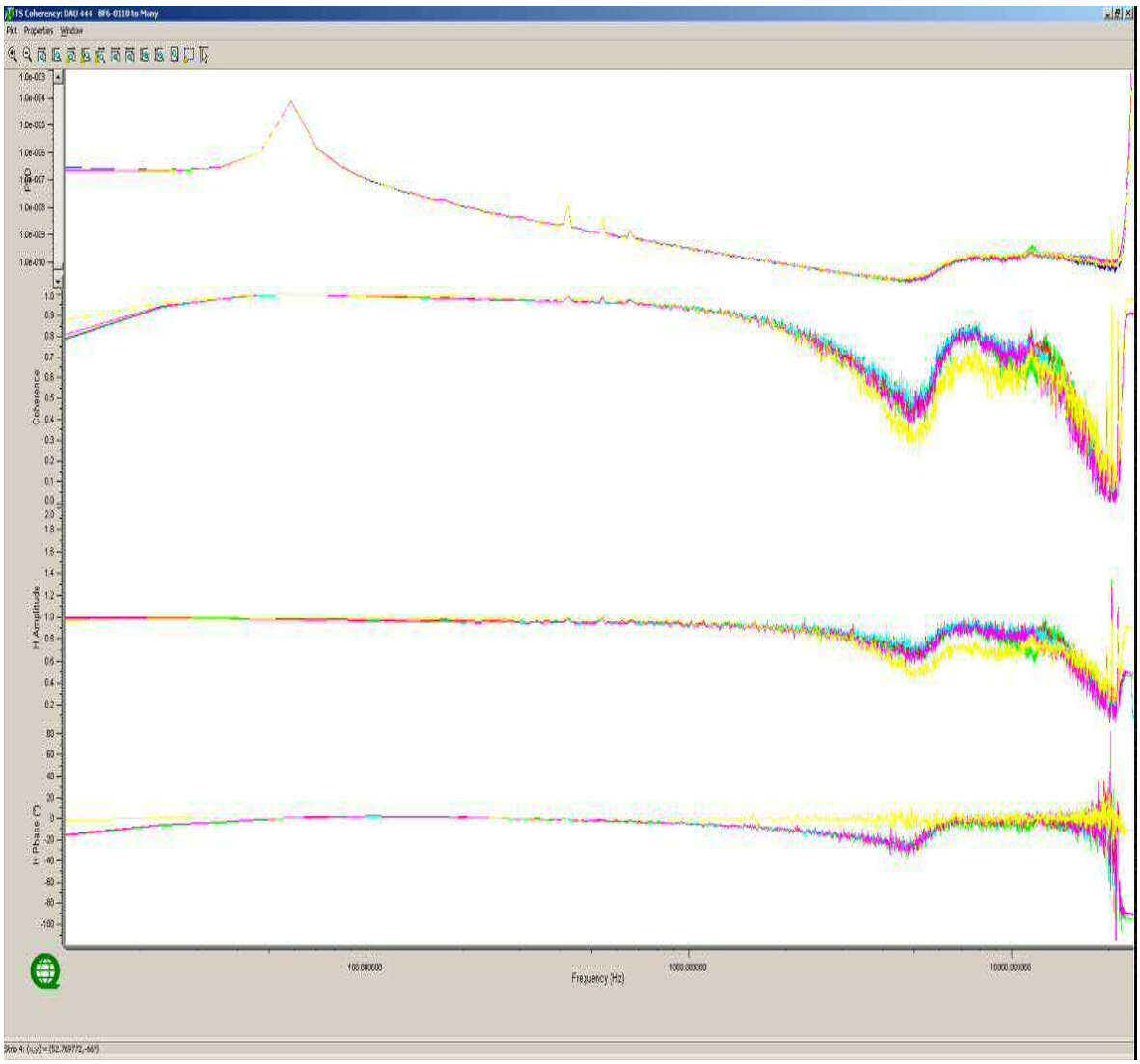

From top to bottom: PSD of channels and Coherency and Response Function (Amplitude and Phase) compared to Reference Channel – Logarithmic frequency scale.

Colour	Channel	Notes
Blue	BF6-0110	All ok
Green	P30-1939	Deviates from the trend at ~1000Hz (Ln Spare)
Red	P30-1971	
Cyan	P30-1972	
Magenta	P30-1973	
Yellow	BF6-6276	Deviates from the trend at ~500Hz (Rm Spare)

F.2.2 TEST RESULTS: 12KSPS

NetEvent:	9039.000015
Sample Rate:	12ksps
TS Length:	1,500,000 samples (~2min)

Results:

BF6-6276	Higher phase than the other coils

Time Series

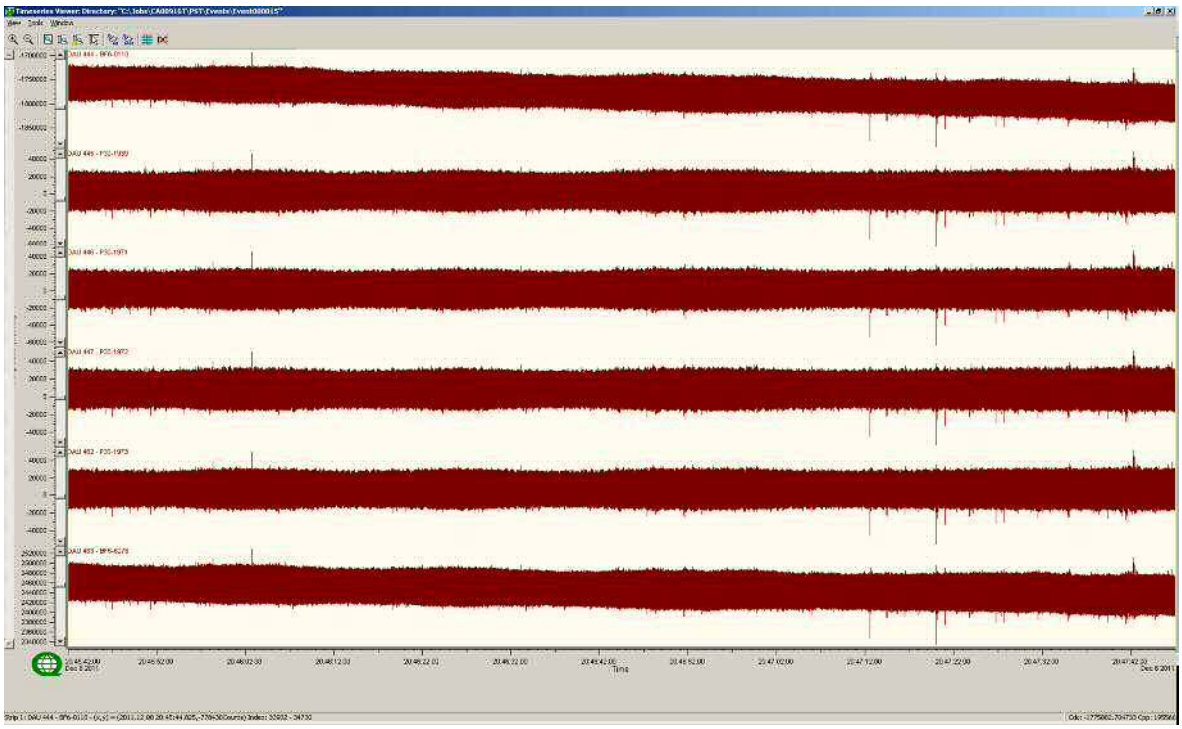

Complete time series 12ksps.

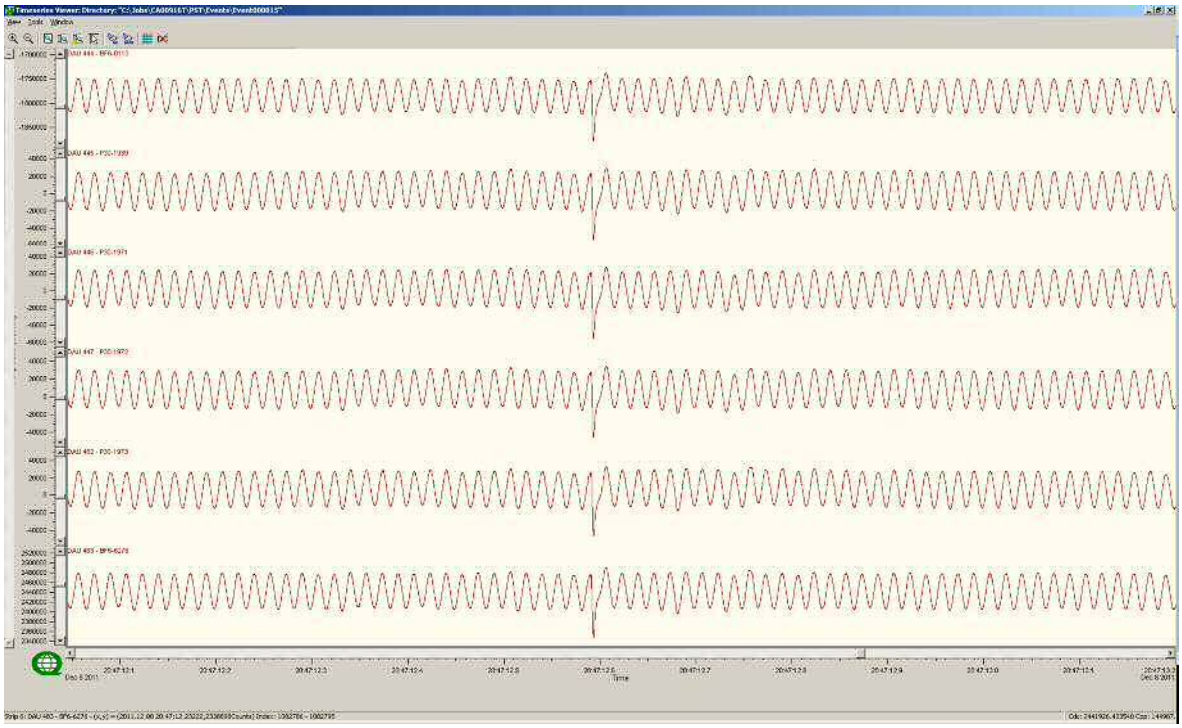

Focus on 1s of the time series 12ksps.

High Frequency (12k) Coil Results ***Coherency to BF6-0110 (Blue)***

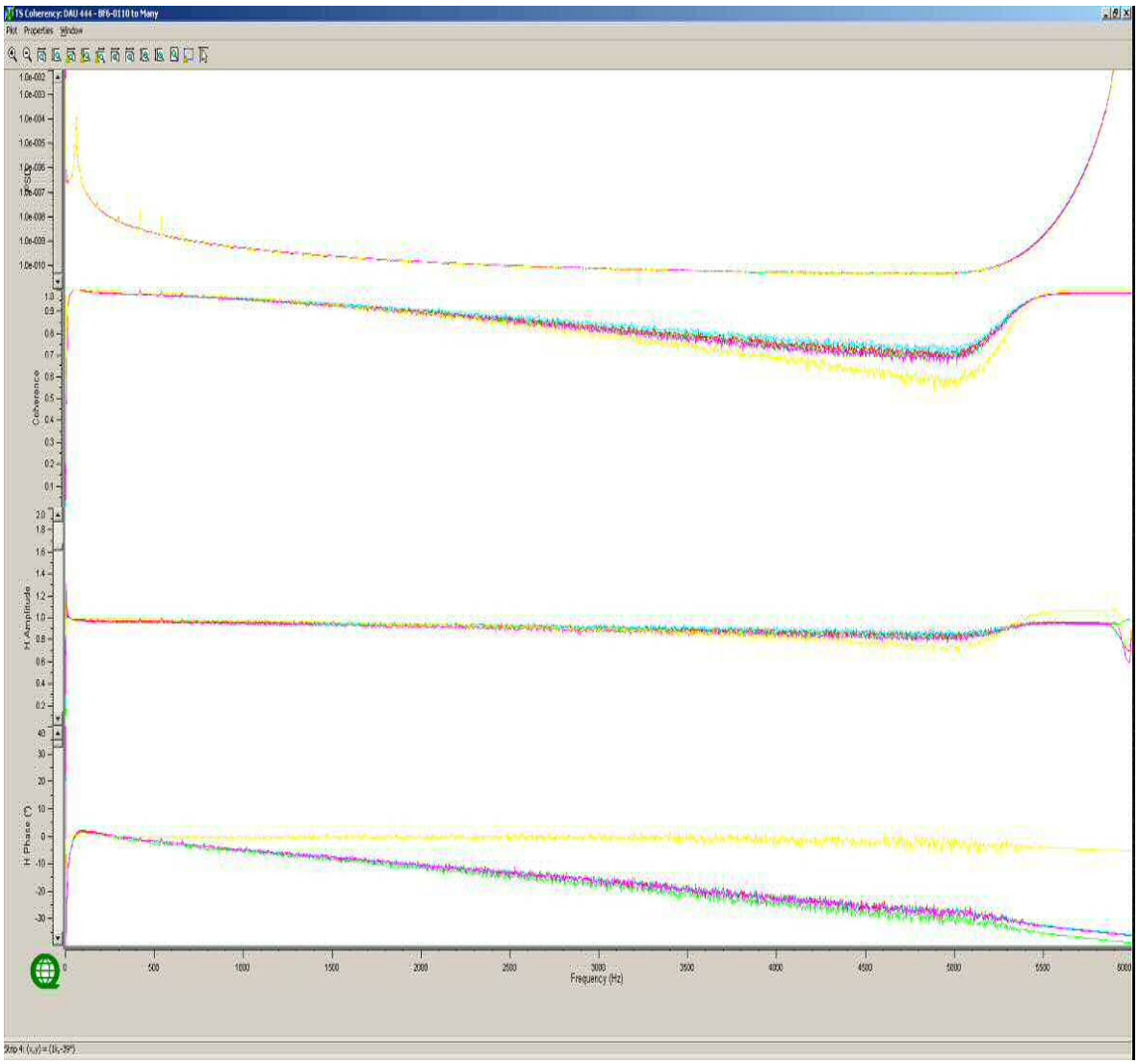

<u>From top to bottom: PSD of channels and Coherency and Response Function (Amplitude and Phase) compared to Reference Channel – Linear frequency scale.</u>

Colour	Channel	Notes
Blue	BF6-0110	
Green	P30-1939	
Red	P30-1971	
Cyan	P30-1972	
Magenta	P30-1973	
Yellow	BF6-6276	Phase response much different from other coils

High Frequency (12k) Coil Results (Continued) **Coherency to BF6-0110 (Blue)**

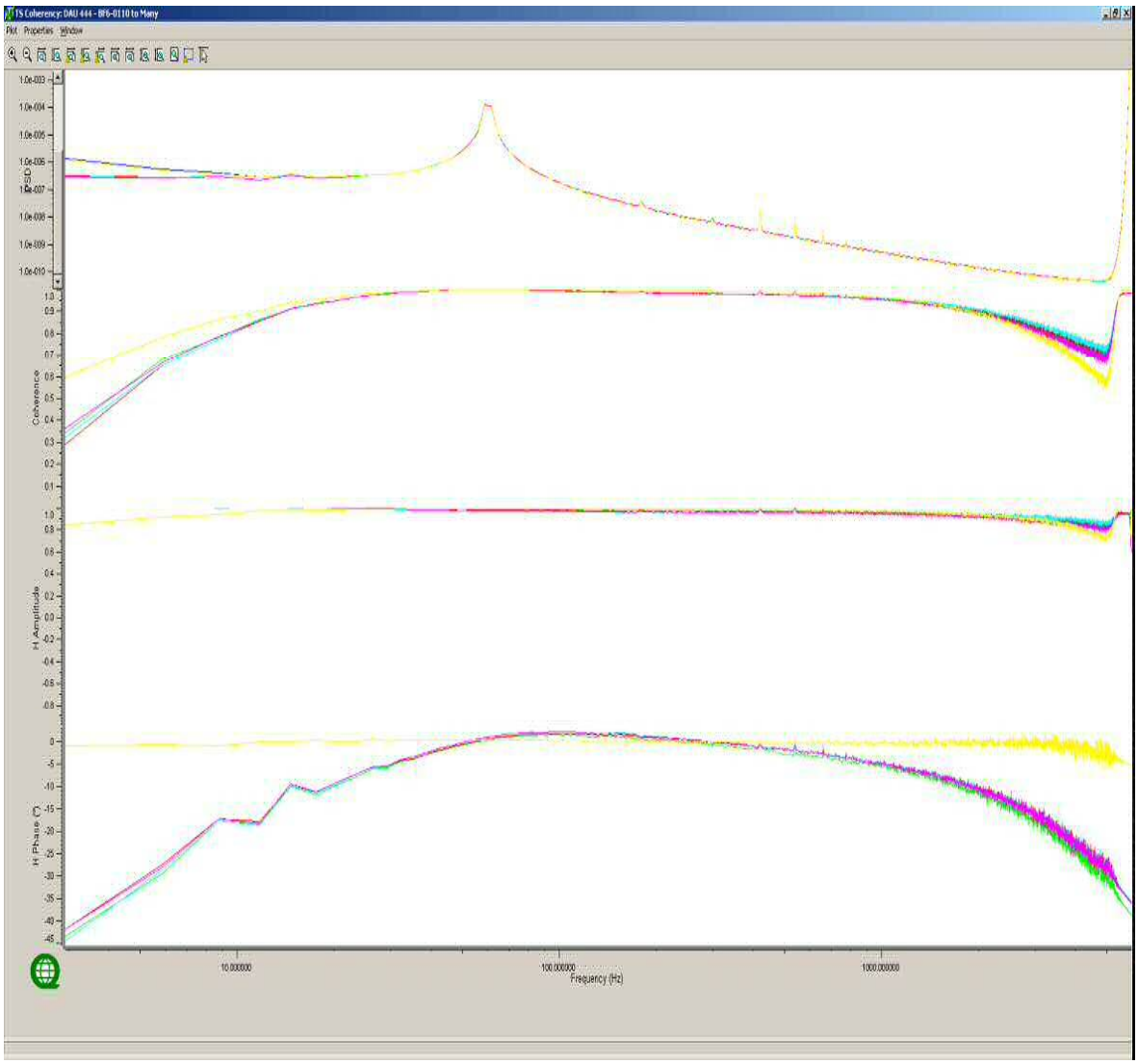

From top to bottom: PSD of channels and Coherency and Response Function (Amplitude and Phase) compared to Reference Channel – Logarithmic frequency scale.

Colour	Channel	Notes
Blue	BF6-0110	
Green	P30-1939	
Red	P30-1971	
Cyan	P30-1972	
Magenta	P30-1973	
Yellow	BF6-6276	Coherency drops off at the highest frequencies

G MT REMOTE TEST – UNREFERENCED DATA

Project	**CA00916T**		
Date:	December 9st, 2011		
Report by:	Mojtaba Daneshvar		
QuickLay Version	4.00.041		
Common folder	V1.52.00		
Remote Location:	565102mE / 5388934mN (WGS 84 / Zone 17 U)		
Mag Declination:	10°West		
Sensor Azimuth:	**Ex**	00°North	dipole = 80m
	Ey	90° West	dipole = 80m
	Hx	00° North	
	Hy	90° East	
Culture:	Non		

Details below ALL the data used and processed for the test

TITAN DATA

Sample Rate	Net Events	TS Length	Observations
48kps	9039.000022	31s	Noisy Time Series
12kps	9039.000023	2.05 min	Noisy Time Series
120sps	9039.000025	10 min	N/A

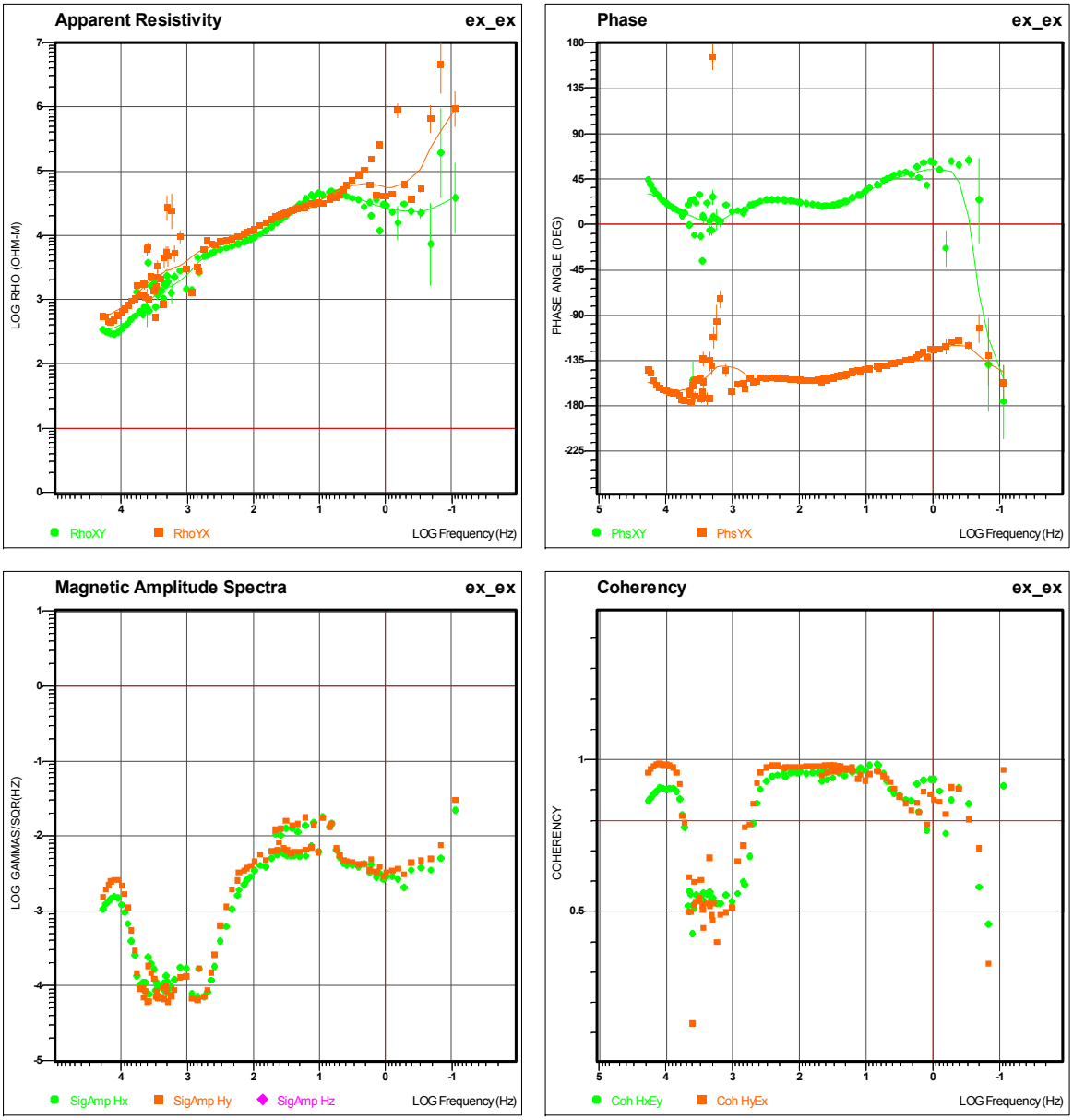

Apparent resistivity, phases, magnetic signal amplitude and off-diagonal coherences of the MT remote, data processed unreferenced.

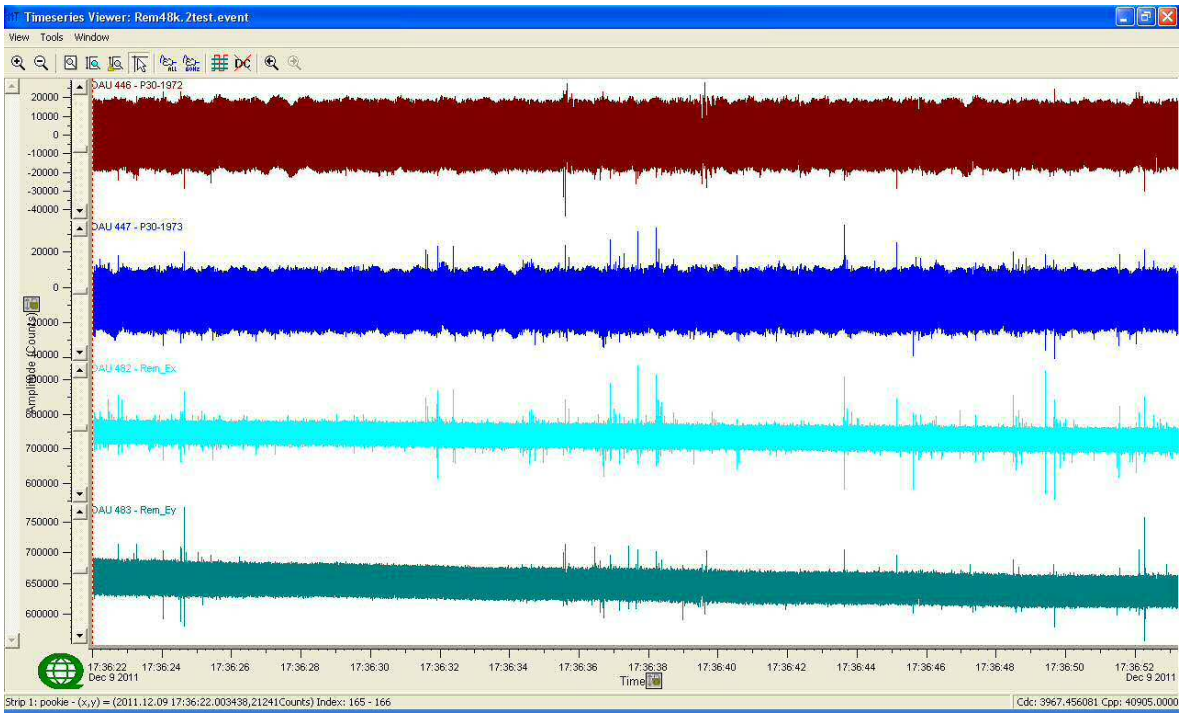

Screen Capture of MT time series, sample rate at 48ksps.

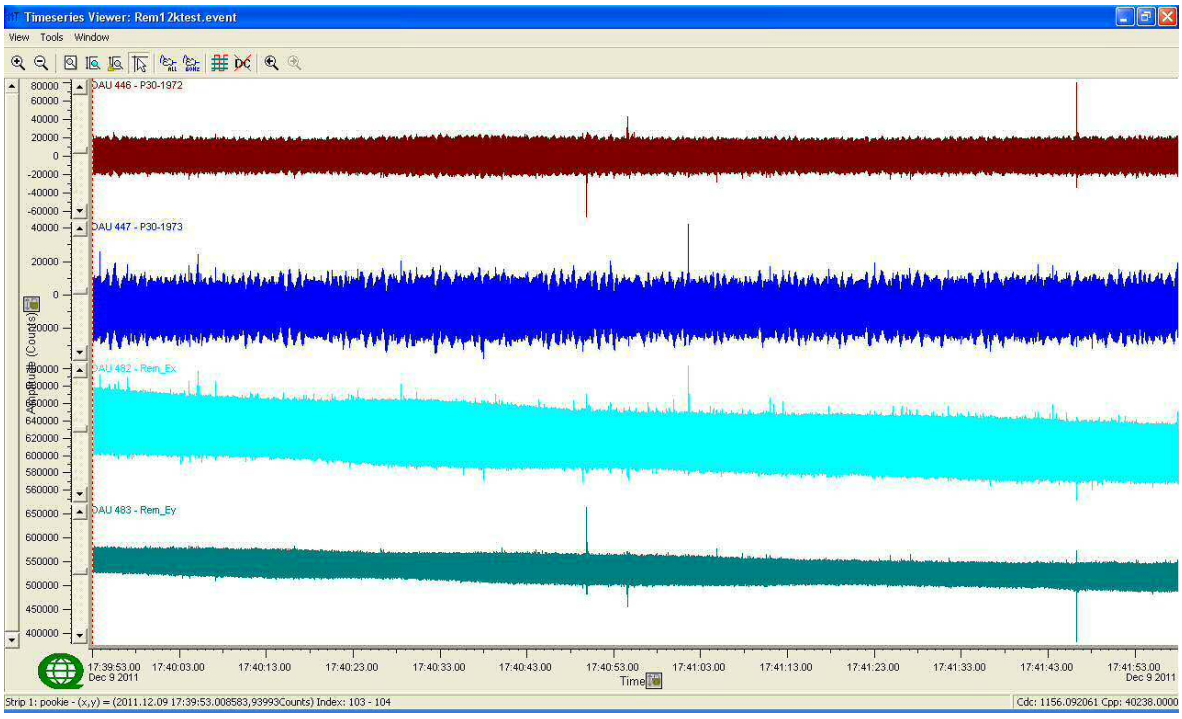

Screen Capture of MT time series, sample rate at 12ksps.

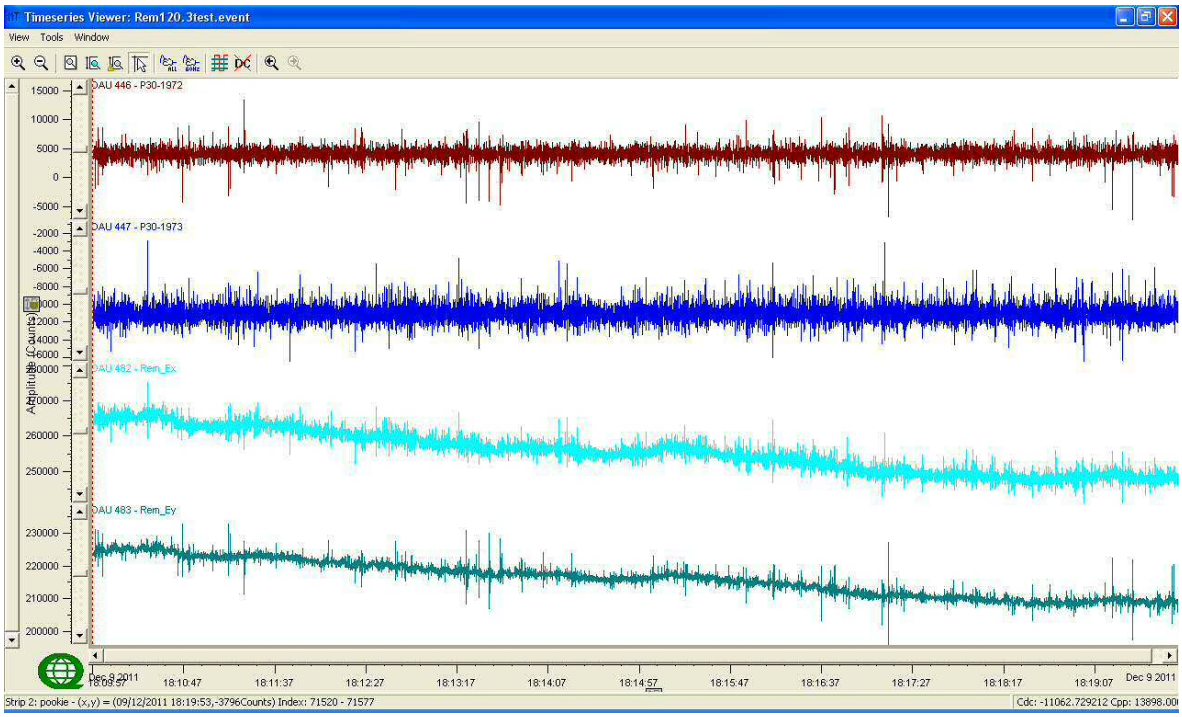

Screen Capture of MT time series, sample rate at 120ksps.

H INSTRUMENTS SPECIFICATIONS

H.1 REF TEK – 120 DATA ACQUISITION SYSTEM

Refraction Technology Inc. – Plano, Texas

Specifications:

Specification	Description			
Physical				
Size:	267 x 248 x 184 mm 10.5 x 9.75 x 7.25 in.			
Weight:	3.7kg 305 g 8 lbs (2-Channels maximum weight))			
Temperature:	-40°C to 60°C operating range.			
Environmental:	Operates in 1m of water without leaking for 48 hours. Airtight to 1.0 psi.			
Shock:	Remains operational after 1m drop (any corner) onto cement floor.			
Connectors				
Line A & Line B:	A pair of identical 10 pin U77/U style connectors. Each connector provides 3 pairs of lines (+): A (+)/B (-) Receive telemetry data and/or commands C (+)/D (-) Transmit telemetry data and/or commands E (+)/F (-) Sync			
Power:	PTO7A12-8S style connector. Provides input +12 VDC supplied from battery.			
Sensor:	PU283/U style connector. Provides for a direct connection from the AM to the sensor.			
Power Requirements				
Battery:	Two 12 volt lead acid battery (7 Ah).			
Signal Input				
Input Impedance:	10 megohms, 330pF, differential			
Broadband Dynamic Range:	130dB (noise power ratio test @ 125 sample per second [sps])			
ADC Type:	Delta-sigma modulation			
Sample Rage:	Multiple 50 to 48,000			
Gain Settings:	Four – programmable for 1, 4, 16 and 64.			
Sensor Input Signal Range:		**24-Bit High Speed A/D**		**24-Bit Low Speed A/D**
	Gain	**Actual**	**Reported**	**Actual**	**Reported**

Specification	Description				
	1	1.192μV	78.12mV	1.907μV	125.0mV
	4	298.0nV	19.53mV	476.8nV	31.25mV
	16	74.51nV	4.883mV	119.2nV	7.812mV
	64	18.63nV	1.221mV	29.80nV	1.953mV
Data Storage					
Data Size:	32-bit two's compliment.				
Base Memory:	128K EPROM 6.5Mb SRAM				
Base Capacity:	Better than 1.5 million samples or approximately 3 hours 10 minutes continuous data @ 125 sps.				
AM Telemetry					
Protocol:	Full duplex synchronous data link control (SDLC).				
Error Correction:	Packet acknowledge with modulo 8 sliding window.				
Speed	3.072Mb/second				
Encoding:	Bi-phase pulse = 1, missing pulse = 0				
Line Impedance:	100 Ohm				
Synchronization					
Timing:	Each AM on-line is timed and synchronized for simultaneous sampling within + 1.50 μsecond.				
Protection					
Electrical Protection:	Line A and Line B signals circuits are protect by: - A surge arrestor located on the RT514 board (SS1-14). - A line isolation transformer located on the RT514 board (T1-6) with over-voltage diodes (D1-4) on both sides of each secondary windings				
State-of-Health					
Information Provided:	The AM reports information on battery status, clock setting, gain setting, calibration mode and the communications link.				

Acquisition Parameters

Acquisition parameters include the sample rate, transmitter frequency and number of samples desired. The operator can also determine whether the AMs calibration signal is activated during data collection.

In typical use, the acquisition parameters are set according to the specific application configuration and event type. For each event type, several recording sessions are made, each at a different transmitter frequency and sample rate. The recording period is set based on event type and transmitter frequency.

The listing below shows several examples of event type, typical transmitter frequency (Hz), sample rates (with applicable ADC resolution) and the corresponding number of samples (record period).

Event Type	Transmit Frequency	Sample Rate	ADC Resolution	Number of Sample
Geophysical Response	375 Hz	48,000	24	124,032
Gain Test	375	48,000	24	65,536
Geophysical Response	75	9,600	24	130,176
Gain Test	75	9,600	24	65,536
Geophysical Response	25/8	3,200	24	139,264
Gain Test	25/8	3,200	24	32,768
Sensor Impedance	N/A	1,600	24	8,704
Ambient Noise	N/A	1,600	24	8,192
Geophysical Response	25/128	800	24	147,456
Gain Test	25/128	800	24	16,384
Geophysical Response	25/2048	100	24	212,992
Gain Test	25/256	100	24	4,096
Gain Test	N/A	50	24	4,096
Geophysical Response	N/A	50	24	65,536

Sensor Calibration

The AM can source a 12.5Hz, 50μA signal to the sensor input for measuring the source impedance of the attached sensor. The user can also specify frequency in amplitude of calibration signal.

Telemetry Cable

The telemetry cable is a *Category V* specification cable and is supplied by the customer.

Sample Rates

The following table shows all available sample rates, based on a 12.288 Mhz oscillator. A 24-bit resolution ADC is used for sample rates 48000 through 4800 and a 24-bit resolution ADC is used for sample rates 3200 and below. The correct ADC is selected automatically by the AM, based on the sample rate.

Typically, different sample rates and transmitter frequencies are used in 50 Hz and 60 Hz power environments to minimize AC power effects on the data. In the table, the shaded areas indicate the sample rates typically used in a 60 Hz power environment. A few rates are typically used in both environments.

Sample Rate	Power Line
48000	50 & 60
24000	50 & 60
19200	60
16000	50
12000	50 & 60
9600	50 & 60
6400	50
4800	60
3200	50
1920	60
1600	50
960	60
800	50
480	60
400	50
240	60
200	50
120	60
100	50
60	60
50	50
60/2	60
50/2	50
60/4	60
50/4	50
60/8	60
50/8	50
60/16	60
50/16	50
60/32	60
50/32	50

H.2 BF-6 MAGNETIC FIELD INDUCTION SENSOR

Schlumberger –EMI (Electromagnetic Instruments Inc.)Technology Center

The BF-6 sensor utilizes a magnetic feedback design to provide a stable flat response over several decades of frequency. The sensors respond as a B field detector over the flat band regions. Both the amplitude and phase responses are highly stable with variations of less than 0.1dB in amplitude and +/- one degree in phase between sensors. For the frequencies below the flat response region, the sensor response is proportional to signal frequency so that the sensor acts as a dB/dt detector. The coil is potted with epoxy and housed inside a rugged impact-resistant ABS tube. A matched low noise preamplifier is connected to the coil in a waterproof case and powered by an external +/- 12V power supply.

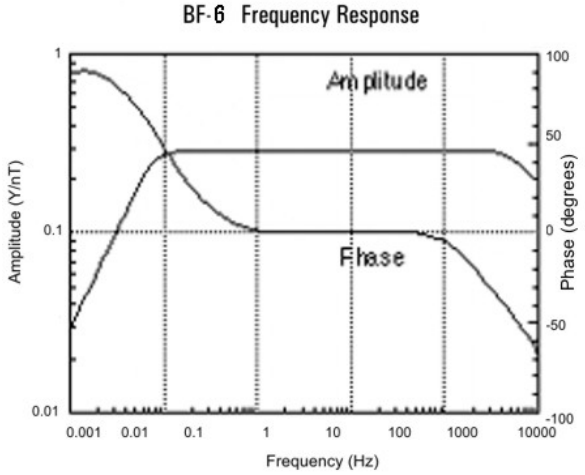

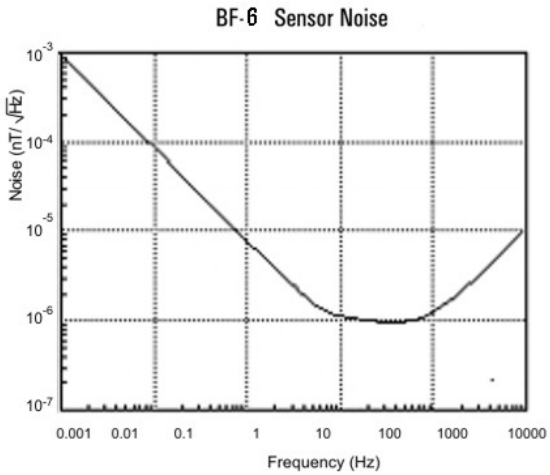

Features

High sensitivity
Very low noise
Magnetic feedback design
Ruggedized and waterproof
Light weight and compact
Low power consumption (210 mW)
Stable phase response

Applications

Magnetotellurics
Audiomagnetotellurics
Controlled-source electromagnetics
Magnetometric resistivity
Time domain electromagnetics

Performance

Frequency Range: 1 Hz to -100 kHz or 1 Hz to 25 kHz
3 dB frequency corners: 10 Hz, 25 kHz or 10 Hz, 100 kHz
Sensitivity (flat region): 0.3 V/nT (standard)
Power consumption: 9mA at +/-12V

Physical

Housing: High Impact ABS Straight Tube
Length: 73 cm (29 inches)
Diameter: 5 cm (2 inches)
Weight: 1.7 kg (3.7 lbs)
Connector: 8-pin Tajimi

H.3 AMTC 30 (P30) SERIES MAGNETIC SENSORS

Phoenix Geophysics Ltd

AMTC-30 magnetic sensor coils are used for AMT magnetic data acquisition. Weighing about 3 kg and measuring only 82 cm, AMTC-30 sensors are compact and portable while providing high-quality magnetic data at frequencies between 10 000 Hz and 1 Hz.

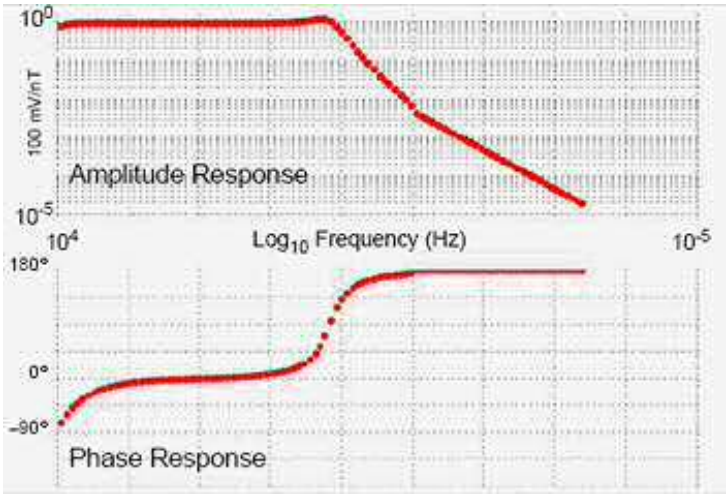

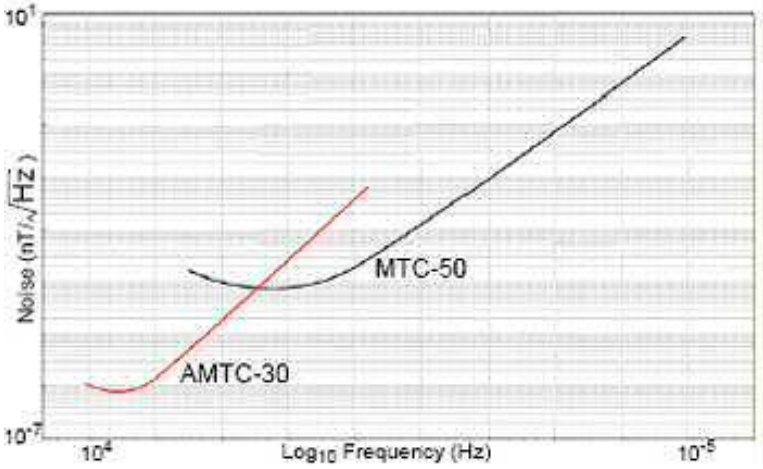

Technical Specifications

Overall Length : 82 cm
Outside Diameter : 6.0 cm
Weight : 3.0 kg
Frequency Range (for MT) : 10,000 Hz to 1 Hz

H.4 MTC 50 (P50) SERIES MAGNETIC SENSORS

Phoenix Geophysics Ltd

MTC-50 magnetic sensor coils weigh just over 10 kg, and measure only 141 cm. They provide magnetotelluric data at frequencies between 400 Hz to 0.00002 Hz.

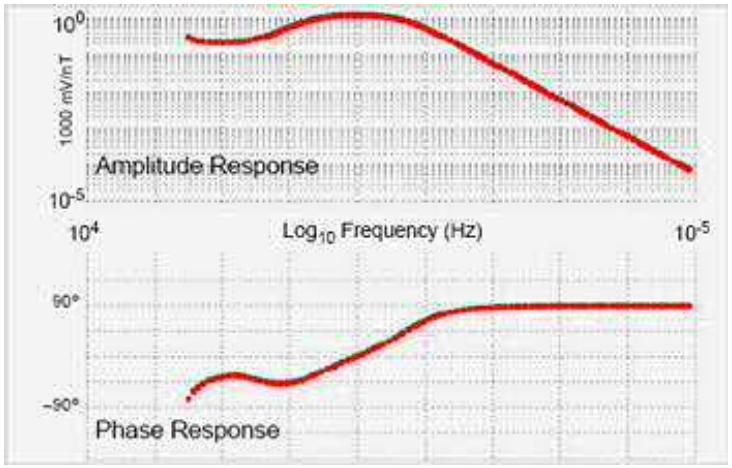

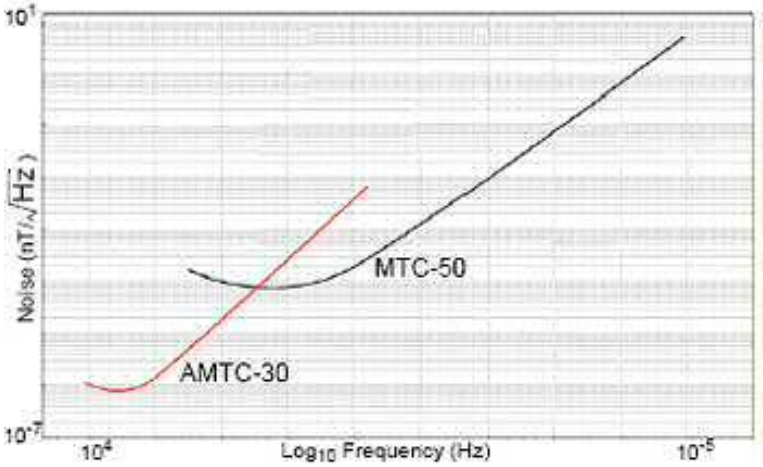

Technical Specifications

Overall Length : 141 cm
Outside Diameter : 6.0 cm
Weight : 10.5 kg
Frequency Range (for MT) :
400 Hz to 0.00002 Hz

I GEOSOFT SECTIONS

I.1 LINE 1E

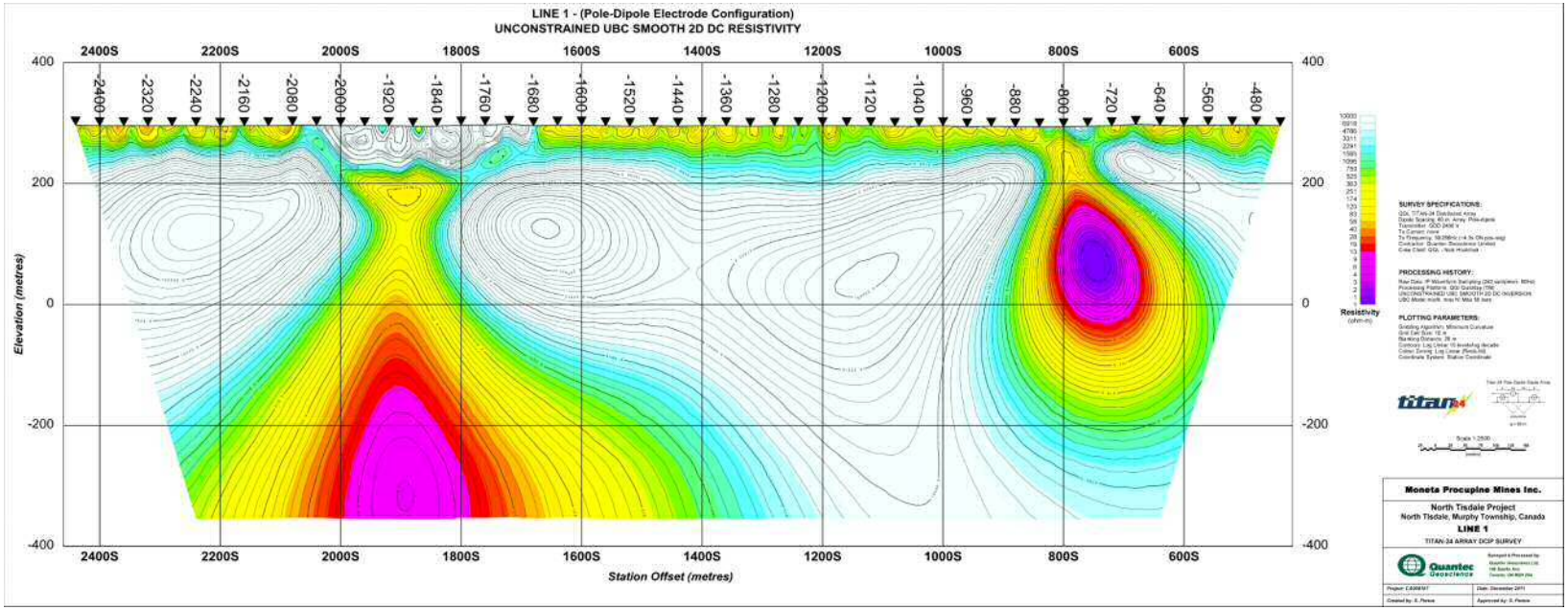

Line 1E –DC Resistivity 2D Model – Pole-Dipole Electrode Configuration

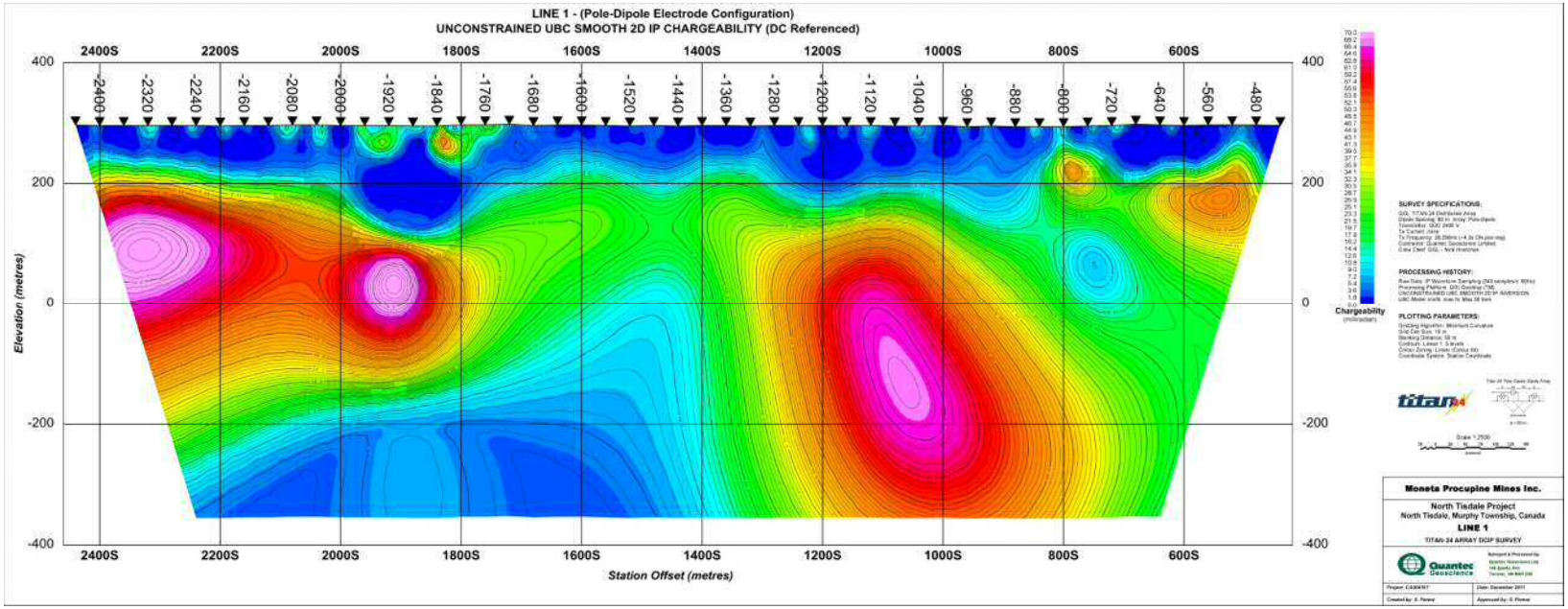

Line 1E – IP Chargeability 2D Model (using DC model as reference) – Pole-Dipole Electrode Configuration

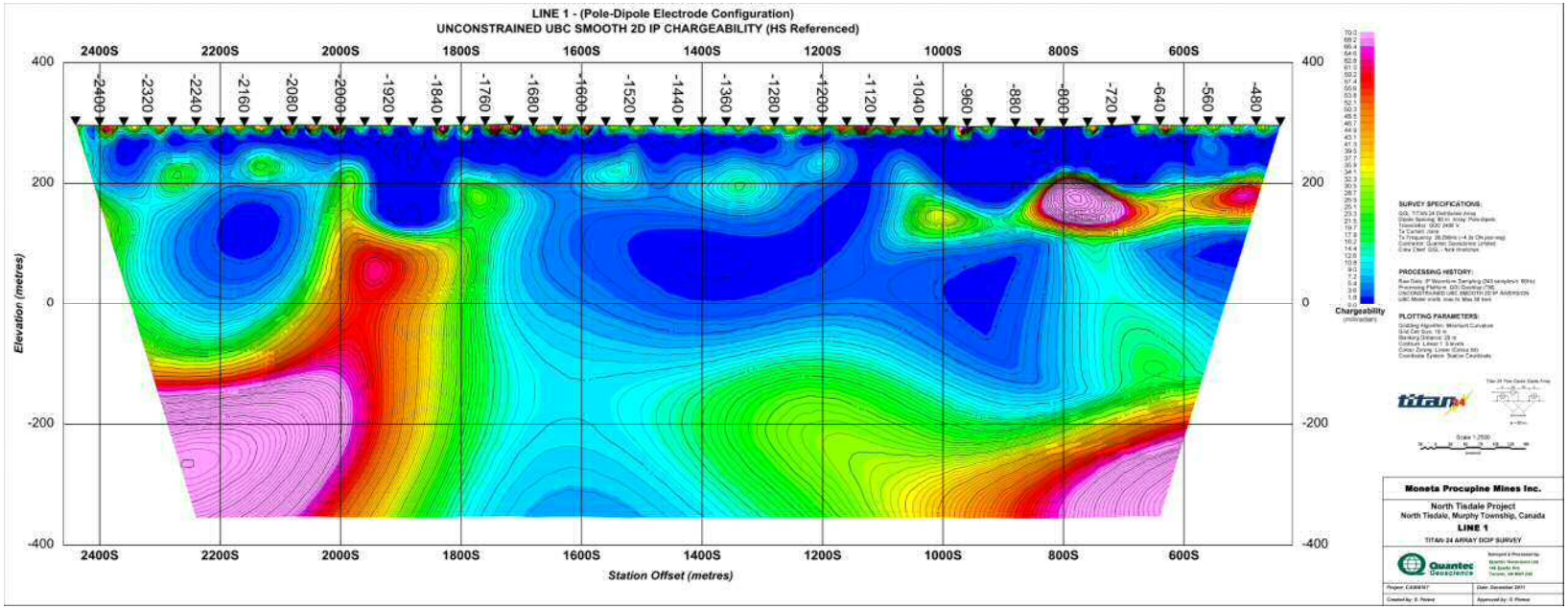

<u>Line 1E – IP Chargeability 2D Model (using HS model as reference) – Pole-Dipole Electrode Configuration</u>

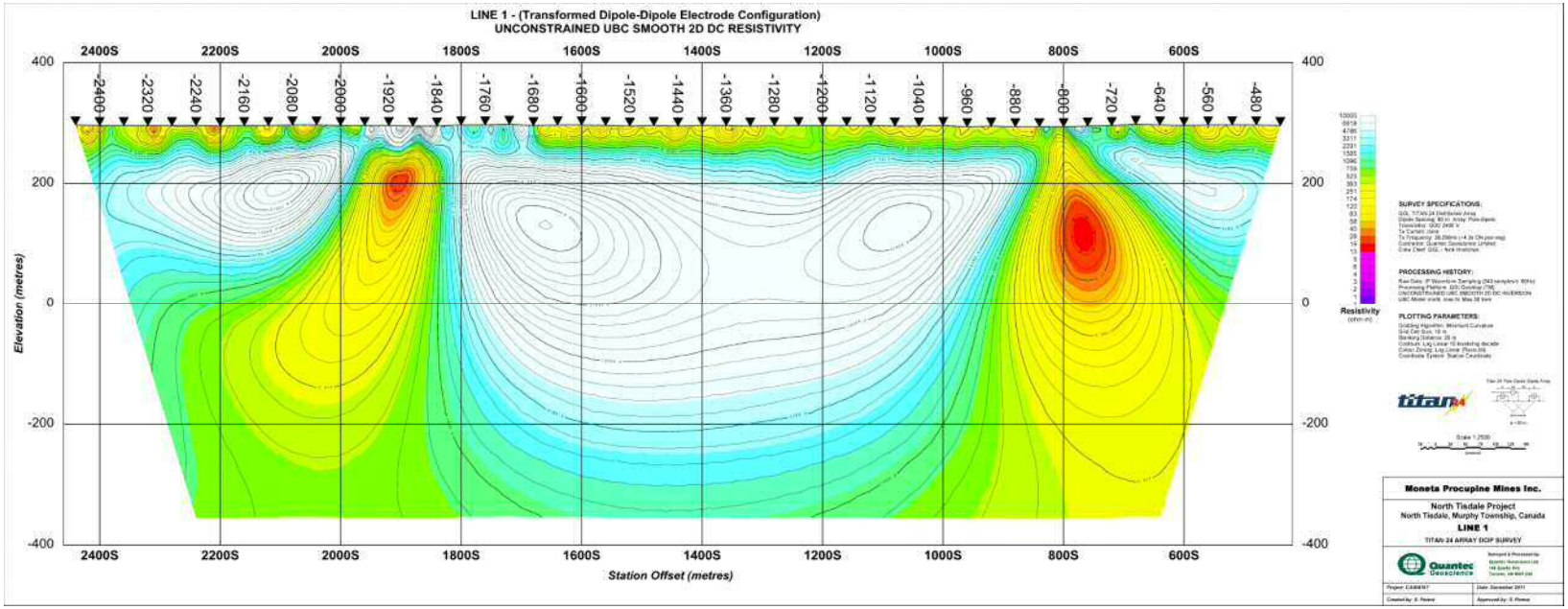

Line 1E –DC Resistivity 2D Model – Transformed Dipole-Dipole Electrode Configuration

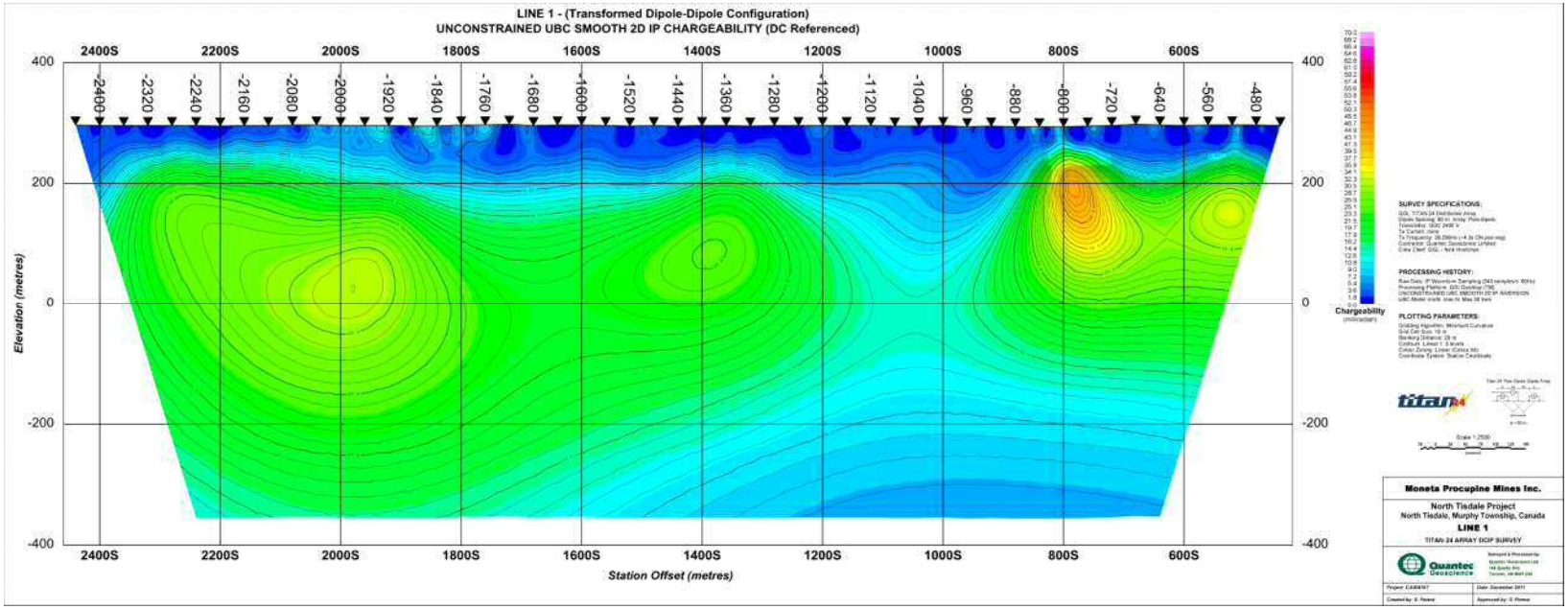

Line 1E – IP Chargeability 2D Model (using DC model as reference) – Transformed Dipole-Dipole Electrode Configuration

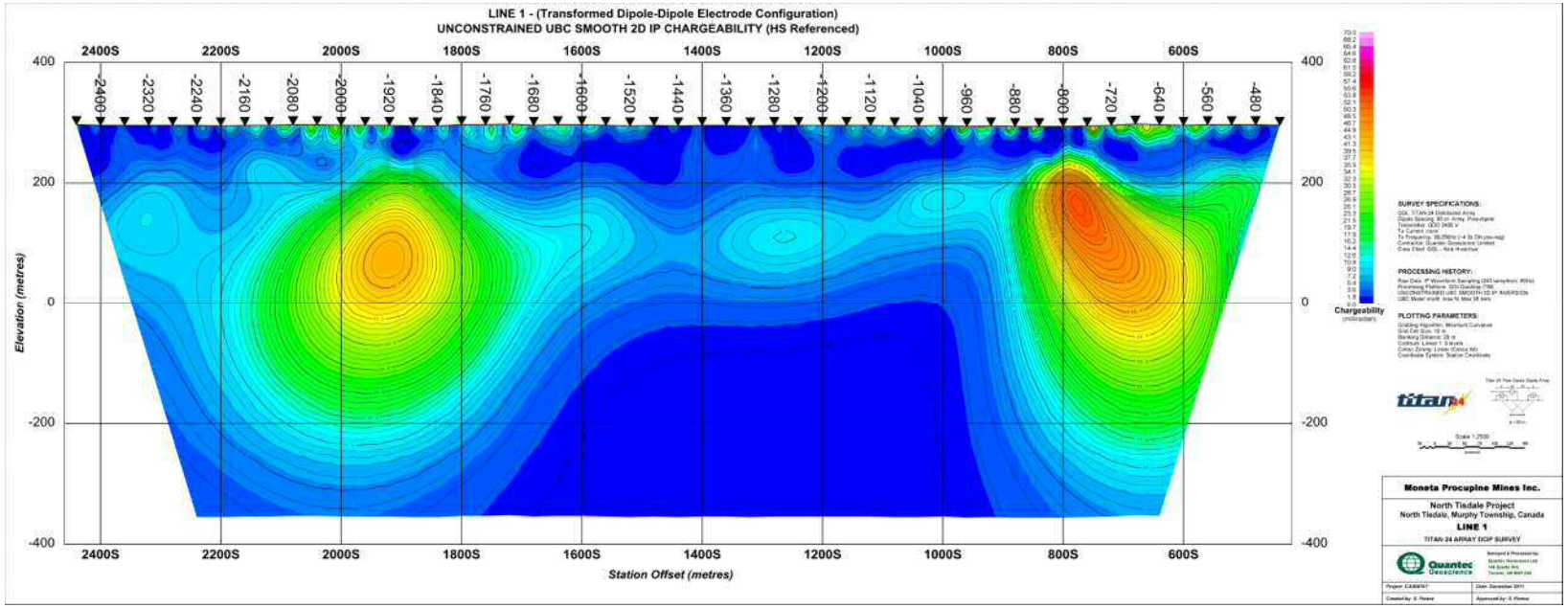

Line 1E – IP Chargeability 2D Model (using HS model as reference) – Transformed Dipole-Dipole Electrode Configuration

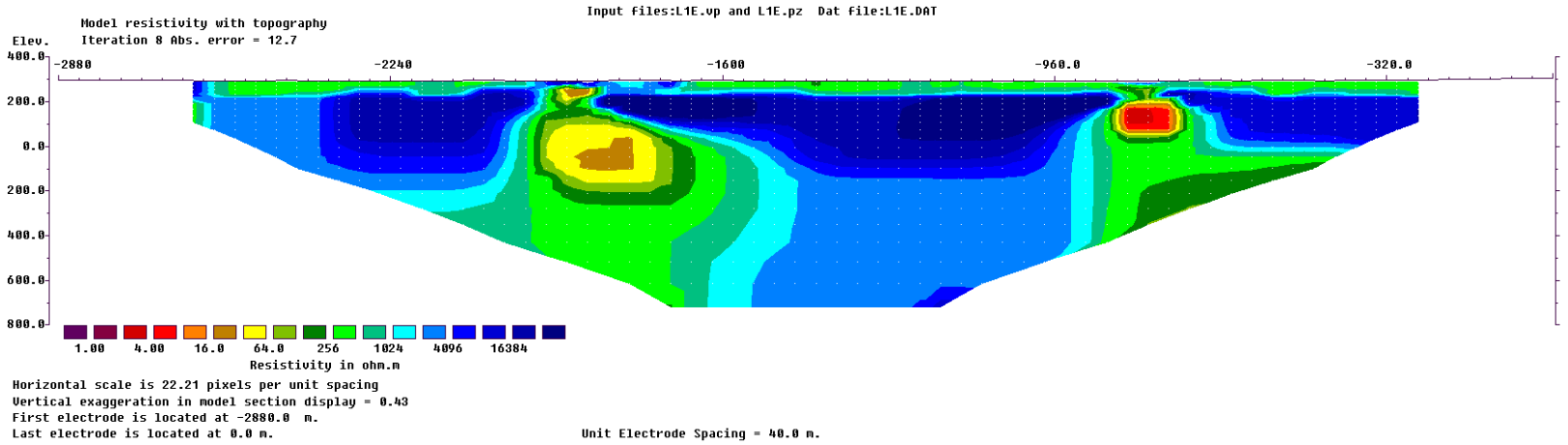

Line 1E –Loke Inversion DC Resistivity 2D Model – Pole-Dipole Electrode Configuration

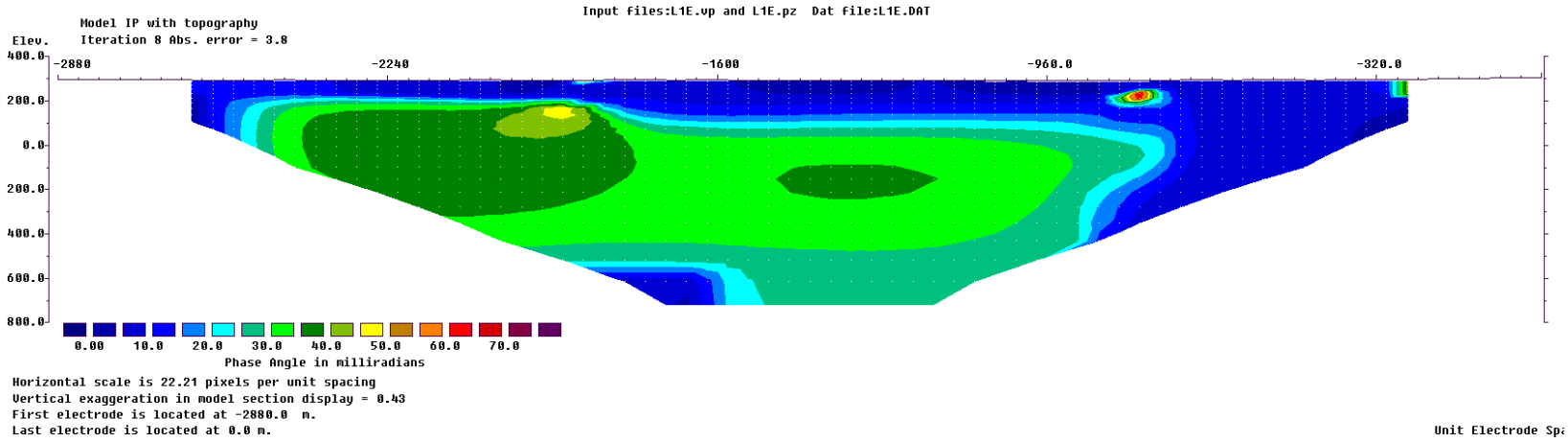

Line 1E – Loke Inversion IP Chargeability 2D Model (using DC model as reference) – Pole-Dipole Electrode Configuration

I.2 LINE 2E

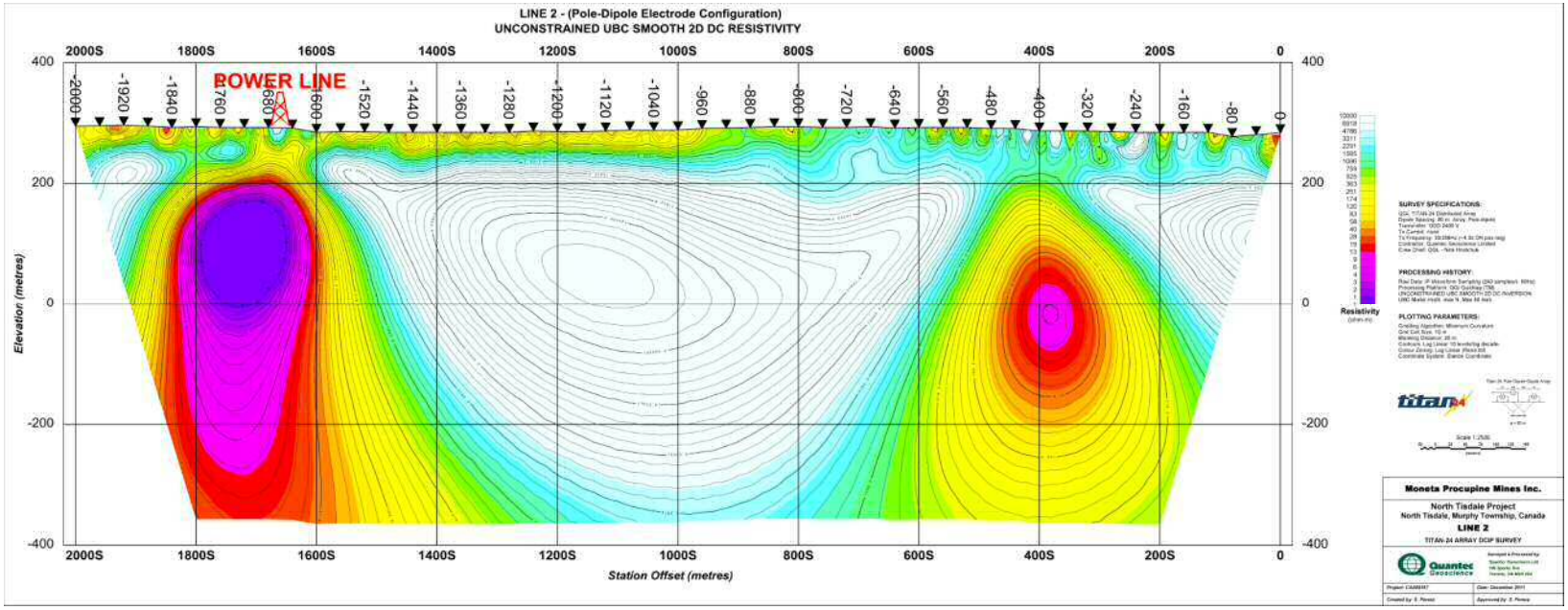

Line 2E –DC Resistivity 2D Model – Pole-Dipole Electrode Configuration

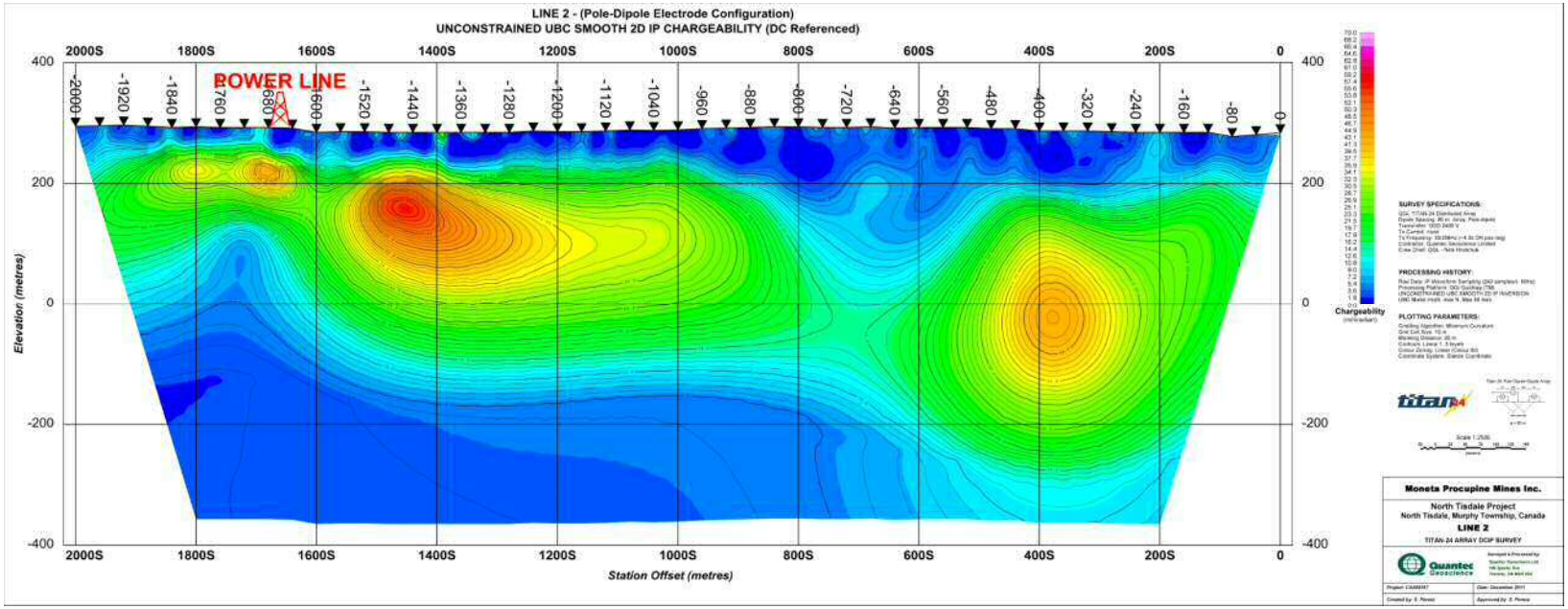

Line 2E – IP Chargeability 2D Model (using DC model as reference) – Pole-Dipole Electrode Configuration

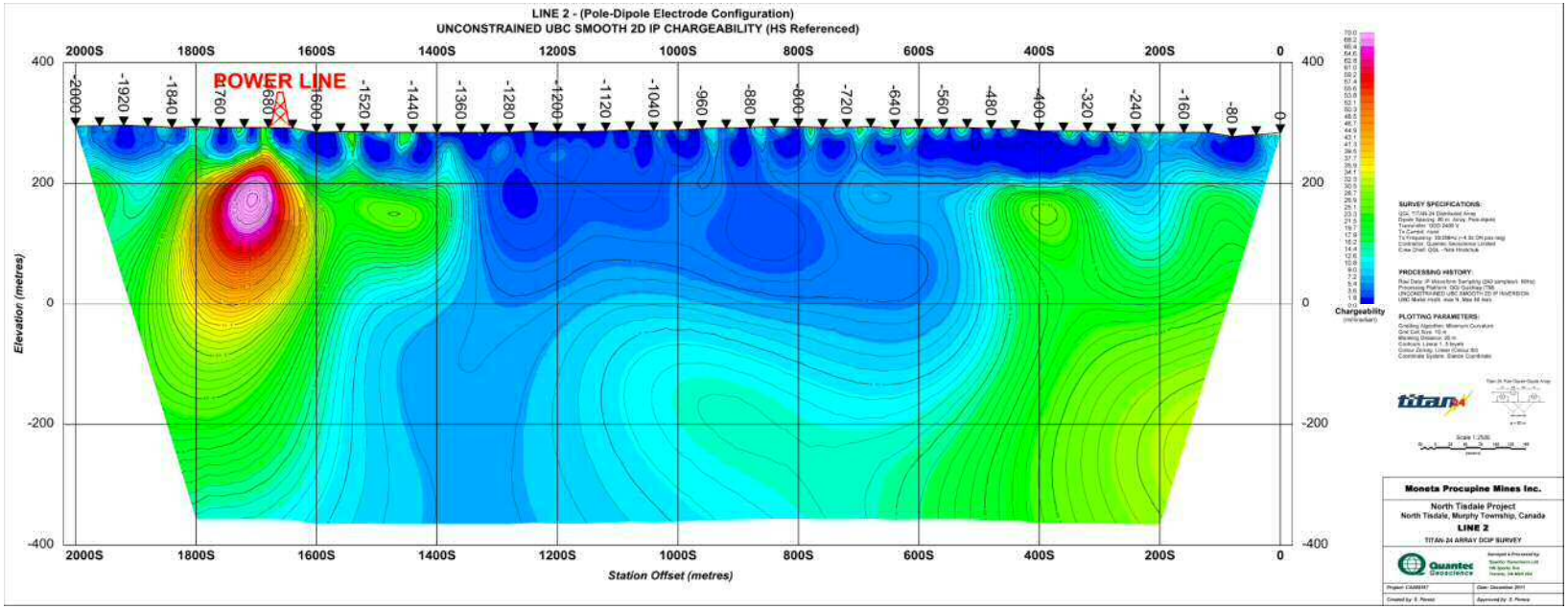

Line 2E – IP Chargeability 2D Model (using HS model as reference) – Pole-Dipole Electrode Configuration

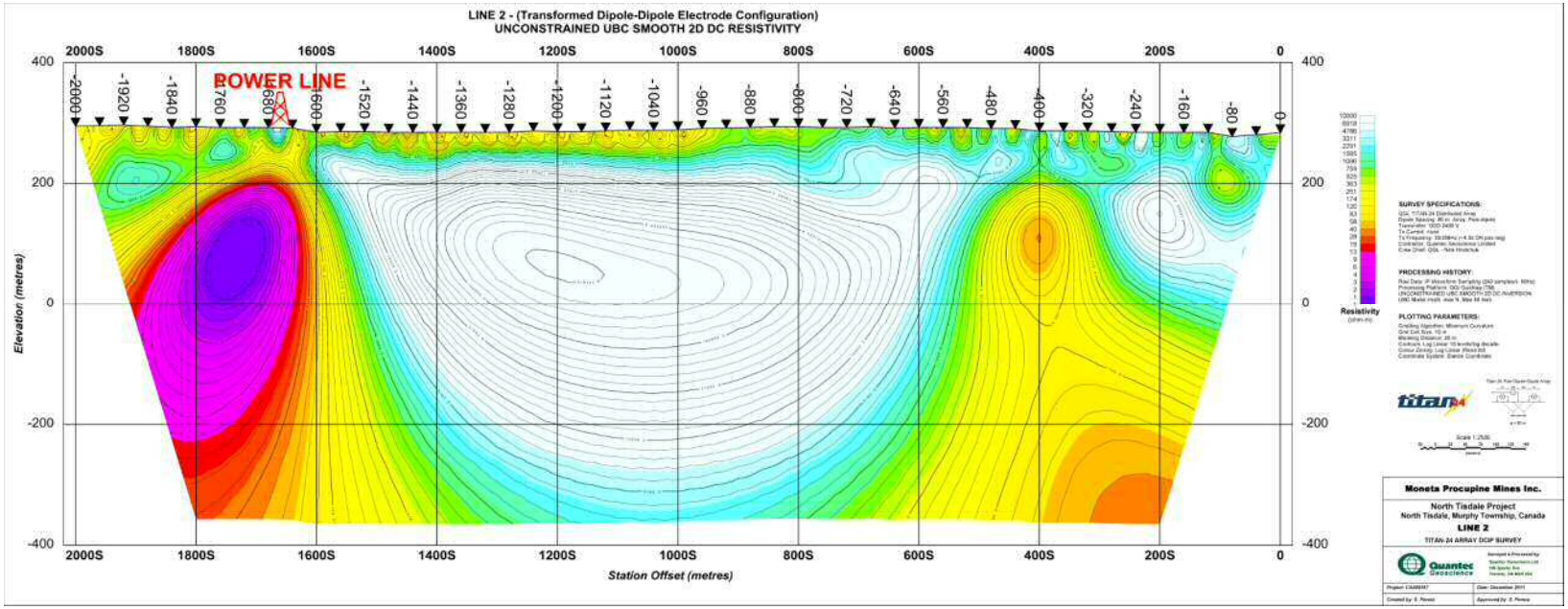

Line 2E –DC Resistivity 2D Model – Transformed Dipole-Dipole Electrode Configuration

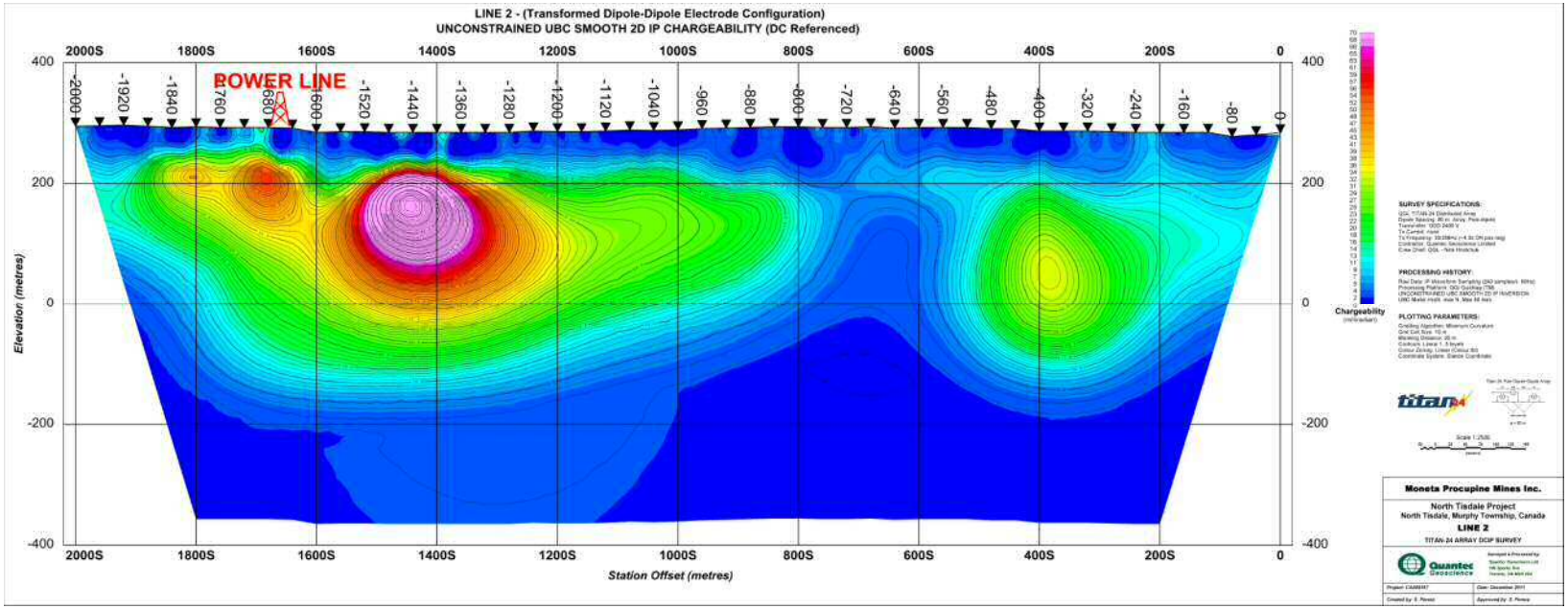

Line 2E – IP Chargeability 2D Model (using DC model as reference) – Transformed Dipole-Dipole Electrode Configuration

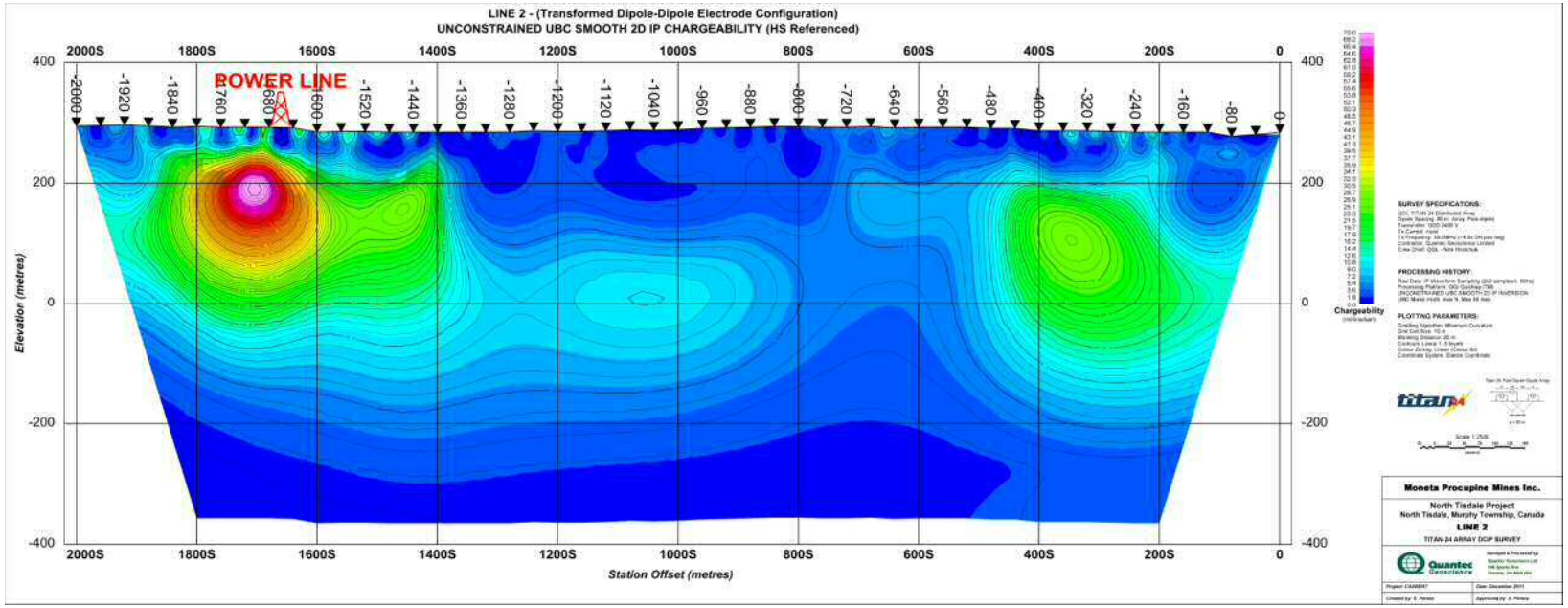

Line 2E – IP Chargeability 2D Model (using HS model as reference) – Transformed Dipole-Dipole Electrode Configuration

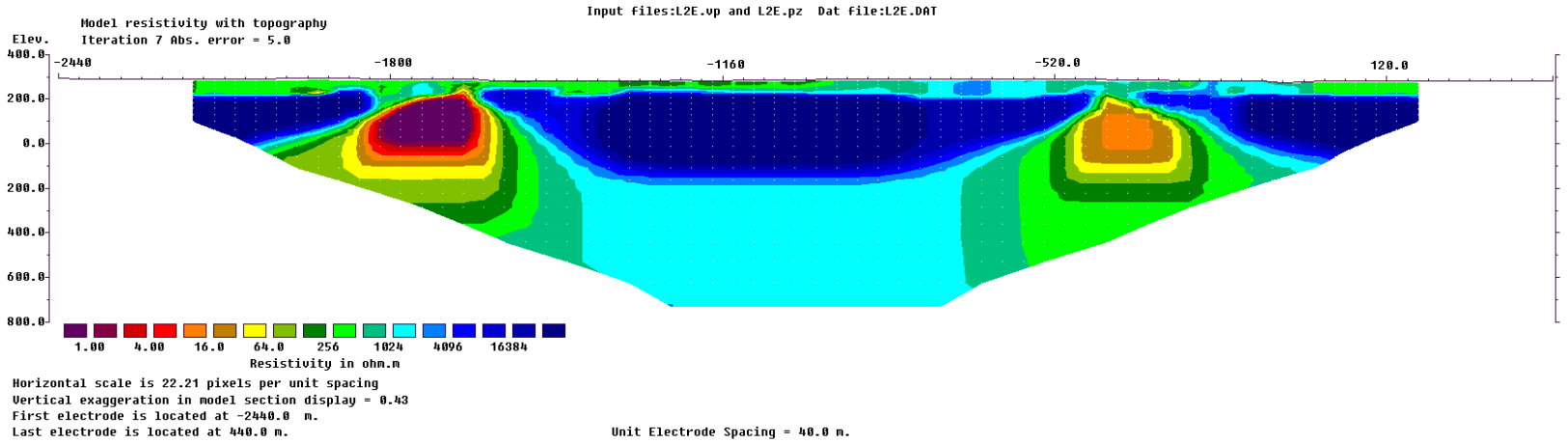

Line 2E –Loke Inversion DC Resistivity 2D Model – Pole-Dipole Electrode Configuration

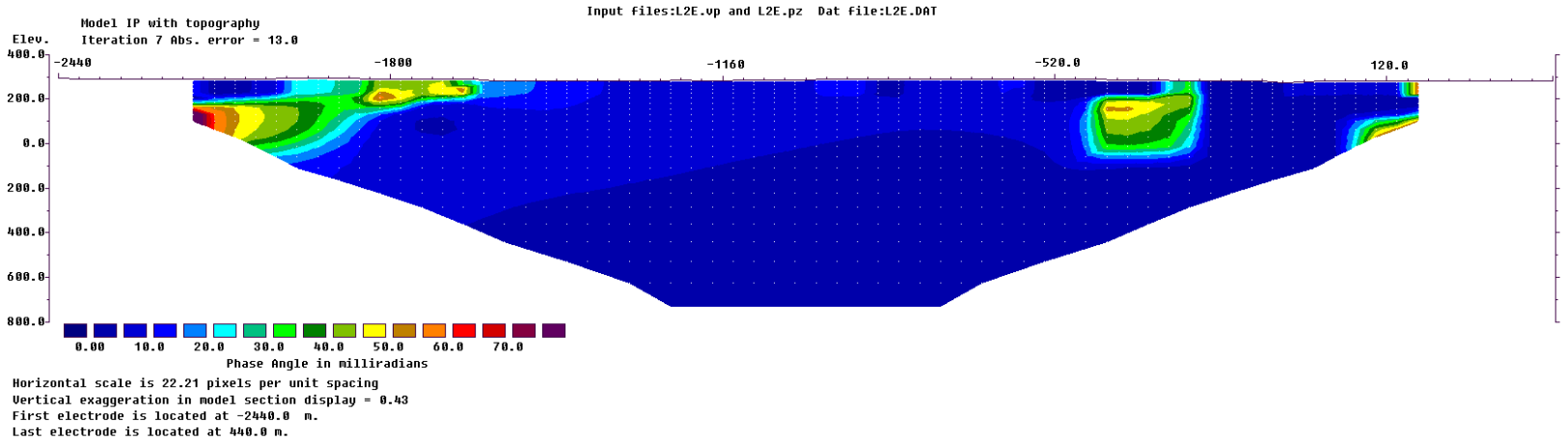

Line 2E – Loke Inversion IP Chargeability 2D Model (using DC model as reference) – Pole-Dipole Electrode Configuration

J AN INTRODUCTION TO TITAN-24 DIRECT CURRENT (DC) RESISTIVITY AND INDUCED POLARISATION (IP) METHODS

J.1 INTRODUCTION

Titan-24 is a 24-bit multi-channel, distributed acquisition system that allows for the collection of high quality Direct Current (DC) Resistivity and Induced Polarization (IP) data (Sheard 1998). The system provides high multiplicity data sets and records full-waveform time-series utilizing 24-bit Sigma Delta Analog to Digital (A/D) conversion. Like other conventional resistivity methods, acquisition is performed by the injection of an artificial controlled source of current, usually a series of full duty cycle[14] square pulses, into the ground through the transmitter electrode. The voltages, normalized by the injected current, are measured at the receiver electrodes as time series.

The use of 24-bit A/D converter allows the Titan-24 system to record the full waveform at the receivers, thus permitting the accurate removal or deconvolution of the source effects from the recorded time series. What is left of the time series after the deconvolution consist of mainly the responses of the ground and noise.

DC resistivity method is quite sensitive to small variations in resistivity near surface, and its effectiveness will be limited by high level of noise in the presence of a shallow conductive layer in the ground. On the other hand, in the desert or coarse-grained sandy environments, DC resistivity method can suffer from poor electrical contact with the ground. As a result, very little or no current can be injected into the ground, and no meaningful data can be collected.

The resistivity is among the most variable of all geophysical parameters, with a range exceeding 10^6 ohm-m. The resistivity of rocks depends primarily on their porosity, permeability and particularly the salinity of fluids contained, according to Archie's Law. Therefore, DC resistivity method can be utilized in a wide variety of applications in mineral exploration, mainly for mapping of resistivity structures and locating of conductive targets.

The chargeability responds to the presence of polarisable minerals (metals, sub-metallic sulphides and oxides, and graphite), in minute amounts. Both the quantity of individual chargeable grains present and their distributions within subsurface current flow paths are significant in controlling the level of response. The IP method can be used to directly detect disseminated to massive sulphides.

More detailed descriptions on the theory and application of the DCIP method can be found in Telford et al. (1976).

[14] *Duty cycle is the ratio between the pulse duration and the period of a square waveform*.

J.2 TITAN-24 DCIP SURVEY

Titan-24 is a distributed DCIP acquisition system. A typical survey layout, or spread, is 2400m long and has 25 inline (Ex) 100m potential dipoles and the current injections sites. With current extensions, a typical Titan-24 spread can be stretched to 3600m. If requested, the dipole length can be changed to 50m or 200m, and the resulting length Titan-24 spread will be 1200m or 4800m. Also, cross line dipoles (Ey) can be deployed as well.

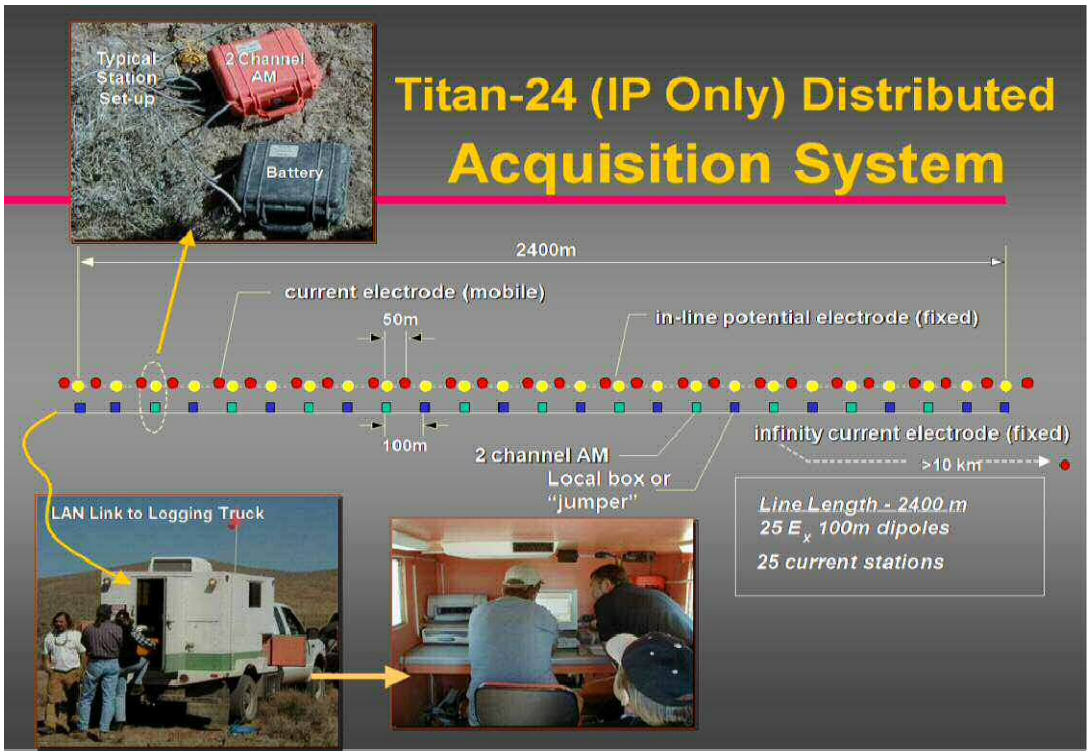

Titan-24 Distributed Acquisition System (IP-only) layout.

In a normal Titan-24 survey, the transmitter (Tx) and receiver (Rx) configuration is the pole-dipole-dipole array, combining pole-dipole right (PDR) and pole-dipole left (PDL). The current is injected at the mid-point between two potential electrodes. However, with special safety arrangements made to the system, the current can be injected at the potential electrode locations.

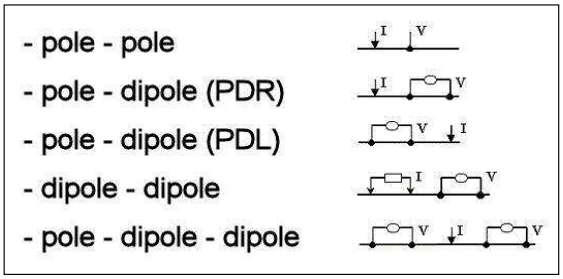

Titan-24 Transmitter (Tx) and Receivers (Rx) configurations.

J.3 TITAN-24 DCIP DATA PROCESSING

For one potential electrode pair, the data acquired with one current injection event is a time series of measured voltages at the electrodes normalized by the current, Vp in mV/A. A typical Titan-24 time series are shown below.

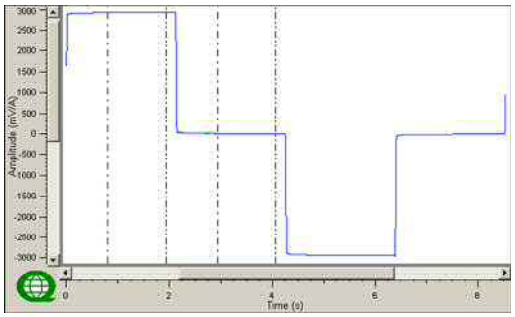

A typical Titan-24 (pole-dipole) Vp time series (8.5s duration)

Vp: voltage measured by the receiver (Rx) dipole normalized by current.

Vp of one current cycle.

The data in the time window between the dash lines are used for IP processing.

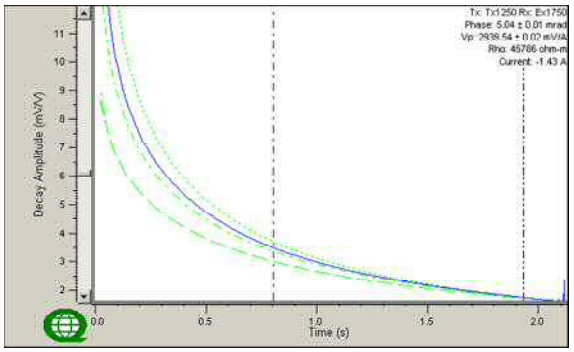

Typical Titan-24 DCIP time series.

A single injection event usually lasts approximately three minutes. The time series of an event are stacked twenty times per second in order to increase the signal to noise (S/N) ratio. The data processing is done in the frequency domain. Current waveform deconvolution and digital filtering of power line noise (60/50Hz, and their harmonics) are applied to the frequency domain data.

J.4 HALVERSON-WAIT CHARGEABILITY

Titan-24 IP chargeability are described using the Halverson-Wait spectral model (Halverson et al., 1981), which is not well known, but is similar to the Cole-Cole model proposed by Pelton et al. (1978) which is a simple relaxation model that fits complex (frequency-dependant) resistivity results.

The time domain chargeability, originally proposed by Siegel (1959), is defined (Telford et al., 1976) as:

$$M = \frac{1}{V_c}\int_{t1}^{t2} V(t)dt$$

where $\boldsymbol{V(t)}$ is the residual or secondary voltage at a time $\boldsymbol{t}$ that is decaying after the current is cut off, between time $\boldsymbol{t_1}$ and $\boldsymbol{t_2}$ with the steady voltage $\boldsymbol{V_c}$ during the current flow interval. The ratio $\boldsymbol{V(t)/V_c}$ is expressed in millivolts per volts (mV/V).

In the frequency domain, the "frequency effect" is defined as:

$$FE = \frac{(\rho_{DC} - \rho_{AC})}{\rho_{AC}}$$

where $\boldsymbol{\rho_{DC}}$ and $\boldsymbol{\rho_{AC}}$ are the apparent resistivities measured at dc and "very high" frequency, usually in the 0.1 to 10 Hz range.

The Cole-Cole model for the chargeability $\mathbf{m}$, as defined by Pelton et al. (1978) is given by the following:

$$Z(\omega) = R_0\left[1 - m\left(1 - \frac{1}{1 + (i\omega\tau)^C}\right)\right]$$

where $\boldsymbol{Z(\omega)}$ is the complex impedance with $\boldsymbol{\omega}$ the angular frequency in Hz, $\boldsymbol{R_0}$ the DC resistivity, $\boldsymbol{m}$ the chargeability in volts per volt, $\boldsymbol{\tau}$ the time constant in seconds, and $\boldsymbol{c}$ is the frequency dependence (unit less). The latter two physical properties describe the shape of the decay curve in time domain or the phase spectrum in frequency domain, and commonly range between 0.01s to +100s and 0.1 to +0.5, respectively (Johnson, 1984).

The Halverson-Wait model was proposed by Halverson et al. (1981) as an extension to the Wait (1959) model of the impedance of "volume loading" of spheres, given by:

$$Z(\omega) = \frac{\rho}{G}\left[1 - 3\nu\left(1 - \frac{3\delta}{1 + 2\delta}\right)\right]$$

where $\boldsymbol{G}$ is a geometric factor, $\boldsymbol{\rho}$ the resistivity of the media, $\boldsymbol{\nu}$ the volume loading (the volume fraction of chargeable "spheres"), $\boldsymbol{\delta}$ the sphere surface impedance. The Wait model was designed to provide an explanation of the differences in the shape of decay curves from different polarisable targets, but does not describe very well the physical attributes of the rocks.

The Halverson-Wait model expands the Wait coated sphere IP model to include a new formulation of the sulphide-rock interface impedance, based on field studies and laboratory tests on samples. It is closely correlated to the Pelton et al. (1978) Cole-Cole model and is given by:

$$Z(\omega) = \frac{\rho}{G}\left[1 - 3\nu\left(1 - \frac{3/2}{1 + r[i\omega]^K}\right)\right]$$

where $\boldsymbol{r}$ is the sphere radius and is equivalent to $\boldsymbol{\tau}$ - the Cole-Cole time constant ($r = \boldsymbol{\tau}^{\boldsymbol{K}}$). The $\boldsymbol{\nu}$ volume loading compares well to $\boldsymbol{m}$ – the Cole-Cole chargeability (see equation below) – and the exponent $\boldsymbol{K}$ is equal to $\boldsymbol{c}$ - the Cole-Cole frequency dependence (Halverson et al., 1981). For sulphide systems, the $\boldsymbol{r}$-factor reflects the size or inter-connectedness of the sulphide grains and the $\boldsymbol{k}$-factor reflects the electrical characteristics of the sulphide surfaces.

An example of time domain Halverson-Wait model responses is shown below:

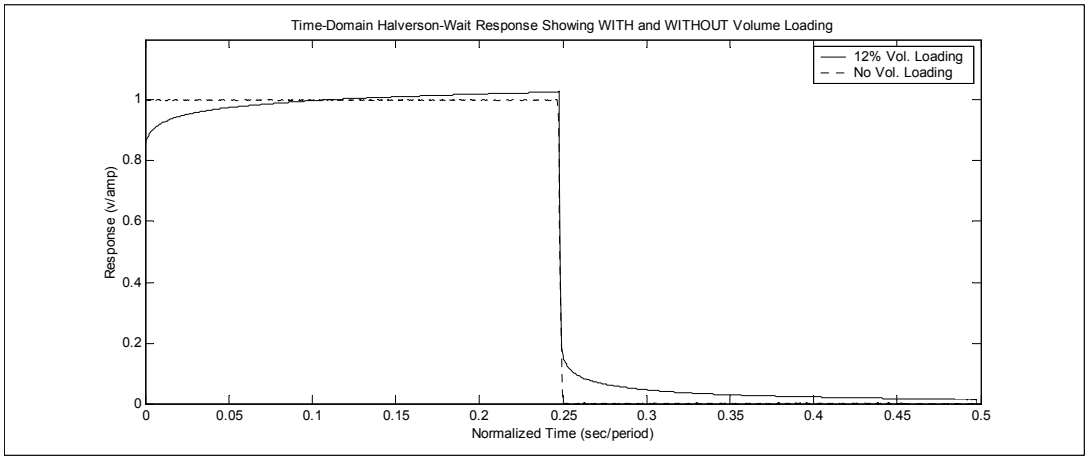

Polarisable versus Non-Polarisable TD-IP response using Halverson-Wait Model.

In the Halverson-Wait model the theoretical Percentage Frequency Effect (PFE)[15] (for infinite bandwidth), which equates to the theoretical chargeability in the Cole-Cole equation, is thereby defined by the volume loading:

$$\frac{PFE_0^{\infty}}{100} = m_0 = \frac{9v}{(2+3v)}$$

and is output in units of milliradians (mrads).

J.5 TITAN-24 IP CHARGEABILITY DEFINITION (QTN001)

Quantec prefers to estimate IP responses using a time domain half-duty square-wave excitation standard, but convert those chargeability results to units of phase. The specific procedure and algorithm is as follows:

1. Determine the earliest time for which EM coupling has died out sufficiently. This time is called the averaging or integration *start time* or . A typical value for is 0.8s;
2. Determine the latest charge/decay time that is minimally affected by sigma-delta and low-pass (usually Hanning window moving average) filtering - called the averaging or integration *end time* or . A typical value for is 1.95s;
3. Adjust the *start time* ( ) so that (equated to number of samples) exactly spans an integer number of power-line signal periods. This can only be done for transmitted (fundamental) frequencies that are much lower than the power-line frequency;
4. Using the charge and decay sample numbers that equate to the averaging window[16] defined by and , calculates the average charge and decay voltages. This average may involve a non-uniform weighting to further improve rejection of power-line noise;
5. Calculate the theoretical Halverson-Wait half-duty time-domain response using identical filtering to that applied to the measured data response estimate, and presuming the following spectral parameters:

[15] The classical definition of PFE is $100 \times (\rho_0 - \rho_\infty) / \rho_0$.

[16] In practice this averaging window is tapered slightly to widen the stop-band notches and thereby provide enhanced power-line noise rejection.

a. volume loading: 0.125 (this value is not important)

b. r – value: 1.0

c. k – value: 0.2

6. For the standard Halverson-Wait spectral parameters mentioned, the synthesized time-domain response and the $t_1 – t_0$ averaging window, convert all estimated/measured charge and decay voltages (using the specified averaging window) to chargeability (millivolts/volt) and then to phase (milliradians).

This is the algorithm used in the Titan-24 data processing. The relationship between Titan-24 chargeability unit, phase in milliradians, and other frequency domain systems is straightforward – Quantec's time-domain based phase equates to frequency domain based phase, see figures below.

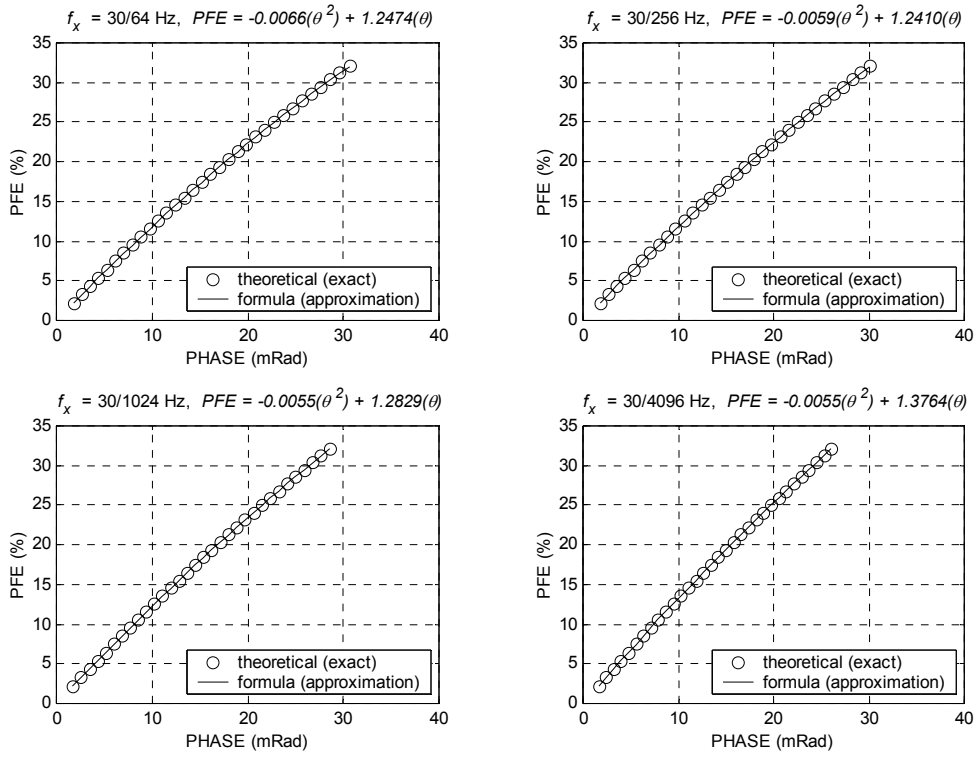

Phase vs. PFE for various pulse lengths and presuming standard Halverson-Wait spectral parameters (r-value = 1.0 and k-value = 0.2).

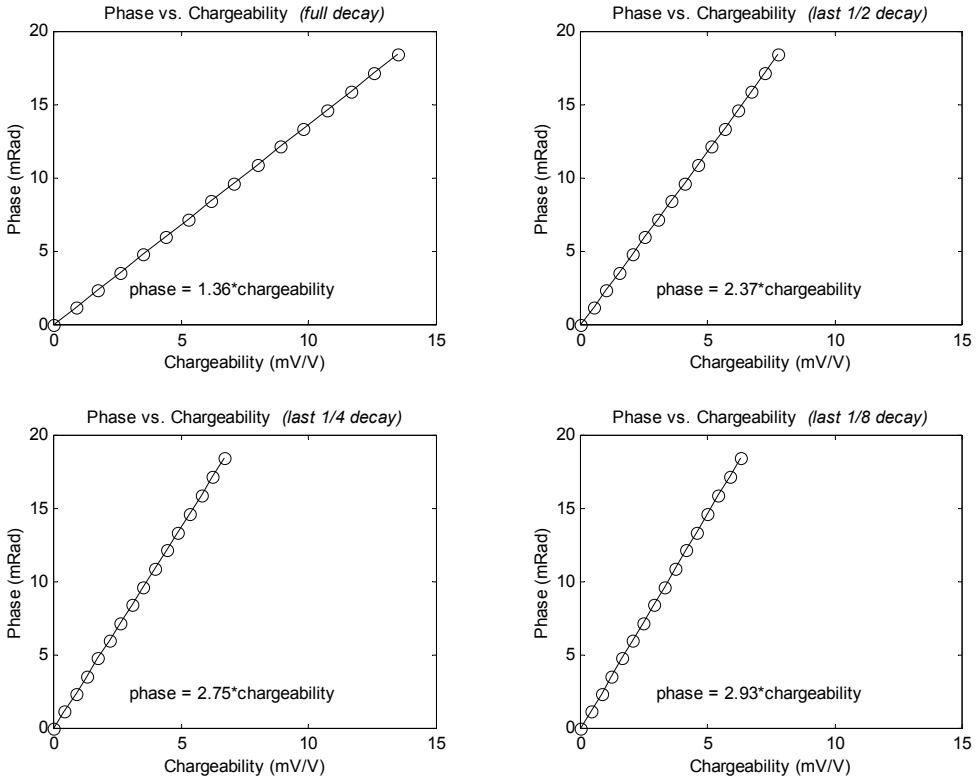

Illustration of the proportional relationship between phase (mrad) and chargeability (mV/V) for various charge/decay averaging windows

J.6 DCIP2D INVERSION

An excellent overview and introduction to both the theory and use of inversions in geophysics is available on the University of British Columbia (UBC) website (Oldenburg et al., 1998).

The DCIP2D inversion algorithms are developed by UBC-Geophysical Inversion Facility.

Mathematically, inversion is the process of fitting the observed data to a model through minimizing a function. The choice of which function to minimize ultimately defines the inversion model. In the inversion algorithm developed by UBC, this function is:

$$\phi = \phi_d + \beta \phi_m = \text{(misfit)} + \beta\,\text{(model norm)}$$
$$0 < \beta < \infty \quad \text{is a constant}$$

The function to be minimized consists of a function, ϕ_d, that minimizes the data misfit, and a function ϕ_m that finds a "smooth" model. Beta, the regularization parameter, represents a relative weighting between fitting the data and smoothing the model.

Clearly, the data misfit function must be defined in more detail. One approach might be

$$\phi_d = \sum_{i=1}^{N} \left(\frac{F_i[m] - d_i^{obs}}{\varepsilon_i} \right)^2 .$$

This function defines the data misfit as the sum of the individual misfits squared (L2 norm), normalized by the errors associated with each data point. It is the least-squares definition of the data misfit.

The model misfit function must also be defined in more detail. One of the most flexible definitions is the one used by UBC

$$\phi_m(m,m_0) = \alpha_s \int_{vol} (m-m_0)^2 dv + \alpha_x \int_{vol} \left(\frac{\partial (m-m_0)}{\partial x} \right)^2 dv + \alpha_z \int_{vol} \left(\frac{\partial (m-m_0)}{\partial z} \right)^2 dv$$

In this definition there are three components to the "model norm" (or "smoothness" constraint, or "regularization"), each of which contains an α constant (α_s, α_x, α_z) that are commonly referred to as "alpha parameters", and a fourth variable m_o that refers to the starting or reference model – either a half-space or geophysical constraint – that also has a profound influence on the model-misfit.

The three "alpha" parameters represent a relative weighting of each component:

- the first component is simply an overall difference between the model and a "target" model;
- the second component is a horizontal smoothness;
- the third component is a vertical smoothness.

J.7 APPARENT RESISTIVITY OF UNIFORM HALF SPACE

From p.636, Telford et al. 1976, the apparent resistivity $\boldsymbol{\rho_a}$ is given as:

$$\rho_a = \frac{2\pi V_p}{G_f}$$

where $\boldsymbol{G_f}$ is the geometric factor defined as:

$$G_f = \left(\frac{1}{r_1} - \frac{1}{r_2}\right) - \left(\frac{1}{r_3} - \frac{1}{r_4}\right)$$

with:

$\boldsymbol{r_1}$ the distance between current electrode P1 and potential electrode C1;

$\boldsymbol{r_2}$ the distance between current electrode P1 and potential electrode C2;

$\boldsymbol{r_3}$ the distance between current electrode P2 and potential electrode C1;

$\boldsymbol{r_4}$ the distance between current electrode P2 and potential electrode C2;

J.8 DC INVERSION USING A SYNTHETIC MODEL

A synthetic resistivity model and its apparent resistivity pseudo section based on Titan-24 configuration are shown here. The model consists of a background of 1,000 ohm-m and a vertical dyke of 1 ohm-m. The synthetic DC data, V_p's, are computed using UBC's 2D forward modeling tool DCIPF2D

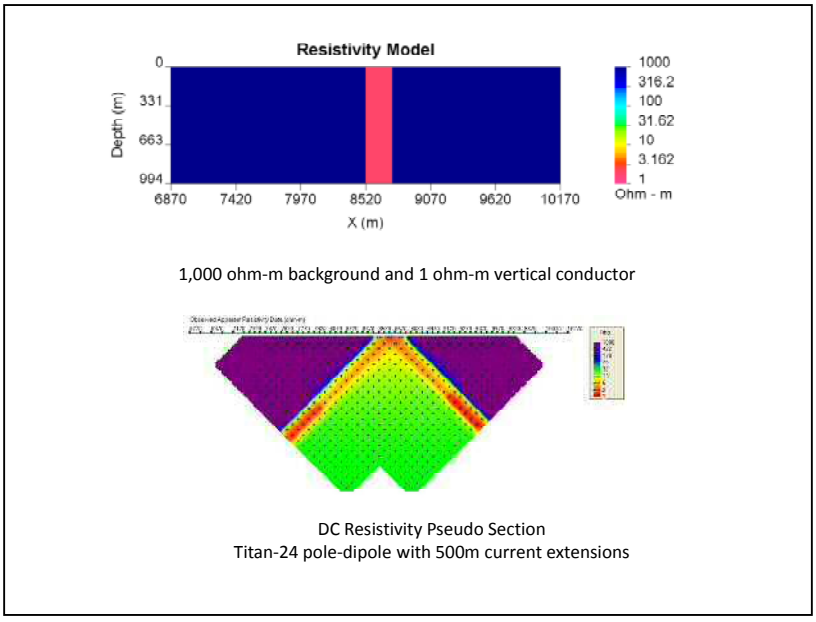

A synthetic model and its apparent resistivity pseudo section

The inverted resistivity model and the convergence curves are displayed below.

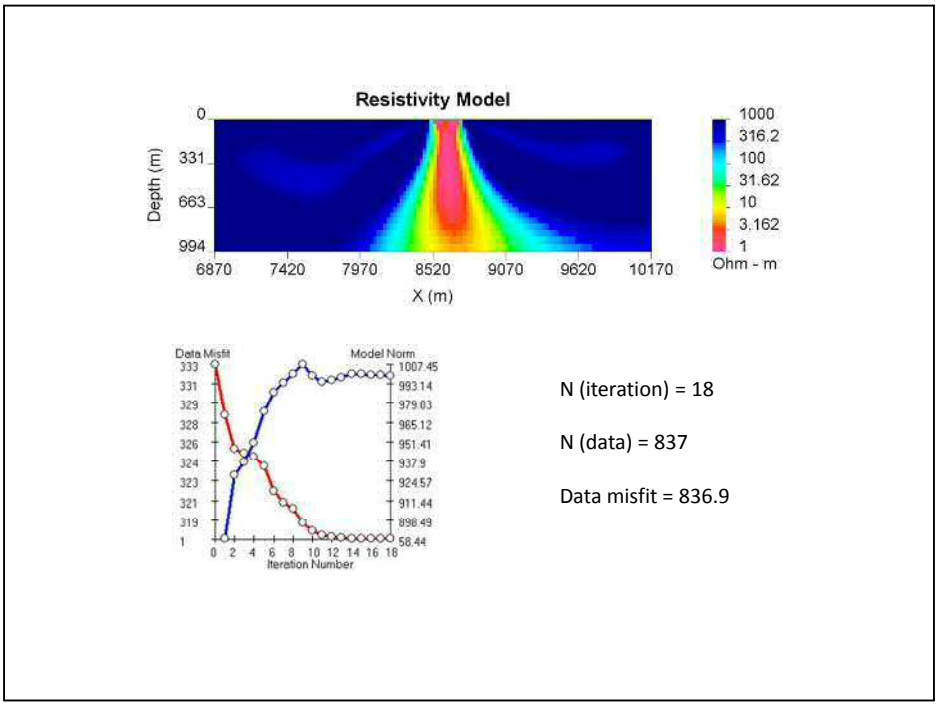

Inversion model, convergence curves and inversion statistics

J.9 IP INVERSIONS

For IP inversions, the apparent chargeability η is computed by carrying out two DC resistivity forward modeling with conductivity distributions $\sigma(x_i,z_i)$ and $(1-\eta)\sigma(x_i,z_i)$ (Oldenburg and Li, 1994), where (x_i, z_i) specifies the location in a 2D mesh.

The conductivity distributions used in IP inversions can be the inverted DC model or a half space of uniform conductivity. The IP inversion, generated through the use of a half space, is called the "NullCon" or "HSref" IP model

K INTRODUCTION TO THE MAGNETOTELLURIC METHOD

K.1 INTRODUCTION

The magnetotelluric (MT) method utilizes time-variations in the Earth's natural electric (E) and magnetic (H) fields to image the resistivity of the subsurface structure. The natural electromagnetic (EM) signals are assumed to be of plane-wave source over the frequency range with which the MT surveys are usually carried out. The plane-wave source is simpler to model compared with the complex transmitter geometries and signals used in the other EM methods. It makes the MT responses easier to understand and interpret with respect to the subsurface resistivity variations.

The E and H fields are measured over a broad range of frequencies. Typically, the frequencies can range from above 10 kHz to below 0.001Hz. Considering the conductivity of the Earth's materials and the frequency range over which the MT data are measured, the EM fields propagate in a diffusive regime. High frequency signals are attenuated more rapidly in the subsurface. Therefore, high frequency data are indicative of shallow resistivity structure while low frequency data are indicative of deep resistivity structure.

At frequencies below 1Hz the EM signal source is due to oscillations of the Earth's ionosphere as it interacts with the solar wind. At frequencies above 1Hz the signal source is due to worldwide lightning activities. There is a lack of natural signal around 1Hz, often referred to as the "hole". Modern 24-bit recording hardware and signal processing techniques, however, have largely eliminated the data quality degradations that have been traditionally seen around the 1Hz signal hole.

Between about 8Hz and 300Hz the signal from worldwide lightning activity propagates in a "resonant" cavity (the resistive atmosphere) between the conductive ionosphere and the conductive Earth's surface. Above 3 kHz the signal propagates as a ground wave. Between 300Hz and 3 kHz there is a "dead-band" where the signal does not propagate well. Despite hardware and signal processing improvements this dead-band remains problematic. When signal (atmospheric activity) is present within several hundreds of miles of the survey area the data quality improves. When no signal is being generated in the vicinity of the survey area the data quality is poor.

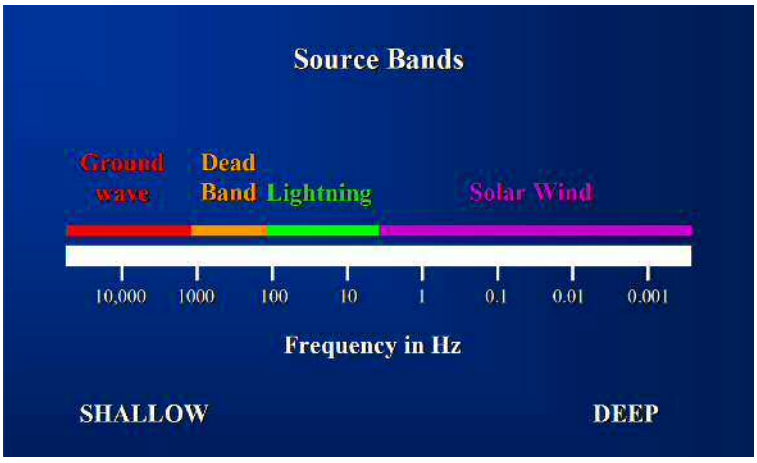

K.2 MEASUREMENTS

Both the electric and magnetic fields are measured at each site. The measured field strengths depend on the ionosphere and lightning activities and are essentially of random nature. While the E and H field strengths are random the ratio of these two fields depends on the frequency and the subsurface resistivity structure. For a homogeneous and a 1D earth resistivity structures, the magnetic field is perpendicular to the electric field. However, it is possible for a complex subsurface resistivity structure to rotate the fields. Therefore, full tensor data, including two perpendicular electric and two perpendicular magnetic fields, are usually measured.

In the field surveys, the electric and magnetic fields are measured as a function of time. The electric field is measured using two orthogonal grounded dipoles. The magnetic field is also measured using induction coils parallel to the electric dipoles.

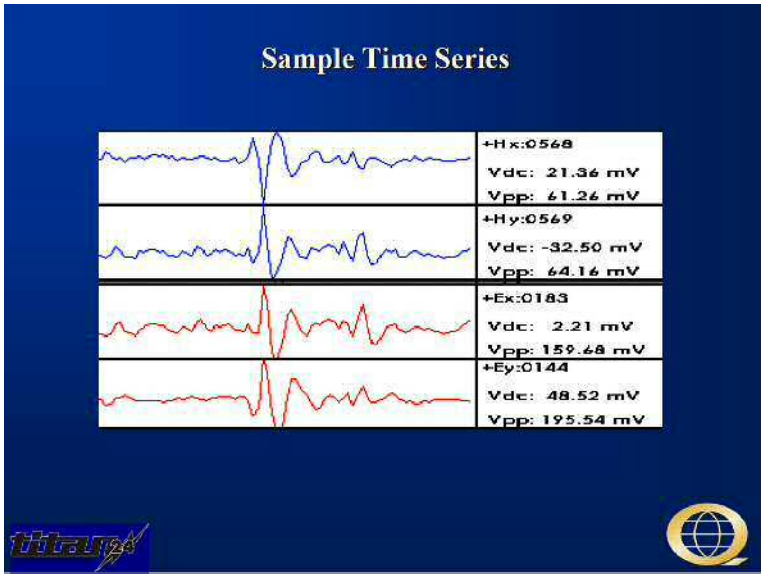

K.3 DATA PROCESSING

Extracting the subsurface resistivity structure from the measured magnetic and electric fields is a multi-step process. First, time series are transformed into frequency domain and sophisticated processing techniques are used to estimate the MT impedance tensor from the electric and magnetic fields. The impedance tensor is then used to calculate the apparent resistivity and phase data. In interpretation stage, inversion techniques are used to invert the apparent resistivity and phase data in to the subsurface true resistivity image. Finally, the resistivity image must be interpreted in terms of geologic units.

In time series processing, the measured magnetic and electric fields are Fourier transformed into the frequency domain. Calibration curves are applied to the measured fields to remove the acquisition system response. The Fourier coefficients represent the amplitude and phase of the electric and magnetic fields as a function of frequency.

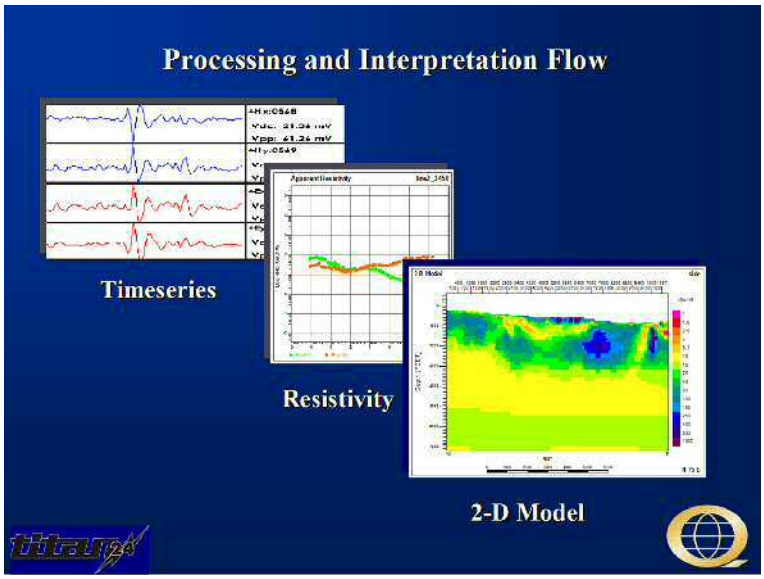

A variety of complex signal processing techniques are used to minimize noise and bias in the estimation of geophysical parameters from the measured fields. The approaches include:

- Spatial isolation of noise. A remote reference magnetic station is used to separate signal from local noise in the magnetic field data;
- Coherency sieves to find coherent signal. First the local and remote magnetic field measurements are compared and coherent signal are kept. Then the local magnetic and electric fields are compared for coherency;
- Frequency isolation of noise. Long Fourier transforms are used to provide extremely sharp isolation of noise in frequency;
- Time isolation of noise. Short Fourier transforms are used to remove noise that is isolated in time (noise spikes, or noise that is randomly turning off and on);
- Robust statistics that minimize biasing effects of a few isolated measurements.

The geophysical parameters are estimated after the processing is completed. In frequency domain, the ratio between the two measured components (E and H) is called electrical impedance (Z) and is defined as $|Z| = |E/H|$. The primary geophysical parameters are usually represented as plots of the apparent resistivity versus frequency and the phase versus frequency. The impedance values are used to calculate apparent resistivity and phase data as follows:

$$\rho_a(\Omega m) = \frac{1}{\mu\omega}|Z|^2 \quad \text{and} \quad \varphi = \arg(Z)$$

The apparent resistivity is a function of the frequency. The apparent resistivity can be considered as a volumetric weighted average of the resistivity and thickness of the rocks being sampled. Consequently, it is a smoothly varying function of the frequency. It can be shown theoretically that on a log-log plot of the apparent resistivity vs. frequency the curve cannot exceed a slope of +/- 45 degrees for a layered earth model. For a homogenous half-space or a one-dimensional (1D) earth the phase is related to the apparent resistivity through the Hilbert transform. This association does not exist for the 2D and the 3D earth models.

K.4 INTERPRETATION

Plots of apparent resistivity and phase data versus frequency in a log-log scale are a conventional

way of looking at the data before interpretation. If the survey involves several MT sites located along a line pseudo-sections of the apparent resistivities and phases in both components provides a first impression of the resistivity variation of the subsurface along the survey line.

The depth of penetration of the EM signal depends on the frequency of the data and the resistivity of the subsurface. The depth at which the signal amplitude attenuates to 37% (1/e) of its initial value is called the electromagnetic skin depth (δ) and is defined as:

$$\delta(m) = \sqrt{\frac{2}{\mu\omega\sigma}} = 503\left(\sqrt{\frac{\rho}{f}}\right)$$

where δ (m) is the skin depth, μ the magnetic permeability, σ (S/m) the conductivity (1/resistivity), ω the angular frequency (=2πf), f (Hz) the frequency, and ρ (Ωm) the resistivity (1/conductivity)

The skin depth concept provides an estimation of the maximum depth of investigation of the MT data.

The following plots illustrate example of the apparent resistivity curves for two MT sites as well as the apparent resistivity cross-sections along a MT line over a simple geological model.

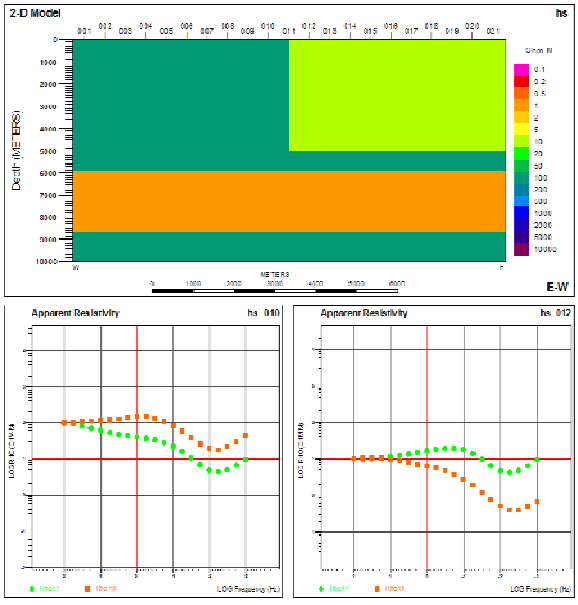

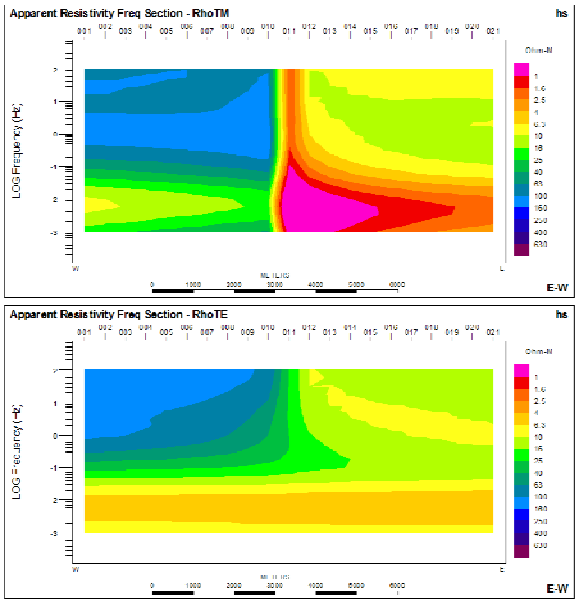

Interpretation of the MT data is performed using the maps of true resistivity of the subsurface. Inversion algorithms in one-dimension (1D), two-dimension (2D), and three-dimension (3D) are used to invert the apparent resistivity and phase data in to the maps of true resistivity of the subsurface. A simple layered subsurface structure generally can adequately be reproduced using the 1D inversion. In the case of more complex 2D or 3D structures, the MT response will be affected by lateral variations in resistivity. Consequently, a 2D or 3D inversion algorithm is required to allow the lateral resistivity variations.

In 1D earth assumption, off-diagonal elements of the impedance tensor are equal and of opposite signs and the diagonal elements are zero. The 1D inversion of the MT data produces a resistivity-depth profile for each MT site. The results represent a first order approximation of the resistivity variations with depth using a layered-earth model.

If there are lateral variations in the resistivity of the subsurface along one direction only (perpendicular to the strike) then a 2D inversion and interpretation is required. In this case, for a data rotated to the strike direction, off-diagonal elements of the impedance tensor are of opposite signs but not equal and the diagonal elements are zero. Because the electrical conductivity is constant along the strike direction (for example x-direction) all derivatives with respect to x will be zero. Therefore, Maxwell's equations are simplified and can be separated into two distinct modes so-called Transverse Electric (TE) and Transverse Magnetic (TM). The TE-mode represents the condition where the electric field is parallel to the strike direction while the TM-mode represents the condition where the magnetic field is parallel to the strike direction.

A cross-section of the true resistivity variations perpendicular to the assumed strike direction is created in the 2D inversion and is used in interpretation. For more complex geological structures a 3D inversion is essential to adequately describe the resistivity variation of the subsurface. In this case, none of the elements in the impedance tensor are equal or zero.

One of the factors that can affect the multi-dimensional MT data and interpretation is "static shift". The apparent resistivity curves can be biased (shifted up or down) by lateral resistivity contrasts with dimensions smaller than the minimum wavelength of the EM fields. These small features cannot be resolved by the MT data and they introduce a DC shift on the log-log apparent resistivity plots. This effect can be recognized by examining the sounding resistivity curves from the neighbouring MT sites and most be treated before the interpretation. Note that there are no static shift effects in the

phase data.

L REFERENCES

L.1 TITAN-24 METHOD AND APPLICATION

Donohue, J.G., and Sheard, S.N., 2001. Geophysics in North West Queensland – Improving the use of electrical geophysics. AIG Journal Paper 2001-01.

Garner, S., and Webb, D., 2000. Broadband MT and IP electrical property mapping with MIMDAS. SEG Technical Program Expanded Abstracts, 1085-1088.

Goldie, M., 2007. A comparison between conventional and distributed acquisition induced polarization surveys for gold exploration in Nevada. The Leading Edge, 26 (2), 180-183.

Hollyer, G, and Hearst, R., 2009. Deep exploration technologies for discovery in the shadow of head frames. First Break, 27 (July), 99-105.

Kingman, J., and Garner, S., 2003. Benefits of large channel capacity systems in electrical geophysics. ASEG 16th Geophysical Conference and Exhibition, Adelaide.

Legault, J., Carriere, D., and Petrie, L., 2008. Synthetic model testing and distributed acquisition dc resistivity results over an unconformity uranium target from the Athabasca Basin, northern Saskatchewan. The Leading Edge, 27 (1), 46-51.

Sheard, N., 1998. MIMDAS: A new direction in geophysics. Proceedings of the ASEG 13th International Conference, Hobart, Tasmania.

White, M., and Gordon, R., 2003. Deep imaging: New technology lowers cost of discovery. Canadian Mining Journal, April, 27-28.

L.2 DIRECT CURRENT (DC) AND INDUCED POLARISATION (IP) METHODS

Halverson, M.O., Zinn, W.G., McAlister, E.O., Ellis, R., and Yates, W.C., 1981. Assessment of results of broad-band spectral IP field test. In: Advances in Induced Polarization and Complex Resistivity, 295-346, University of Arizona.

Johnson, I.M., 1984. Spectral induced polarization parameters as determined through time-domain measurements. Geophysics, v. 49, 1993-2003.

Li, Y., and Oldenburg, W., 2000. 3-D inversion of induced polarization data. Geophysics, v 65 (6), 1931-1945.

Loke, M.H., 2004. Tutorial: 2D and 3D electrical imaging surveys, Res2Dinv and Res3Dinv manual [www.geoelectrical.com].

Oldenburg, D., and Li, Y., 1994. Inversion of induced polarization data. Geophysics, 59, 1327-1341.

Oldenburg, D., Li, Y., and Jones, F., 1998. Tutorial: Inversion (Res/IP) Methodology. In: The UBC-GIF Tutorials [http://www.geop.ubc.ca/ubcgif].

Oldenburg, D., and Li, Y., 1999. Estimating depth of investigation in DC and IP surveys. Geophysics, 64, 403-416.

Pelton, W.H., Ward, S.H., Hallof, P.G., Sill, W.R. and Nelson, P.H., 1978. Mineral discrimination and removal of inductive coupling with multi-frequency IP. Geophysics, v.43, 588-609.

Quantec, 2009. Standard chargeability calculations in Titan-24 IP measurements. Quantec Technical Note 001.

Seigel, H., 1959. Mathematical formulation and type curves for induced polarization. Geophysics, 24, 547-565.

Telford., W.M., Geldart, L., Sheriff, R., and Keys, D., 1976. Applied Geophysics. Cambridge University

Press, New York, NY.

Van Blaricom, R., 1992. Practical Geophysics for the Exploration Geologist. Nortwest Mining Association, Spokane, WA.

Wait, J., 1959. Overvoltage Research and Geophysical Applications. Pergammon Press.

L.3 MAGNETOTELLURIC (MT) METHOD

Bahr, K., and Simpson, F., 2005, Practical Magnetotellurics, Cambridge University Press.

Constable, S.C., Parker, R.L., and Constable, C.G., 1987. Occam's inversion - A practical algorithm for generating smooth models from electromagnetic sounding data. Geophysics, 52 (3), 289-300.

de Lugao, P.P., and Wannamaker, P.E., 1996. Calculating the two-dimensional magnetotelluric Jacobian in finite elements using reciprocity. Geophysical Journal International, 127, 806-810.

Marquardt, D.W., 1963. An algorithm for least-squares estimation of non-linear parameters. J. Sot. Ind. Appl. Math., 11, 431–441.

Nabighian, M.N., 1987. Electromagnetic Methods in Applied Geophysics, Volume 2: Application (Parts A and B). Society of Exploration Geophysicists (SEG), Tulsa.

Orange, A.S., 1989. Magnetotelluric exploration for hydrocarbons. Proceedings of the IEEE, 77, 287-317.

Rodi, W., and Mackie, R.L., 2001. Nonlinear conjugate gradients algorithm for 2D magnetotelluric inversions. Geophysics, 66, 174-187.

Siripunvaraporn, W., Egbert, G., Lenbury, Y., and Uyeshima, M., 2005. Three-Dimensional Magnetotelluric: Data Space Method. Physics of the Earth and Planetary Interiors, 150, 3-14.

Vozoff, K., 1972. The Magnetotelluric method in the Exploration of Sedimentary basins. Geophysics, 37, 98-141.

Wannamaker, P.E., Stodt, J.A., and Rijo, L., 1987. A stable finite-element solution for two-dimensional magnetotelluric modeling. Geophysical Journal of the Royal Astronomical Society, 88, 277-296.

Wight, D.E., 1987. MT/EMAP Data Interchange Standard, Revision 1.0. Society of Exploration Geophysicists (SEG). (Document available at the SEG web site: www.seg.org).

SUMMARY TABLE

SUMMARY TABLE	
CLIENT	
Client / Company Name	Moneta Porcupine Mines Inc.
Client Main Location	(Timmins, Ontario, Canada)
Client Representative	Rainer Skeries
Phone Number	(705) 264-2296
Fax Number	(705) 267-7490
Email Contact (if available)	RSkeries@monetaporcupine.com
PROJECT	
Project Grid Name	North Tisdale Project
Project Grid Location	(Ontario, Canada)
Survey Type	Titan-24 DC - IP - MT
Survey Period (YY/MM/DD to YY/MM/DD)	2011/12/06 to 2011/12/14
Quantec Project Number	CA00916T
Geophysicist(s) in charge	Data QAQC: Kevin Killin, Mojtaba Daneshvar Chris Furey Processing, Inversion & Interpretation: (list if different to QAQC person)
REPORT	
Signed by	Saman Perera, Mehran Gharibi
Report Date	17/02/2012